Title
Genome-wide analysis of re-replication initiation and elongation in Saccharomyces cerevisiae

Author
Morreale, Richard J

Publication Date
2007-08-31

Peer reviewed|Thesis/dissertation

Genome-wide analysis of re-replication initiation and elongation in Saccharomyces cerevisiae

by

Richard J Morreale

DISSERTATION

Submitted in partial satisfaction of the requirements for the degree of

DOCTOR OF PHILOSOPHY

in

Genetics

in the

GRADUATE DIVISION

of the

UNIVERSITY OF CALIFORNIA, SAN FRANCISCO

[redacted]

Dedicated to

Heather Finlay-Morreale

Mary Morreale

Jerry Morreale

Michelle Morreale

Acknowledgements

I would first like to express my gratitude to my advisor, Joachim Li, whose guidance has been instrumental for my development as a scientist. Joachim taught me many skills including how to solve problems systematically, communicate effectively and perhaps most importantly, to remain optimistic in the face of failure.

My sincere thanks to thank my thesis committee, Sandy Johnson and Hiten Madhani, both of whom helped me see the big picture and gave me excellent advice on the direction of my project. I would like to thank Sandy for encouraging me to consider my future career plans sooner than I would have otherwise. I wish to express my gratitude to Hiten for his continued interest in my research and his many helpful experimental suggestions.

I wish to thank my fellow graduate students and partners in crime Brian Green, Leslie Chu and Muluye Liku. Their friendship, encouragement, and numerous helpful discussions have been invaluable to me. I am particularly obliged to Brian Green from whom I learned to balance carefulness and speed. I am indebted to Emily Wang, who helped me to PCR amplify nearly every base pair of the yeast genome and to Bilge Ozaydin who performed the first microarray experiments in our lab. In addition, I wish to thank current and former lab members Van Nguyen, Erin Quan, Laura Goodwin, Annie Arguello, Nima Afshar, Jeff Farrell, Ken Finn and Chris Richardson for making the lab a fun and rewarding place to work. I wish to express my gratitude to Marian Tse and Frank Castro for their tireless efforts to keep the lab running.

I wish to extend my warm thanks to my family. I am grateful for my parents who have been encouraging and supportive throughout graduate school, even when they wondered why it seemed to take such a long time. I wish to thank my sister, Michelle, who first introduced me to San Francisco and who has always been willing to listen.

Finally, and most importantly, I would like to thank my wife, Heather, for her generosity and support throughout graduate school. Heather has been both an inspiration and a great source of comfort. Her patience, understanding and love have made this work possible.

Chapter 2 and Appendix 1 of this dissertation are reprints of material as it appears in Green BM, Morreale RJ, Ozaydin B, Derisi JL, Li JJ (2006). Genome-wide mapping of DNA synthesis in *Saccharomyces cerevisiae* reveals that mechanisms preventing reinitiation of DNA replication are not redundant. Mol Biol Cell *17*, 2401-14. Chapter 3 and Appendix 2 of this dissertation are reprints of material that have been submitted for publication, Morreale, RJ and Li, JJ (2007).

Contributions to Described Work

The work in Chapter 2 and Appendix 1 was published in *Molecular Biology of the Cell* by myself, Brian Green, Bilge Ozaydin, Joe DeRisi and Joachim Li. Brian Green and I were co-first authors. I contributed to the design of all experiments and contributed to writing and editing the manuscript. I executed the experiments in Figures 1A, 1B, 1C, 1D, 1E, 2B, 3A, 3B, 4C, 5E, 6E, 7B, and 7C with help from Bilge Ozaydin for Figures 4C, 4D and 6E. Brian Green wrote the computer program used to analyze and display Figures 1B, 1D, 2B, 2D, 3B, 4C, 4D, 5E, 6E, 7B and 7C. Brian Green executed the experiments in Figures 2A, 2C, 4A, 4B, 5A, 5B, 5C, 5D, 6A, 6B, 6C, 6D and 7A.

The work in Chapter 3 and Appendix 2 has been submitted for publication. I contributed to the design of all experiments, executed all experiments and contributed to writing and editing the manuscript.

Genome-wide analysis re-replication initiation and elongation in *Saccharomyces cerevisiae*

Richard J. Morreale

To maintain genomic stability, re-initiation of eukaryotic DNA replication within a single cell cycle is blocked by multiple mechanisms that inactivate or remove replication proteins after G1 phase. Our lab had previously shown that simultaneous deregulation of three replication proteins, ORC, Cdc6 and Mcm2-7, was necessary to cause detectable bulk re-replication in G2/M phase in *Saccharomyces cerevisiae*. We used microarray comparative genomic hybridization (CGH) to provide a more comprehensive and detailed analysis of re-replication. This genome-wide analysis suggests that re-initiation in G2/M phase primarily occurs at a subset of both active and latent origins, but is independent of chromosomal determinants that specify the timing of origins in S phase. We demonstrate that re-replication can be induced within S phase, but differs in amount and location from re-replication in G2/M phase, illustrating the dynamic nature of DNA replication controls. Finally, we re-examined the issue of mechanistic redundancy and showed that very limited re-replication can be detected by microarray CGH when only two replication proteins are deregulated demonstrating that the mechanisms blocking re-replication are overlapping rather than redundant.

Deregulation of these mechanisms leads to incomplete re-replication of the genome and has been shown to cause DNA damage checkpoint activation and double strand breaks. To understand the link between re-replication and DNA damage I

performed a genome-wide kinetic analysis of fork progression using microarray CGH. I determined that fork progression was severely impaired during re-replication. During re-replication forks progressed at least five-fold slower than S phase forks and failed to complete duplication of the chromosomes. In addition, analysis of the progression of existing forks suggested that the forks were stalled or collapsed. I next investigated the potential source of this impairment and determined that impaired fork progression was not due to insufficient nucleotides. I also provided evidence that fork progression was impaired even when fork head-to-tail collisions due to multiple rounds of reinitiation were prevented. Thus this impairment is likely occurring at individual forks and is consistent with a model in which replication fork failure during re-replication leads to DNA lesions.

Table of Contents

List of Tables

List of Figures

APPENDIX I

APPENDIX 2

CHAPTER 1

Introduction

Introduction

One of the most fundamental tasks performed by a cell is faithfully transmitting an exact copy of its genome to subsequent generations. In order to accomplish this task, DNA replication is tightly controlled to ensure that every chromosomal segment is replicated once and only once per cell cycle. Precisely time coordination is critical because eukaryotic genomes initiate DNA replication from hundreds to thousands of sites, called origins of replication each cell cycle. A cell must simultaneously promote replication initiation from these many origins while at the same time preventing even a single origin from initiating a second time.

The Initiation of DNA replication

Cells initiate DNA replication using a highly coordinated process that is universally conserved among eukaryotes (for review see (Bell and Dutta, 2002)). Origins of replication direct the stepwise assembly of a multiprotein machine called the pre-replicative complex (pre-RC). The basic function of the pre-RC is to load Mcm2-7, the putative replicative helicase, at origins (Bell and Dutta, 2002). Pre-RC formation occurs in G1 phase by the sequential binding of the Origin Recognition Complex (ORC), Cdc6, Cdt1 and Mcm2-7 (Kelly and Brown, 2000). The activation of origins in S phase causes a series of steps that culminate in the formation of two bi-directional replication forks (Waga and Stillman, 1998). The activation an origin in S phase is accompanied by disassembly of the pre-RC. The control of this process is intimately linked to the cell cycle such that a single round of assembly and activation can occur at each origin.

Eukaryotes initiate DNA replication at DNA segments called origins of replication. In *Saccharomyces cerevisiae* each replication origin is composed of a discrete sequence element of approximately 150 bp called an autonomously replicating sequence (ARS) (Bell *et al.*, 1995). The yeast genome contains approximately 450 potential replication origins (Wyrick *et al.*, 2001; Xu *et al.*, 2006). This is far greater than the number of origins that are actually needed to replicate the yeast genome. Thus only a subset of all the potential origins actually initiates DNA replication in a given cell cycle (Dershowitz and Newlon, 1993; Raghuraman *et al.*, 2001; Wyrick *et al.*, 2001; Pasero *et al.*, 2002). Origin activation is additionally regulated because each origin initiates in a reproducible temporal order throughout S phase through a mechanism which is not understood (Donaldson, 2005). As a consequence, late replicating origins are often replicated passively by forks from neighboring initiation sites (Santocanale *et al.*, 1999).

In metazoan cells, there can be upwards of thousands of origins and the sequence specificity of initiation appears to be more permissive. Origins tend to be much larger, several kilobases, and consist of zones of initiation where replication can initiate from a number of different sequences (Gilbert, 2004). During the rapid embryonic cell cycles of *Drosophila melanogaster* and *Xenopus laevis*, it appears that nearly any sequence of DNA will initiate efficiently, indicating that a specific site is not an absolute requirement of initiation (Gilbert, 2004).

In all eukaryotes, potential replication origins are first selected by the process of ORC binding to the DNA (Bell and Dutta, 2002). In budding yeast ORC is bound to origins during all phases of the cell cycle (Santocanale and Diffley, 1996). ORC was first identified in *S. cerevisiae* using biochemical (ORC1-5) (Bell and Stillman, 1992) and

genetic (ORC6) (Li and Herskowitz, 1993) methods. In budding yeast, ORC binds to short AT-rich sequence called the ARS consensus sequences (ACS) ((Bell and Stillman, 1992)) and recruits other pre-RC members to the origin (Bell and Dutta, 2002). ORC binding also facilitates initiation by positioning nucleosomes adjacent to the origin (Lipford and Bell, 2001). Three of the ORC subunits (Orc1, Orc4 and Orc5) are members of the nucleotide binding AAA+ superfamily. ATP binding but not hydrolysis, is essential for origin DNA binding (Klemm *et al.*, 1997). The hydrolysis of ORC is essential for the loading of multiple Mcm2-7 complexes onto origins (Bowers *et al.*, 2004).

Two additional proteins, Cdc6 and Cdt1 bind to ORC and recruit Mcm2-7 the origin. Cdc6, like ORC, is a member of the AAA+ ATPase superfamily. Binding to ORC and the origin stimulates the ATPase activity of Cdc6. ATP hydrolysis by Cdc6 functions prior to ATP hydrolysis by ORC to load Mcm2-7 onto DNA (Randell *et al.*, 2006). The coordinated ATP hydrolysis of ORC and Cdc6 function as a molecular machine that loads multiple Mcm2-7 complexes onto the origin. The second protein, Cdt1 is required to load Mcm2-7 though its precise molecular function is not known (Maiorano *et al.*, 2000; Nishitani *et al.*, 2000; Wohlschlegel *et al.*, 2000; Tanaka and Diffley, 2002).

The heterohexameric Mcm2-7 complex is thought to be the replicative helicase, although definitive proof of this has been elusive (Forsburg, 2004). The Mcm2-7 complex is loaded onto origins and upon origin activation travels with the replication forks presumably to unwind the DNA (Aparicio *et al.*, 1997). A large body of indirect evidence supports the notion that Mcm2-7 is a helicase (Forsburg, 2004). The Mcm2-7

complex is essential for replication elongation (Labib *et al.*, 2000). The complex is composed of six different subunits each with ATPase activity. Importantly the ATPase domain on each subunit is stimulated by a domain on an adjacent subunit ensure only the fully formed complex is functional (Schwacha and Bell, 2001). Purified complexes of Mcm2-7 proteins, however, exhibit only weak helicase activity in vitro (Bell and Dutta, 2002). Recently, a large complex containing Mcm2-7 and additional replication proteins has been isolated from *Drosophila* cells. This complex displays robust helicase activity suggesting that Mcm2-7 is a component of a larger molecular machine that unwinds the DNA (Moyer *et al.*, 2006).

Passage through the G1 phase commitment point, Start, is accompanied by a rise in the activity of S phase CDKs and a second kinase Cdc7-Dbf4 (Buck *et al.*, 1991; Epstein and Cross, 1992; Schwob and Nasmyth, 1993). This allows the recruitment of additional initiation proteins, origin unwinding, and assembly of the replication fork machinery (Zou and Stillman, 2000). CDK phosphorylation of two proteins, Sld2 (Masumoto *et al.*, 2002) and Sld3, (Tanaka *et al.*, 2007; Zegerman and Diffley, 2007) is required for replication initiation. The direct target of Cdc7-Dbf4 has not been firmly established but is likely to be a member of the Mcm2-7 complex (Bell and Dutta, 2002). During this stage, two additional sequential sets of replication proteins assemble at the origin. The first set includes Cdc45, Sld3, Sld2, Dpb11, and the GINS complex (Kamimura *et al.*, 1998; Zou and Stillman, 1998; Kamimura *et al.*, 2001; Takayama *et al.*, 2003). The second set includes proteins involved in DNA synthesis including RPA, PCNA and the DNA polymerases (Bell and Dutta, 2002). Some of the proteins in this large initiation complex are incorporated into the replication fork, while others dissociate

from the origin leaving only ORC behind. Thus, any new initiation event requires both assembly of a new pre-RC and re-activation of the origin.

Preventing re-replication in yeast

Re-replication is prevented by dividing the process of replication initiation into two mutually exclusive stages (reviewed in (Bell and Dutta, 2002; Diffley, 2004; Machida *et al.*, 2005)). In the first stage, which is restricted to G1 phase, potential origins are selected by assembly of the pre-RC. In the second stage, which is restricted to S, G2, and M phases, potential origins are activated to initiate DNA replication by the two kinases, Cdk1 and Cdc7. The activation of CDKs prevents pre-RC assembly. This block persists through S, G2, and M phases until the CDKs are inactivated in G1. Likewise, origin activation is excluded from G1 phase, because the two kinases that trigger initiation are inactive. In this manner passage through the cell cycle is coupled to exactly one round of replication.

In *S. cerevisiae*, the block to re-replication is primarily enforced by CDK phosphorylation of the pre-RC components. CDKs down regulate ORC through inhibitory phosphorylation of Orc2 and Orc6 (Nguyen *et al.*, 2001) as well as by direct binding to Orc6 (Wilmes *et al.*, 2004). The direct binding of Orc6 by Cdk1-Clb5 is thought to occlude the binding site for a component of the pre-RC. The mechanism through which CDK phosphorylation of Orc2 and Orc6 inactivates the complex is not known. Mutation of the phosphorylation sites only modestly reduces the binding to Orc6 by Cdk1-Clb5 (Wilmes *et al.*, 2004). Additionally, the ATPase activity of the subunits is likewise an unlikely mode of regulation since this activity is essential for viability REF.

Further investigation will be required to understand how CDK phosphorylation inhibits the activity of ORC.

CDKs inhibit Cdc6 in *S. cerevisiae* using three separate mechanisms. CDKs down regulate the expression of *CDC6* by phosphorylating the transcription factor Swi5 and preventing its import (Moll *et al.*, 1991). The CDK phosphorylation of two domains on Cdc6 stimulates its degradation (Perkins *et al.*, 2001). During G1/S phase, CDK phosphorylation causes ubiquitylation of Cdc6 by SCF^{CDC4} E3 ubiquitin ligase and subsequent degradation by the proteasome (Drury *et al.*, 1997; Elsasser *et al.*, 1999: Drury, 2000 #29). CDKs use similar a mechanisms to promote destruction of Cdc6 homolog, Cdc18, in fission yeast (Jallepalli *et al.*, 1997). Finally, CDK phosphorylation of the Cdc6 n-terminus causes the mitotic cyclin Clb2, complexed with Cdk1, to directly bind and inhibit Cdc6 (Mimura *et al.*, 2004). The complex regulation of Cdc6 demonstrates that control of this protein is critical to prevent re-replication.

CDKs phosphorylation promotes the net nuclear export of Mcm2-7 in budding yeast (Labib *et al.*, 1999; Nguyen *et al.*, 2000). CDKs directly phosphorylate critical phosphorylation sites on Mcm3 that cluster around a nuclear export signal (NES) (Liku *et al.*, 2005). Phosphorylation of these sites likely alters the activity of the NES and may also affect a bipartite nuclear localization signal (NLS) found on Mcm2 and Mcm3. The localization of Cdt1 closely mirrors that of Mcm2-7 and it has been shown that the localization of these two proteins is interdependent (Tanaka and Diffley, 2002). Thus deregulating the localization of the Mcm2-7 complex also changes the localization of Cdt1.

Preventing re-replication in metazoans

The principle of temporally separating the two stages of initiation appears to be universal among eukaryotes, but the specific targets and modes of regulation vary between organisms. Despite this variation, all eukaryotes use the basic strategy of regulating the stability, activity, and localization of pre-RC components to prevent re-replication (for review see (Blow and Dutta, 2005: Arias, 2007 #242)). CDKs have been implicated in the degradation of Orc1 and the nuclear exclusion of Cdc6 (Diffley, 2004). In addition, Cdk1 can inhibit re-replication in *Xenopus* extracts in metaphase by an unknown mechanism (Tada *et al.*, 2001).

Unlike in budding yeast, not all mechanisms in metazoan cells are directly dependent upon CDK activity. At least two CDK-independent mechanisms have been identified that regulate Cdt1. Metazoans contain a protein, geminin that directly binds Cdt1 and inhibits prevent it from associating with Mcm2-7 and recruiting it to origins (Wohlschlegel *et al.*, 2000; Tada *et al.*, 2001). The periodic destruction of geminin in G1 phase frees Cdt1 to participate in pre-RC formation (McGarry and Kirschner, 1998).

Experiments in *Xenopus* and human cells have identified a second CDK-independent mechanism to prevent re-replication: the replication-coupled destruction of Cdt1 during S phase (Arias and Walter, 2005; Takeda *et al.*, 2005). Following origin activation and assembly of the replisome, Cdt1 binds to the replication processivity clamp, PCNA. This stimulates Cdt1 ubiquitylation by the Cul4-Ddb1^{Cdt2} E3 ubiquitin ligase and degradation by the proteasome (Arias and Walter, 2006; Jin *et al.*, 2006; Senga *et al.*, 2006).

In addition, mammalian cells have a second mode of CDT1 destruction that does require the activity of the CDK. In G2 and M phase Cdk1 phosphorylates Cdt1 and stimulates its degradation through ubiquitylation by a different E3 ubiquitin ligase, SCF^{Skp2} (Nishitani *et al.*, 2006). Interestingly, it is thought that geminin binding in G2 acts to sequester Cdt1 and protect it from this degradation (Ballabeni *et al.*, 2004). Upon entry into G1 phase, geminin degradation releases this pool of Cdt1 allowing for rapid pre-RC assembly.

The role of multiple mechanisms in the block to re-replication

Obtaining clear evidence of re-replication within a single cell cycle has generally required the simultaneous disruption of multiple mechanisms, leading to the presumption that these mechanisms are functionally redundant (Diffley, 2004; Blow and Dutta, 2005). In budding yeast, for example, simultaneous deregulation of ORC phosphorylation, Mcm2-7 localization, and Cdc6 protein levels is needed to detect re-replication in G2/M phase (Nguyen *et al.*, 2001). Similarly, in fission yeast, regulation of Cdc6/Cdc18 expression and phosphorylation, regulation of Cdt1 expression, and Orc2 phosphorylation have been proposed to act redundantly to prevent re-replication (Gopalakrishnan *et al.*, 2001; Vas *et al.*, 2001; Yanow *et al.*, 2001). In *Xenopus* regulation of Cdt1 by degradation and geminin inhibition appear to work together to prevent re-replication (McGarry and Kirschner, 1998; Arias and Walter, 2005; Li and Blow, 2005; Yoshida *et al.*, 2005). In those cases where individual overexpression of Cdc6/Cdc18 or Cdt1 was associated with re-replication, the perturbations used to

deregulate these proteins likely affected other regulatory mechanisms as well (Nishitani and Nurse, 1995; Muzi Falconi *et al.*, 1996; Thomer *et al.*, 2004).

In metazoans, several of these mechanisms typically must be deregulated to detect re-replication using current assays (McGarry and Kirschner, 1998; Arias and Walter, 2005; Li and Blow, 2005; Yoshida *et al.*, 2005**)**. The only examples where precise disruption of a single replication control mechanism has led to re-replication are provided by depletion of geminin in certain metazoan cell lines (Mihaylov *et al.*, 2002; Melixetian *et al.*, 2004; Zhu *et al.*, 2004). Even in these cases, other unknown factors may be contributing to the observed re-replication as: (1) many cells in the affected cell lines do not exhibit re-replication (Mihaylov *et al.*, 2002; Melixetian *et al.*, 2004); (2) not all geminin depleted cell lines experience detectable re-replication (Nishitani *et al.*, 2004); and (3) geminin depletion in whole metazoan organisms either does not cause overt re-replication (McGarry, 2002; Yanagi *et al.*, 2005) or is limited to prolonging DNA synthesis primarily in cell types that normally undergo endoreduplication or gene amplification (Quinn *et al.*, 2001). Regardless, these results support the model, discussed further in Chapter 2, that re-replication controls are not redundant and rather provide overlapping protection from re-replication.

The consequences of re-replication

In budding yeast, re-replication causes activation of the DNA damage checkpoint and cell inviability. In addition clear evidence of double strand breaks and chromosomal fragmentation are observed (Green and Li, 2005). In metazoan cells re-replication induced by overexpression of Cdc6 and Cdt1 or by depletion of geminin activates a DNA

damage response and causes a loss of viability (Vaziri *et al.*, 2003; Melixetian *et al.*, 2004; Zhu *et al.*, 2004; Li and Blow, 2005). Induction of re-replication results in the appearance of DNA damage-associated H2AX foci and DNA double strand breaks are detected (Melixetian *et al.*, 2004; Lovejoy *et al.*, 2006; Zhu and Dutta, 2006). While it is likely that re-replication itself is causing the DNA damage in these systems, it is unclear how re-replication creates these lesions.

One mechanism through which re-replication is able to cause DNA damage has been demonstrated in *Xenopus* (Davidson *et al.*, 2006). When high levels of Cdt1 induced massive re-replication, fragmented DNA that appeared to be extruded from the chromosome was observed. The authors proposed that the excessive Cdt1 levels induced multiple rounds of re-initiation, generating successive re-replication forks that followed each other down the chromosome. The second fork could potentially chase the first fork causing a collision. If this were to occur on either side of an origin this could result in extrusion of the newly synthesized daughter strands. It was unclear, however, whether the extruded DNA was the source the DNA damage. The authors failed to convincingly prove that the chromosomal DNA was unbroken. In addition, there are two peculiarities of the Xenopus embryonic replication system, which make it difficult to generalize this result. First, the DNA is not actively transcribed which means that replication can initiate from any sequence. Secondly, the average distance between origins is only 10 kb (Blow *et al.*, 2001) which is far smaller than the 45 kb in budding yeast (Lengronne *et al.*, 2001) and 115 kb in mammalian somatic cells (Lebofsky *et al.*, 2006).

Dissertation overview

In this dissertation I will discuss research to understand re-replication using the budding yeast, *Saccharomyces cerevisiae.* In Chapter 2 (Green *et al.*, 2006), I discuss our efforts to understand how the mechanisms that prevent re-replication cooperate to achieve stringent control of initiation. I will also describe work investigating the control of re-replication during different phases of the cell cycle. Finally, I will discuss our characterization of re-replication initiation on a genome-wide level in which we determine the location and nature of origins that re-initiated. In Chapter 3 (submitted), I will discuss our efforts to obtain a better mechanistic understanding of why re-replication causes DNA lesions by characterizing fork progression during re-replication.

References

Aparicio, O.M., Weinstein, D.M., and Bell, S.P. (1997). Components and dynamics of DNA replication complexes in S. cerevisiae: redistribution of MCM proteins and Cdc45p during S phase. Cell *91*, 59-69.

Arias, E.E., and Walter, J.C. (2005). Replication-dependent destruction of Cdt1 limits DNA replication to a single round per cell cycle in Xenopus egg extracts. Genes Dev *19*, 114-126.

Arias, E.E., and Walter, J.C. (2006). PCNA functions as a molecular platform to trigger Cdt1 destruction and prevent re-replication. Nat Cell Biol *8*, 84-90.

Ballabeni, A., Melixetian, M., Zamponi, R., Masiero, L., Marinoni, F., and Helin, K. (2004). Human geminin promotes pre-RC formation and DNA replication by stabilizing CDT1 in mitosis. Embo J *23*, 3122-3132.

Bell, S.P., and Dutta, A. (2002). DNA replication in eukaryotic cells. Annu Rev Biochem *71*, 333-374.

Bell, S.P., Mitchell, J., Leber, J., Kobayashi, R., and Stillman, B. (1995). The multidomain structure of Orc1p reveals similarity to regulators of DNA replication and transcriptional silencing. Cell *83*, 563-568.

Bell, S.P., and Stillman, B. (1992). ATP-dependent recognition of eukaryotic origins of DNA replication by a multiprotein complex. Nature *357*, 128-134.

Blow, J.J., and Dutta, A. (2005). Preventing re-replication of chromosomal DNA. Nat Rev Mol Cell Biol *6*, 476-486.

Blow, J.J., Gillespie, P.J., Francis, D., and Jackson, D.A. (2001). Replication origins in Xenopus egg extract Are 5-15 kilobases apart and are activated in clusters that fire at different times. J Cell Biol *152*, 15-25.

Bowers, J.L., Randell, J.C., Chen, S., and Bell, S.P. (2004). ATP hydrolysis by ORC catalyzes reiterative Mcm2-7 assembly at a defined origin of replication. Mol Cell *16*, 967-978.

Buck, V., White, A., and Rosamond, J. (1991). CDC7 protein kinase activity is required for mitosis and meiosis in Saccharomyces cerevisiae. Mol Gen Genet *227*, 452-457.

Davidson, I.F., Li, A., and Blow, J.J. (2006). Deregulated replication licensing causes DNA fragmentation consistent with head-to-tail fork collision. Mol Cell *24*, 433-443.

Dershowitz, A., and Newlon, C.S. (1993). The effect on chromosome stability of deleting replication origins. Mol Cell Biol *13*, 391-398.

Diffley, J.F. (2004). Regulation of early events in chromosome replication. Curr Biol *14*, R778-786.

Donaldson, A.D. (2005). Shaping time: chromatin structure and the DNA replication programme. Trends Genet *21*, 444-449.

Drury, L.S., Perkins, G., and Diffley, J.F. (1997). The Cdc4/34/53 pathway targets Cdc6p for proteolysis in budding yeast. Embo J *16*, 5966-5976.

Elsasser, S., Chi, Y., Yang, P., and Campbell, J.L. (1999). Phosphorylation controls timing of Cdc6p destruction: A biochemical analysis. Mol Biol Cell *10*, 3263-3277.

Epstein, C.B., and Cross, F.R. (1992). CLB5: a novel B cyclin from budding yeast with a role in S phase. Genes Dev *6*, 1695-1706.

Forsburg, S.L. (2004). Eukaryotic MCM proteins: beyond replication initiation. Microbiol Mol Biol Rev *68*, 109-131.

Gilbert, D.M. (2004). In search of the holy replicator. Nat Rev Mol Cell Biol *5*, 848-855.

Gopalakrishnan, V., Simancek, P., Houchens, C., Snaith, H.A., Frattini, M.G., Sazer, S., and Kelly, T.J. (2001). Redundant control of rereplication in fission yeast. Proc Natl Acad Sci U S A *98*, 13114-13119.

Green, B.M., and Li, J.J. (2005). Loss of rereplication control in Saccharomyces cerevisiae results in extensive DNA damage. Mol Biol Cell *16*, 421-432.

Green, B.M., Morreale, R.J., Ozaydin, B., Derisi, J.L., and Li, J.J. (2006). Genome-wide mapping of DNA synthesis in Saccharomyces cerevisiae reveals that mechanisms preventing reinitiation of DNA replication are not redundant. Mol Biol Cell *17*, 2401-2414.

Jallepalli, P.V., Brown, G.W., Muzi-Falconi, M., Tien, D., and Kelly, T.J. (1997). Regulation of the replication initiator protein p65cdc18 by CDK phosphorylation. Genes Dev *11*, 2767-2779.

Jin, J., Arias, E.E., Chen, J., Harper, J.W., and Walter, J.C. (2006). A family of diverse Cul4-Ddb1-interacting proteins includes Cdt2, which is required for S phase destruction of the replication factor Cdt1. Mol Cell *23*, 709-721.

Kamimura, Y., Masumoto, H., Sugino, A., and Araki, H. (1998). Sld2, which interacts with Dpb11 in Saccharomyces cerevisiae, is required for chromosomal DNA replication. Mol Cell Biol *18*, 6102-6109.

Kamimura, Y., Tak, Y.S., Sugino, A., and Araki, H. (2001). Sld3, which interacts with Cdc45 (Sld4), functions for chromosomal DNA replication in Saccharomyces cerevisiae. Embo J *20*, 2097-2107.

Kelly, T.J., and Brown, G.W. (2000). Regulation of chromosome replication. Annu Rev Biochem *69*, 829-880.

Klemm, R.D., Austin, R.J., and Bell, S.P. (1997). Coordinate binding of ATP and origin DNA regulates the ATPase activity of the origin recognition complex. Cell *88*, 493-502.

Labib, K., Diffley, J.F., and Kearsey, S.E. (1999). G1-phase and B-type cyclins exclude the DNA-replication factor Mcm4 from the nucleus. Nat Cell Biol *1*, 415-422.

Labib, K., Tercero, J.A., and Diffley, J.F. (2000). Uninterrupted MCM2-7 function required for DNA replication fork progression. Science *288*, 1643-1647.

Lebofsky, R., Heilig, R., Sonnleitner, M., Weissenbach, J., and Bensimon, A. (2006). DNA replication origin interference increases the spacing between initiation events in human cells. Mol Biol Cell *17*, 5337-5345.

Lengronne, A., Pasero, P., Bensimon, A., and Schwob, E. (2001). Monitoring S phase progression globally and locally using BrdU incorporation in TK(+) yeast strains. Nucleic Acids Res *29*, 1433-1442.

Li, A., and Blow, J.J. (2005). Cdt1 downregulation by proteolysis and geminin inhibition prevents DNA re-replication in Xenopus. Embo J *24*, 395-404.

Li, J.J., and Herskowitz, I. (1993). Isolation of ORC6, a component of the yeast origin recognition complex by a one-hybrid system. Science *262*, 1870-1874.

Liku, M.E., Nguyen, V.Q., Rosales, A.W., Irie, K., and Li, J.J. (2005). CDK Phosphorylation of a Novel NLS-NES Module Distributed between Two Subunits of the Mcm2-7 Complex Prevents Chromosomal Rereplication. Mol Biol Cell *16*, 5026-5039.

Lipford, J.R., and Bell, S.P. (2001). Nucleosomes positioned by ORC facilitate the initiation of DNA replication. Mol Cell *7*, 21-30.

Lovejoy, C.A., Lock, K., Yenamandra, A., and Cortez, D. (2006). DDB1 maintains genome integrity through regulation of Cdt1. Mol Cell Biol *26*, 7977-7990.

Machida, Y.J., Hamlin, J.L., and Dutta, A. (2005). Right place, right time, and only once: replication initiation in metazoans. Cell *123*, 13-24.

Maiorano, D., Moreau, J., and Mechali, M. (2000). XCDT1 is required for the assembly of pre-replicative complexes in Xenopus laevis. Nature *404*, 622-625.

Masumoto, H., Muramatsu, S., Kamimura, Y., and Araki, H. (2002). S-Cdk-dependent phosphorylation of Sld2 essential for chromosomal DNA replication in budding yeast. Nature *415*, 651-655.

McGarry, T.J. (2002). Geminin deficiency causes a Chk1-dependent G2 arrest in Xenopus. Mol Biol Cell *13*, 3662-3671.

McGarry, T.J., and Kirschner, M.W. (1998). Geminin, an inhibitor of DNA replication, is degraded during mitosis. Cell *93*, 1043-1053.

Melixetian, M., Ballabeni, A., Masiero, L., Gasparini, P., Zamponi, R., Bartek, J., Lukas, J., and Helin, K. (2004). Loss of Geminin induces rereplication in the presence of functional p53. J Cell Biol *165*, 473-482.

Mihaylov, I.S., Kondo, T., Jones, L., Ryzhikov, S., Tanaka, J., Zheng, J., Higa, L.A., Minamino, N., Cooley, L., and Zhang, H. (2002). Control of DNA replication and chromosome ploidy by geminin and cyclin A. Mol Cell Biol *22*, 1868-1880.

Mimura, S., Seki, T., Tanaka, S., and Diffley, J.F. (2004). Phosphorylation-dependent binding of mitotic cyclins to Cdc6 contributes to DNA replication control. Nature *431*, 1118-1123.

Moll, T., Tebb, G., Surana, U., Robitsch, H., and Nasmyth, K. (1991). The role of phosphorylation and the CDC28 protein kinase in cell cycle-regulated nuclear import of the S. cerevisiae transcription factor SWI5. Cell *66*, 743-758.

Moyer, S.E., Lewis, P.W., and Botchan, M.R. (2006). Isolation of the Cdc45/Mcm2-7/GINS (CMG) complex, a candidate for the eukaryotic DNA replication fork helicase. Proc Natl Acad Sci U S A *103*, 10236-10241.

Muzi Falconi, M., Brown, G.W., and Kelly, T.J. (1996). cdc18+ regulates initiation of DNA replication in Schizosaccharomyces pombe. Proc Natl Acad Sci U S A *93*, 1566-1570.

Nguyen, V.Q., Co, C., Irie, K., and Li, J.J. (2000). Clb/Cdc28 kinases promote nuclear export of the replication initiator proteins Mcm2-7. Curr Biol *10*, 195-205.

Nguyen, V.Q., Co, C., and Li, J.J. (2001). Cyclin-dependent kinases prevent DNA re-replication through multiple mechanisms. Nature *411*, 1068-1073.

Nishitani, H., Lygerou, Z., and Nishimoto, T. (2004). Proteolysis of DNA replication licensing factor Cdt1 in S-phase is performed independently of geminin through its N-terminal region. J Biol Chem *279*, 30807-30816.

Nishitani, H., Lygerou, Z., Nishimoto, T., and Nurse, P. (2000). The Cdt1 protein is required to license DNA for replication in fission yeast. Nature *404*, 625-628.

Nishitani, H., and Nurse, P. (1995). p65cdc18 plays a major role controlling the initiation of DNA replication in fission yeast. Cell *83*, 397-405.

Nishitani, H., Sugimoto, N., Roukos, V., Nakanishi, Y., Saijo, M., Obuse, C., Tsurimoto, T., Nakayama, K.I., Nakayama, K., Fujita, M., Lygerou, Z., and Nishimoto, T. (2006). Two E3 ubiquitin ligases, SCF-Skp2 and DDB1-Cul4, target human Cdt1 for proteolysis. Embo J *25*, 1126-1136.

Pasero, P., Bensimon, A., and Schwob, E. (2002). Single-molecule analysis reveals clustering and epigenetic regulation of replication origins at the yeast rDNA locus. Genes Dev *16*, 2479-2484.

Perkins, G., Drury, L.S., and Diffley, J.F. (2001). Separate SCF(CDC4) recognition elements target Cdc6 for proteolysis in S phase and mitosis. Embo J *20*, 4836-4845.

Quinn, L.M., Herr, A., McGarry, T.J., and Richardson, H. (2001). The Drosophila Geminin homolog: roles for Geminin in limiting DNA replication, in anaphase and in neurogenesis. Genes Dev *15*, 2741-2754.

Raghuraman, M.K., Winzeler, E.A., Collingwood, D., Hunt, S., Wodicka, L., Conway, A., Lockhart, D.J., Davis, R.W., Brewer, B.J., and Fangman, W.L. (2001). Replication dynamics of the yeast genome. Science *294*, 115-121.

Randell, J.C., Bowers, J.L., Rodriguez, H.K., and Bell, S.P. (2006). Sequential ATP hydrolysis by Cdc6 and ORC directs loading of the Mcm2-7 helicase. Mol Cell *21*, 29-39.

Santocanale, C., and Diffley, J.F. (1996). ORC- and Cdc6-dependent complexes at active and inactive chromosomal replication origins in Saccharomyces cerevisiae. Embo J *15*, 6671-6679.

Santocanale, C., Sharma, K., and Diffley, J.F. (1999). Activation of dormant origins of DNA replication in budding yeast. Genes Dev *13*, 2360-2364.

Schwacha, A., and Bell, S.P. (2001). Interactions between two catalytically distinct MCM subgroups are essential for coordinated ATP hydrolysis and DNA replication. Mol Cell *8*, 1093-1104.

Schwob, E., and Nasmyth, K. (1993). CLB5 and CLB6, a new pair of B cyclins involved in DNA replication in Saccharomyces cerevisiae. Genes Dev *7*, 1160-1175.

Senga, T., Sivaprasad, U., Zhu, W., Park, J.H., Arias, E.E., Walter, J.C., and Dutta, A. (2006). PCNA is a cofactor for Cdt1 degradation by CUL4/DDB1-mediated N-terminal ubiquitination. J Biol Chem *281*, 6246-6252.

Tada, S., Li, A., Maiorano, D., Mechali, M., and Blow, J.J. (2001). Repression of origin assembly in metaphase depends on inhibition of RLF-B/Cdt1 by geminin. Nat Cell Biol *3*, 107-113.

Takayama, Y., Kamimura, Y., Okawa, M., Muramatsu, S., Sugino, A., and Araki, H. (2003). GINS, a novel multiprotein complex required for chromosomal DNA replication in budding yeast. Genes Dev *17*, 1153-1165.

Takeda, D.Y., Parvin, J.D., and Dutta, A. (2005). Degradation of Cdt1 during S phase is Skp2-independent and is required for efficient progression of mammalian cells through S phase. J Biol Chem *280*, 23416-23423.

Tanaka, S., and Diffley, J.F. (2002). Interdependent nuclear accumulation of budding yeast Cdt1 and Mcm2-7 during G1 phase. Nat Cell Biol *4*, 198-207.

Tanaka, S., Umemori, T., Hirai, K., Muramatsu, S., Kamimura, Y., and Araki, H. (2007). CDK-dependent phosphorylation of Sld2 and Sld3 initiates DNA replication in budding yeast. Nature *445*, 328-332.

Thomer, M., May, N.R., Aggarwal, B.D., Kwok, G., and Calvi, B.R. (2004). Drosophila double-parked is sufficient to induce re-replication during development and is regulated by cyclin E/CDK2. Development *131*, 4807-4818.

Vas, A., Mok, W., and Leatherwood, J. (2001). Control of DNA rereplication via Cdc2 phosphorylation sites in the origin recognition complex. Mol Cell Biol *21*, 5767-5777.

Vaziri, C., Saxena, S., Jeon, Y., Lee, C., Murata, K., Machida, Y., Wagle, N., Hwang, D.S., and Dutta, A. (2003). A p53-dependent checkpoint pathway prevents rereplication. Mol Cell *11*, 997-1008.

Waga, S., and Stillman, B. (1998). The DNA replication fork in eukaryotic cells. Annu Rev Biochem *67*, 721-751.

Wilmes, G.M., Archambault, V., Austin, R.J., Jacobson, M.D., Bell, S.P., and Cross, F.R. (2004). Interaction of the S-phase cyclin Clb5 with an "RXL" docking sequence in the initiator protein Orc6 provides an origin-localized replication control switch. Genes Dev *18*, 981-991.

Wohlschlegel, J.A., Dwyer, B.T., Dhar, S.K., Cvetic, C., Walter, J.C., and Dutta, A. (2000). Inhibition of eukaryotic DNA replication by geminin binding to Cdt1. Science *290*, 2309-2312.

Wyrick, J.J., Aparicio, J.G., Chen, T., Barnett, J.D., Jennings, E.G., Young, R.A., Bell, S.P., and Aparicio, O.M. (2001). Genome-wide distribution of ORC and MCM proteins in S. cerevisiae: high-resolution mapping of replication origins. Science *294*, 2357-2360.

Xu, W., Aparicio, J.G., Aparicio, O.M., and Tavare, S. (2006). Genome-wide mapping of ORC and Mcm2p binding sites on tiling arrays and identification of essential ARS consensus sequences in S. cerevisiae. BMC Genomics *7*, 276.

Yanagi, K., Mizuno, T., Tsuyama, T., Tada, S., Iida, Y., Sugimoto, A., Eki, T., Enomoto, T., and Hanaoka, F. (2005). Caenorhabditis elegans geminin homologue participates in cell cycle regulation and germ line development. J Biol Chem *280*, 19689-19694.

Yanow, S.K., Lygerou, Z., and Nurse, P. (2001). Expression of Cdc18/Cdc6 and Cdt1 during G2 phase induces initiation of DNA replication. Embo J *20*, 4648-4656.

Yoshida, K., Takisawa, H., and Kubota, Y. (2005). Intrinsic nuclear import activity of geminin is essential to prevent re-initiation of DNA replication in Xenopus eggs. Genes Cells *10*, 63-73.

Zegerman, P., and Diffley, J.F. (2007). Phosphorylation of Sld2 and Sld3 by cyclin-dependent kinases promotes DNA replication in budding yeast. Nature *445*, 281-285.

Zhu, W., Chen, Y., and Dutta, A. (2004). Rereplication by depletion of geminin is seen regardless of p53 status and activates a G2/M checkpoint. Mol Cell Biol *24*, 7140-7150.

Zhu, W., and Dutta, A. (2006). An ATR- and BRCA1-mediated Fanconi anemia pathway is required for activating the G2/M checkpoint and DNA damage repair upon rereplication. Mol Cell Biol *26*, 4601-4611.

Zou, L., and Stillman, B. (1998). Formation of a preinitiation complex by S-phase cyclin CDK-dependent loading of Cdc45p onto chromatin. Science *280*, 593-596.

Zou, L., and Stillman, B. (2000). Assembly of a complex containing Cdc45p, replication protein A, and Mcm2p at replication origins controlled by S-phase cyclin-dependent kinases and Cdc7p-Dbf4p kinase. Mol Cell Biol *20*, 3086-3096.

CHAPTER 2

Genome-wide mapping of DNA synthesis in *Saccharomyces cerevisiae* reveals that mechanisms preventing reinitiation of DNA replication are not redundant

ABSTRACT

To maintain genomic stability, re-initiation of eukaryotic DNA replication within a single cell cycle is blocked by multiple mechanisms that inactivate or remove replication proteins after G1 phase. Consistent with the prevailing notion that these mechanisms are redundant, we previously showed that simultaneous deregulation of three replication proteins, ORC, Cdc6 and Mcm2-7, was necessary to cause detectable bulk re-replication in G2/M phase in *Saccharomyces cerevisiae*. In this study, we used microarray comparative genomic hybridization (CGH) to provide a more comprehensive and detailed analysis of re-replication. This genome-wide analysis suggests that re-initiation in G2/M phase primarily occurs at a subset of both active and latent origins, but is independent of chromosomal determinants that specify the use and timing of these origins in S phase. We demonstrate that re-replication can be induced within S phase, but differs in amount and location from re-replication in G2/M phase, illustrating the dynamic nature of DNA replication controls. Finally, we show that very limited re-replication can be detected by microarray CGH when only two replication proteins are deregulated, suggesting that the mechanisms blocking re-replication are not redundant. Therefore we propose that eukaryotic re-replication at levels below current detection limits may be more prevalent and a greater source of genomic instability than previously appreciated.

INTRODUCTION

Eukaryotic cells must replicate each portion of their genome precisely once per cell cycle to faithfully transmit that genome to succeeding generations. This cell cycle control is enforced at the hundreds to thousands of replication origins where replication is initiated. As part of this regulation, cells must prohibit re-initiation within a single cell cycle at every origin for many successive generations. Even a small or occasional slip in this control will lead to re-replication, which can potentially compromise genome integrity. Hence, the block to re-initiation must be absolutely effective and reliable.

Studies from many labs have led to a model for the block to re-initiation that is based on the division of the initiation event into two mutually exclusive stages (reviewed in (Bell and Dutta, 2002; Diffley, 2004; Machida *et al.*, 2005)). In the first stage, which is restricted to G1 phase, potential origins are selected on chromosomal DNA by assembly of the Origin Recognition Complex (ORC), Cdc6, Cdt1, and the putative replicative helicase, Mcm2-7 into pre-replicative complexes (pre-RCs). In the second stage, which is restricted to S, G2, and M phases, potential origins are activated to initiate DNA replication by two kinases, a cyclin-dependent kinase (CDK) and Cdc7 kinase. Since CDK activity prevents pre-RC assembly in S, G2 and M phases and origins are not activated in G1 phase, passage through the cell cycle is coupled to exactly one round of replication.

Although this model provides a framework for understanding once and only once initiation, it does not explain how the block to re-initiation can be maintained with such high fidelity. This fidelity can be readily incorporated into the model if multiple overlapping mechanisms prevent pre-RC reassembly. In fact, multiple CDK-dependent

inhibitory mechanisms that target pre-RC components have been identified in a number of eukaryotic organisms. In budding and fission yeast, CDKs appear to down regulate ORC through inhibitory phosphorylation of Orc2 and/or Orc6 (Nguyen *et al.*, 2001; Vas *et al.*, 2001) as well as by direct binding to Orc6 (Wilmes *et al.*, 2004). Additionally, CDKs inhibit Cdc6 (or the *S. pombe* ortholog Cdc18) by promoting Cdc6/Cdc18 degradation (Drury *et al.*, 1997; Jallepalli *et al.*, 1997; Elsasser *et al.*, 1999; Drury *et al.*, 2000), by reducing *CDC6* transcription (Moll *et al.*, 1991), and by directly inhibiting Cdc6/Cdc18 through phosphorylation (Jallepalli *et al.*, 1997) or binding (Mimura *et al.*, 2004). Finally, CDKs also promote the nuclear exclusion of Mcm2-7 and Cdt1 in budding yeast (Labib *et al.*, 1999; Nguyen *et al.*, 2000; Tanaka and Diffley, 2002), in part by direct phosphorylation of Mcm3 (Liku *et al.*, 2005). In metazoans, CDKs have been implicated in Orc1 degradation, Cdt1 degradation and Cdc6 nuclear exclusion (reviewed in (Diffley, 2004)). In addition, metazoan cells have a CDK-independent mechanism involving the protein geminin, which binds to Cdt1 and can prevent it from recruiting Mcm2-7 during S, G2, and M phase (reviewed in (Blow and Dutta, 2005)).

Obtaining clear evidence of re-replication within a single cell cycle has generally required the simultaneous disruption of multiple mechanisms, leading to the presumption that these mechanisms are redundant (Diffley, 2004; Blow and Dutta, 2005). In budding yeast, for example, simultaneous deregulation of ORC phosphorylation, Mcm localization, and Cdc6 protein levels was needed to detect re-replication in G2/M phase (Nguyen *et al.*, 2001). Similarly, disruption of several regulatory mechanisms leads to re-replication in fission yeast (Gopalakrishnan *et al.*, 2001; Vas *et al.*, 2001; Yanow *et*

al., 2001) and in *Xenopus* replication extracts (McGarry and Kirschner, 1998; Arias and Walter, 2005; Li and Blow, 2005; Yoshida *et al.*, 2005).

In addition to the issue of mechanistic redundancy, the model for the block to re-replication makes predictions that are best examined by a genome-wide analysis of re-replication. First, the re-replication that is induced by deregulating pre-RC assembly should initiate from the potential replication origins used during normal replication. Re-initiation from a few origins has been observed by 2-dimensional gel electrophoresis in both budding (Nguyen *et al.*, 2001) and fission (Yanow *et al.*, 2001) yeast, but genome-wide mapping of re-initiation sites is needed to confirm this prediction. Second, deregulation of pre-RC reassembly should be able to induce re-replication throughout the period from S to M phase. Although Cdt1 overexpression has been shown to prolong S phase in *Drosophila* embryos (Thomer *et al.*, 2004), direct evidence for re-replication within S phase is still lacking. Finally, full deregulation of pre-RC reassembly should allow more than one round of re-initiation and result in rampant re-replication. So far, precise deregulation of replication proteins has led to at most a doubling of genomic DNA content, suggesting that additional inhibitory mechanisms remain to prevent re-replication. A more comprehensive analysis of where re-replication occurs in the genome may provide clues to how re-replication is still inhibited.

We have developed a more sensitive and comprehensive assay for re-replication by adapting and streamlining previously published microarray-based assays for analyzing DNA replication in budding yeast. With this assay we present evidence that re-initiation occurs primarily at a subset of the potential origins normally established for S phase without being strongly affected by the chromosomal determinants that specify the

efficiency and timing of these origins in S phase. Our studies suggest that the limited re-replication observed may be due in part to the fewer initiation sites used for re-replication compared to S phase. Additionally, our studies indicate that some of the mechanisms preventing re-replication in G2/M phase also operate in S phase but that the block to re-replication in these two phases is not identical. Finally, we demonstrate that re-initiation from as few as a single origin is detectable when fewer mechanisms are disrupted, consistent with the notion that these mechanisms are not redundant but are each actively maintaining the high fidelity of the block to re-replication.

MATERIALS AND METHODS

Plasmids and Strains

All plasmids are described in Table 1, all strains are described in Table 2 and all oligonucleotides are described in Table 3. Supplemental Methods contains detailed description of plasmid and strain construction.

Yeast media, growth and arrest

Cells were grown in YEP, synthetic complete (SC), or synthetic (S broth) medium (Guthrie and Fink, 1990) supplemented with 2% dextrose (wt/vol), 2% galactose (wt/vol), 3% raffinose (wt/vol), or 3% raffinose (wt/vol) + 0.05% dextrose (wt/vol). For S phase experiments cells were grown overnight in SDC (YJL5038) or SDC-Met,Ura (YJL3248 and YJL5834) and arrested in G1 phase with 50 ng/ml alpha factor (all strains were *bar1*) at 30˚C. Cells were released by filtering, washing, and then resuspending in

prewarmed 30˚C YEPD containing 100 µg/ml pronase, 100 mM hydroxyurea, and 15 µg/ml nocodazole.

To obtain reproducible induction of re-replication, cells were inoculated from a fresh unsaturated culture containing 2% dextrose into a culture containing 3% raffinose + 0.05% dextrose and grown for 12-15 h the night before the experiment. The *GAL1* promoter (*pGAL1*) was induced by addition of 2% galactose and the *MET3* promoter (*pMET3*) was repressed by the addition of 2 mM methionine. All experiments were performed at 30˚C except where noted. For induction of re-replication in G2/M phase, cells grown overnight in SRaffC-Met,Ura + 0.05% dextrose were pelleted and resuspended in YEPRaff + 2 mM methionine and 15 µg/ml nocodazole. Once arrested (>90% large budded cells), galactose was added to a final concentration of 2%. In experiments with strains containing *cdc7-1*, cells were grown and arrested at 23˚C. These cultures were split after arresting in G2/M phase and either kept at 23˚C or shifted to 35˚C for 1 hour followed by addition of 2% galactose to both cultures

For induction of re-replication during the release from G1 phase into a G2/M phase arrest, cells grown overnight in SRaffC-Met,Ura + 0.05% dextrose were arrested with 50 ng/ml alpha factor (all strains were *bar1*). Once arrested (>95% small budded cells), galactose was added to a final concentration of 2% for 30 minutes. Cells were released by filtering, washing, and then resuspending in prewarmed YEPGal + 2 mM methionine, 100 µg/ml pronase, and 15 µg/ml nocodazole. For the induction of re-replication during a release from G1 phase into S phase, cells arrested and released as described above were resuspended in prewarmed YEPGal + 2 mM methionine, 100 µg/ml pronase, and 100 mM hydroxyurea.

Flow cytometry

Cells were fixed and stained with 1 μM Sytox Green (Molecular Probes, Eugene, OR) as previously described (Haase and Lew, 1997).

Pulsed Field Gel Electrophoresis (PFGE)

PFGE was performed as described in Green *et al.* (Green and Li, 2005). Probes for *ARS305*, *ARS607* and *ARS1413* were prepared as described in Nguyen *et al.* (Nguyen *et al.*, 2001).

2-D Gel Electrophoresis

Neutral-neutral two-dimensional (2-D) gel analysis was performed essentially as described at http://fangman-brewer.genetics.washington.edu. The DNA preparation described there is a slight modification of the one used in Huberman *et al.* (Huberman *et al.*, 1987). Modifications to the previous protocols can be found in Supplemental Methods.

Microarray Assay

Microarrays containing 12,034 PCR products representing every ORF and intergenic region were prepared essentially as described (DeRisi *et al.*, 1997; Iyer *et al.*, 2001) (see Supplemental Methods). Genomic DNA was prepared, labeled and hybridized as described in Supplemental Methods.

Data analysis

Raw Cy5/Cy3 ratios from scanned arrays were normalized to the DNA content per cell based on the flow cytometry data to determine absolute copy number of each DNA segment. Raw values were then binned and smoothed using Fourier Convolution Smoothing essentially as described (Raghuraman *et al.*, 2001). Peaks in the replication profiles that were both prominent and reproducible among repetitions of an experiment were identified as origins. Details of data analysis (Supplemental Methods) and examples of raw data (Figure S1) are contained in Supplemental Information. The data discussed in this publication have been deposited in NCBI's Gene Expression Omnibus (GEO, http:://www.ncbi.nlm.nih.gov/geo/) and are accessible through GEO Series accession number GSE4181.

The "experiment variability" was determined using the equation for calculating one standard deviation. Since there were only two DNA preparations used, each of which was hybridized twice, the trials are not truly independent and thus we call these values "experiment variability" rather than standard deviation.

Scatter Plot

For each pro-ARS (Wyrick *et al.*, 2001), the normalized Cy5/Cy3 ratio of that chromosomal locus during replication or re-replication was determined and plotted. See Supplemental Methods for more details.

RESULTS

A simplified microarray CGH assay for DNA replication

We have adapted and streamlined existing microarray assays (Raghuraman *et al.*, 2001; Yabuki *et al.*, 2002) to create a rapid and economical genome-wide assay for yeast DNA replication. Our simplified assay uses comparative genomic hybridization (CGH) to directly measure the increase in DNA copy number arising from replication or re-replication. During S phase replication, the copy number of each DNA segment reflects the timing of its replication because the earlier a DNA segment replicates, the greater the proportion of replicating cells containing a duplication of this segment. Origins, which replicate earlier than neighboring regions, can be localized to chromosomal segments where the copy number reaches a local maxima. Thus, use of microarray CGH to monitor copy number changes across the genome can provide a comprehensive view of the location and efficiency/timing of initiation sites during replication and re-replication.

Figure 1A shows a schematic of our microarray CGH replication assay. Genomic DNA from replicating (or re-replicating) and non-replicating cells is purified and differentially labeled with Cy5 and Cy3. The labeled probes are competitively hybridized to a spotted microarray and the raw Cy5/Cy3 values are normalized such that the average ratio corresponds to the DNA content determined by flow cytometry. Data are smoothed and origins are computationally identified by locating prominent and reproducible peaks in smoothed replication profiles.

Before using the microarray CGH assay to study re-replication, we assessed its reproducibility and its ability to identify known replication origins in the S phase of a wild type S288c strain (flow cytometry data in Figure 1C). Figure 1B and Figure S2

show the mean of the smoothed S phase replication profiles from four hybridizations plus or minus the "experiment variability" (see Methods) for chromosome X. The small variability demonstrates that this technique is highly reproducible. An overlay of our replication profiles with those generated from previously published data (Raghuraman *et al.*, 2001; Yabuki *et al.*, 2002) shows considerable agreement in both peak positions, which reflects origin locations, and peak heights, which reflects origin timing/efficiency. When our peak finding algorithm was applied to our profiles, we obtained origin numbers (212) comparable to those obtained by Rhaguraman *et al.* (332) (Raghuraman *et al.*, 2001) and Yabuki *et al.* (260) (Yabuki *et al.*, 2002). Additionally, the alignment of peaks to origins systematically mapped by 2-D gel electrophoresis or ARS plasmid assay was similar to, or better than, published data (Table S1). Together, these data confirm that our streamlined assay is reproducible and accurate.

Re-replication competent mutant has a mostly normal S phase

We have previously demonstrated that simultaneous deregulation of three pre-RC components (ORC, Mcm2-7, and Cdc6) leads to limited re-replication in G2/M phase arrested cells (Nguyen *et al.*, 2001). These initiation proteins were deregulated by mutations that make the proteins refractory to CDK regulation. First, the CDK consensus phosphorylation sites of two subunits of the origin recognition complex, Orc2 and Orc6, were mutated, preventing Cdc28/Cdk1 phosphorylation of these subunits (*orc2-cdk6A, orc6-cdk4A*). Second, two copies of the SV40 nuclear localization signal were fused to *MCM7* (*MCM7-SVNLS*$_2$) to prevent the Cdc28/Cdk1 promoted net nuclear export of the Mcm2-7 complexes. Finally, an extra copy of *CDC6*, containing a partially stabilizing

N-terminal deletion, was placed under control of the galactose inducible promoter (*pGAL1-*Δ*ntcdc6*). This strain re-replicates when Δntcdc6 is induced by addition of galactose and will be referred to as the OMC re-replicating strain in reference to its deregulation of **O**RC, **M**cm2-7, and **C**dc6.

A major concern in any genetic analysis of replication control is the possibility that the mutations deregulating replication proteins also disrupt their replication activity. Such a nonspecific perturbation would complicate any interpretation of the resulting phenotype. We and others have previously reported that Δnt-cdc6 expressed under the *CDC6* promoter retains full replication initiation function (Drury *et al.*, 2000; Nguyen *et al.*, 2001). To determine whether the mutations deregulating Orc2, Orc6, and Mcm7 in the OMC strain also preserve their initiation function, we compared S phase of the OMC strain (*orc2-cdk6A orc6-cdk4A MCM7-2NLS pGAL1-*Δ*ntcdc6*), when re-replication was not induced, to S phase of the congenic wild-type A364a strain (*ORC2 ORC6 MCM7 pGAL1*). When cells were harvested at the same point in S phase (Figure 1E), the replication profiles for the two strains showed considerable overlap (Figures 1D, S3 and S4) although ORC and Mcm7 mutations cause subtle alterations in the initiation of DNA replication. Because two wild-type strains of different strain backgrounds show nearly identical replication profiles (Figures S5 and S6), we believe these differences reflect subtle alterations in the initiation activity of the mutant ORC and Mcm2-7. Nonetheless, we conclude that, overall, the mutant ORC and Mcm2-7 proteins in the OMC strain retain most of their normal initiation activity.

Mapping re-initiating origins

A key prediction of the current model for eukaryotic replication control is that pre-RC reassembly and re-initiation should only occur where pre-RCs normally assemble, i.e., the potential origins or pro-ARSs identified by Wyrick *et al.* (Wyrick *et al.*, 2001). In our previous characterization of re-replication induced at G2/M phase in the OMC strain (*orc2-cdk6A orc6-cdk4A MCM7-2NLS pGAL1-Δntcdc6*), we observed three active S phase origins re-initiating by 2-D gel-electrophoresis (Nguyen *et al.*, 2001). To comprehensively examine this prediction throughout the genome, we performed microarray CGH on the re-replicating DNA from OMC cells. This re-replicating DNA (flow cytometry in Figure 2A) was competitively hybridized against DNA from a congenic non-re-replicating strain that lacks the inducible Δntcdc6 and will be referred to as the OM strain (*orc2-cdk6A orc6-cdk4A MCM7-2NLS pGAL1*). Another source of non-re-replicating control DNA is OMC DNA from G1 phase cells, and when this was used, virtually identical results were obtained (data not shown).

The OMC G2/M phase re-replication profiles are shown in Figure 2B and Figure S7. These data confirm that the incomplete re-replication observed by flow cytometry is distributed over all sixteen chromosomes, as was first suggested by their limited entry into the gel during pulsed-field gel electrophoresis (PFGE) ((Nguyen *et al.*, 2001) and Figure 2C). The re-replication profiles also show that individual chromosomes re-replicate very unevenly, with some segments preferentially re-replicating more than others do.

Application of a peak finding algorithm to OMC re-replication profiles identified 106 re-initiating origins. Most of these origins appear to correspond to chromosomal loci

that form pre-RCs in G1 phase as more than 80% of the re-initiating origins map to within 10 kb of a pro-ARS identified by Wyrick *et al.* (Wyrick *et al.*, 2001) as sites of pre-RC binding. The mean distance between the OMC re-initiating origins and the closest Wyrick pro-ARS (Wyrick *et al.*, 2001) is 7.0 kb. This value is highly significant ($p < 5x10^{-8}$) when compared to the mean distances calculated for equivalent numbers of randomly selected chromosomal loci, as a value of 12.3 kb would be expected by chance (Figure S8).

In an accompanying manuscript, Tanny *et al*. (Tanny *et al.*, 2006) have analyzed the re-replication profile of a strain similar to our OMC strain containing the additional perturbation of a mutation of an RXL motif in ORC6 that abrogates CDK binding and results in a slightly increased extent of re-replication. Although both manuscripts use slightly different data analysis and presentation, (our profiles are presented to preserve absolute copy number information at the cost of less distinctive peaks) the re-replication profiles are strikingly similar (compare Figure S7 to Tanny *et al*. (Tanny *et al.*, 2006) Figure S2). Like our results, 80% of the 123 re-replication origins identified by Tanny *et al*. (Tanny *et al.*, 2006) are within 10kb of a Wyrick et al pro-ARS, further supporting the notion that re-replication occurs at normal sites of pre-RC formation. Overlap of origins identified in both studies is considerable, with 64% of the origins in this study within 10kb of an origin in Tanny *et al*. (Tanny *et al.*, 2006) (20% would be expected by chance). This overlap becomes even more striking, 80% overlap (expected value is also 20%), when the top 40 highest peaks in our analysis are compared to peaks identified in Tanny *et al*. (Tanny *et al.*, 2006). Together with our previous confirmation by 2-D gel electrophoresis that ARS305, ARS121, and ARS607 re-initiate (Nguyen *et al.*, 2001),

these genomic data suggest that re-initiation primarily occurs at a subset of potential S phase origins.

The efficiency with which these potential origins re-initiate in G2/M phase, however, does not correlate with the efficiency or timing with which they initiate in S phase. For example, only 38% of the active S phase origins re-initiate with enough efficiency to be identified as peaks during re-replication in G2/M phase. Moreover, some regions that normally replicate late in S phase, such as those near the telomeres of chromosome III, re-replicate very efficiently in G2/M phase, apparently from very inefficient or latent S phase origins in those regions. For a systematic comparison of re-replication efficiency versus replication timing of all potential S phase origins, we plotted the re-replication copy number versus the replication copy number for the set of pro-ARSs identified by Wyrick *et al.* (Wyrick *et al.*, 2001) (Figure 2D). The absence of any significant correlation (R^2 of 0.0002) indicates that the efficiency or timing of a replication origin in S phase does not determine its re-replication efficiency during G2/M phase.

Mechanisms that prevent re-replication at G2/M phase also act in S phase

The prevailing model for replication control depicts the prevention of re-replication in S, G2, and M phase as one continuous inhibitory period using a common strategy of preventing pre-RC reassembly. Since CDKs are active throughout this period, the model would predict that mechanisms used by CDKs to regulate replication proteins should prevent re-replication throughout S, G2, and M phase. To determine if CDK regulation of ORC, Mcm2-7, and Cdc6, which prevents re-replication within G2/M

phase, also prevents re-replication in S phase, we induced Δntcdc6 in OMC cells (*orc2-cdk6A orc6-cdk4A MCM7-2NLS pGAL1-Δntcdc6*) as they entered S phase.

OMC cells were arrested in G1 phase with alpha factor, and half the cells were harvested to obtain G1 phase DNA. The remaining cells were induced to express Δntcdc6 and then released from the G1 arrest into a low concentration of HU to delay their replication and allow us to collect them in S phase. Flow cytometry indicated that the released cells were harvested while still in S phase with a DNA content of 1.4 C (Figure 3A). The S phase and G1 phase DNA were competitively hybridized against the yeast genomic microarray to generate a combined replication/re-replication profile for S phase (Figure 3B and Figure S9).

Because normal S phase replication can account for an increase in DNA copy number from 1 to 2, only DNA synthesis beyond this copy number can be unequivocally attributed to re-replication. As seen in Figure 3B and Figure S9, many early origins acquired a DNA copy number greater than 2; in some cases reaching values greater than 3. In the same profiles other chromosomal regions had copy numbers significantly below 2, confirming that cells were indeed in the midst of S phase. In fact, early origins re-initiated while forks from their first round of replication were still progressing and before many late origins had fired. Similar re-replication profiles were observed for re-replicating cells synchronously harvested in S phase in the absence of hydroxyurea (data not shown). These findings thus directly establish that mechanisms used to prevent re-replication in G2/M phase also act within S phase.

Cell cycle position can affect the extent and location of re-replication

To determine if the block to re-replication is modulated during progression through the cell cycle, we compared the re-replication profile of OMC cells (*orc2-cdk6A orc6-cdk4A MCM7-2NLS pGAL1-Δntcdc6*) that were induced to re-replicate through a complete S phase with the profile associated with re-replication in G2/M phase. To obtain the former profile, both OMC and control OM cells (*orc2-cdk6A orc6-cdk4A MCM7-2NLS pGAL1*)) were arrested in G1 phase with alpha factor followed by addition of galactose to induce Δntcdc6 in the OMC strain. Cells were then released from the G1 arrest, allowed to proceed through S phase, and collected at a G2/M arrest 3 hours after the release. DNA prepared from the OMC and OM strains were competitively hybridized to our yeast genomic microarray to obtain a "G1 release" re-replication profile for the OMC cells.

Flow cytometry showed that both the re-replicating OMC and the control OM strain were in the middle of S phase 1 hour after the release (Figure 4A). As expected for actively replicating chromosomes (Hennessy and Botstein, 1991), the chromosomes of these strains were retained in the wells during PFGE (Figure 4B). Two hours after the release, S phase was mostly complete in the control OM strain and its chromosomes reentered the gel during PFGE. In the OMC strain, however, the induction of re-replication prevented chromosomes from reentering the PFGE gel at both 2 and 3 hr timepoints. Because significant re-replication could be induced in OMC cells delayed in S phase, we believe that re-replication during the progression through S phase contributed to the re-replication seen in the G1 release experiment.

Re-replication induced during G1 release of OMC cells was more extensive than re-replication induced in G2/M phase. Despite comparable lengths of induction, flow cytometry reproducibly indicated that the former accumulated a DNA content of 3.2 C while the latter accumulated only 2.7 C (compare 3h time points in Figure 4A to Figure 2A). More extensive re-replication could also be seen by comparing the re-replication profiles induced during the G1 release (Figure 4C and Figure S10) and the G2/M phase arrest (Figure 2B and Figure S7). In general the peaks in the G1 release profiles were taller than the G2/M phase profiles, suggesting that more efficient or more rounds of re-initiation can occur when re-replication is induced during S phase. For example, *ARS305* reached a copy number of 6.6, indicating it re-initiated a second time, as a single round can only generate a maximum copy number of 4. Overall, multiple rounds of re-initiation were observed on more than half of the chromosomes when re-replication was induced during the G1 release. In contrast, multiple rounds of re-initiation occurred at much fewer loci and to a lesser extent when re-replication was induced in G2/M phase.

A peak finding algorithm identified 87 potential re-initiation sites when re-replication was induced during the G1 release experiment. Of these, 85% were located within 10 kb of a Wyrick pro-ARS Wyrick *et al.* (Wyrick *et al.*, 2001). These data suggest that re-replication induced during a G1 release occurs from S phase origins of DNA replication.

In addition to the extent of re-replication, another significant difference between re-replication induced during the G1 release and re-replication induced during G2/M phase was their pattern of origin usage. As discussed above, efficiency of re-replication in G2/M phase was not correlated with origin usage during S phase. In contrast, the

efficiency of re-replication induced during the G1 release exhibited a modest positive correlation with S phase origin timing (Figure 4D). Although we cannot rule out an intrinsic difference in the re-initiation efficiency of early versus late origins when re-replication is induced during the G1 release, the simplest explanation for this correlation is that earlier replicating origins are cleared of pre-RCs earlier, making them available sooner for reassembly of pre-RCs and re-initiation within S phase.

Limited re-replication is detectable with fewer genetic perturbations

Our previous analysis of budding yeast re-replication failed to detect re-replication when only two pre-RC components were deregulated in G2/M phase (Nguyen *et al.*, 2001). This observation is frequently cited as evidence that eukaryotic replication controls are highly redundant. Both the increased sensitivity of the microarray CGH assay and the enhanced re-replication observed during a G1 release provided opportunities to reexamine whether these controls are indeed redundant in budding yeast.

As a first step, we examined an "OC" strain (*orc2-cdk6A orc6-cdk4A pGAL1-*Δ*ntcdc6*), in which only ORC and Cdc6 are deregulated and compared it to a control "O" strain (*orc2-cdk6A orc6-cdk4A GAL1*), where only ORC is deregulated. In accordance with our previous results (Nguyen *et al.*, 2001), induction of Δntcdc6 in G2/M phase generated no significant increase in DNA content by flow cytometry (Figure 5A) or chromosome immobilization during PFGE (Figure 5C). Similarly, microarray CGH of DNA prepared from the OC and O strains after three hours of galactose induction in G2/M phase detected no re-replication on fifteen out of sixteen chromosomes (Figure S11). However, limited re-replication could clearly be observed on both arms of

chromosome III (Figure 5E). Thus, the microarray CGH assay can detect re-replication missed by other assays.

We next asked whether we could detect more re-replication in the OC strain by inducing it during a G1 release. In contrast to the results obtained during a G2/M phase induction, significant re-replication was detected by flow cytometry and PFGE within 2 hours of the G1 release (Figure 5B and Figure 5D). The re-replication profile of the OC strain induced during a G1 release (Figure 5E and Figure S11) showed broad re-replication zones of approximately 200-500 kb in width on all chromosomes. These results, along with the re-replication induced during G2/M phase, establish that deregulating just ORC and Cdc6 is sufficient to induce re-replication and thus these inhibitory mechanisms are not truly redundant. The greater amount of re-replication induced during G1 release versus G2/M arrest underscores the dynamic character of the block to re-replication and, in this case, is likely due to the incomplete expulsion of Mcm proteins from the nucleus during S phase.

Microarray CGH can detect re-replication initiating primarily from a single origin

To further investigate the question of redundancy in replication control, we examined the consequences of deregulating just Mcm2-7 and Cdc6. We were not able to detect re-replication in the "MC" strain (*MCM7-2NLS pGAL1-*Δ*ntcdc6*) whether Δntcdc6 was induced in G2/M phase or during a G1 release (data not shown). Hence, we further deregulated Cdc6 inhibition by mutating the two full CDK consensus phosphorylation sites on Δntcdc6 to generate the MC_{2A} strain (*MCM7-2NLS* Δ*ntcdc6-cdk2A*). These additional mutations increase the stability of Δntcdc6 (Perkins *et al.*, 2001).

Expression of Δntcdc6-cdk2A in the MC_{2A} strain in either G2/M phase or during a G1 release did not cause a detectable increase in DNA content by flow cytometry (Figures 6A and 6B). However, PFGE suggested that chromosome III re-replicated in a small subset of MC_{2A} cells when Δntcdc6-cdk2A was induced under either protocol (Figure 6C and 6D). Microarray CGH provided definitive evidence that re-replication occurred, in this strain, primarily on the right arm of chromosome III (Figure 6E and Figure S12).

To confirm that the very limited DNA re-replication in the MC_{2A} strain arose from a canonical re-initiation event, we asked whether this re-replication depended on known origins and initiation proteins. Our peak finding algorithm implicated an initiation event at approximately 297 kb, close to *ARS317*, an inefficient S phase origin located at 291 kb. 2-dimensional gel analysis of *ARS317* (Figure 7A) detected bubble arcs, indicative of replication initiation, in the MC_{2A} strain but not the control "M" strain (*MCM7-2NLS pGAL1*). The immediately adjacent origins, *ARS316* and *ARS318*, only displayed fork arcs (data not shown), suggesting that most of the re-replication on the right arm of chromosome III originates from *ARS317*. Deletion of *ARS317*, but not *ARS316* or *ARS318*, in the MC_{2A} strain eliminated the bulk of the re-replication detected by microarray CGH (Figure 7B and data not shown), demonstrating that re-replication initiates primarily from a single S phase origin.

We next asked whether this re-replication is dependent on the essential initiation factor, Cdc7-Dbf4 kinase. Both MC_{2A} and MC_{2A} *cdc7-1* strains were induced to re-

replicate in G2/M phase under permissive (23 °C) and restrictive (35 °C) temperatures for the *cdc7-1* allele. Microarray CGH demonstrated that both strains re-replicated to a similar extent at 23ºC (Figure S13), but at 35 °C there was little or no re-replication in the MC_{2A} *cdc7-1* strain (Figure 7C). Together, the dependence on both *ARS317* and Cdc7-Dbf4 indicates that the very limited re-replication induced in the MC_{2A} strain arises primarily from a single *bona fide* re-initiation event.

DISCUSSION

Use of microarray CGH as a routine genome-wide assay for budding yeast replication.

We have refined previously published genome-wide replication assays for budding yeast and made them more amenable for routine and widespread use in the study of eukaryotic DNA replication. The previous assays required significant effort and cost to generate a single replication profile and were only used to characterize the normal wild-type S phase (Raghuraman *et al.*, 2001; Yabuki *et al.*, 2002). We have obtained comparable replication profiles using a streamlined protocol, collection of a single time point and inexpensive spotted microarrays. Thus, it is feasible to use our streamlined assay to examine the genome-wide replication phenotypes associated with many different genotypes or physiological conditions.

Re-initiation induced in G2/M phase largely follows the rules of origin selection, but not the rules of origin activation, that govern S phase replication.

We have taken advantage of our microarray CGH assay to perform a genome wide analysis of eukaryotic re-replication. This comprehensive analysis has allowed us to examine several key tenets of the current model for replication control. One important tenet is that re-initiation that arises from deregulation of ORC, Mcm2-7, and Cdc6 occur from sites of pre-RC formation in S phase. The overall concordance of mapped re-replication origins with pro-ARSs suggests that the re-initiation occurs at sites that normally assemble pre-RCs for S phase replication. Although current limitations of the resolution of microarray data prevent a precise match of replication and re-replication origins, in the few cases where this has been directly tested by 2-D gel electrophoresis or deletion analysis (Figure 7 and (Nguyen *et al.*, 2001)), we have confirmed that this is, in fact, the case. Thus, the sequence determinants that select potential origins in S phase appear to be conserved during re-replication.

In contrast to the selection of potential origins, the activation of these origins during re-replication in G2/M phase differs considerably from origin activation during replication in S phase. During S phase replication, poorly understood chromosomal determinant specify which potential origins are activated early, which are activated late, and which remain latent. During re-replication in G2/M phase, all three classes are among the 106 origins that re-initiate, and there is no correlation between the time/efficiency pro-ARSs replicate in S phase and the efficiency with which they re-replicate in G2/M phase. These results suggest that the chromosomal determinants governing S phase origin activation are not preserved during G2/M phase re-replication.

Such a conclusion is consistent with the finding that the temporal program for origin firing in S phase is lost by G2/M phase and must be reestablished upon entry into each new cell cycle (Raghuraman *et al.*, 1997).

The block to re-replication uses a common fundamental strategy implemented in a dynamic manner across the cell cycle

Another important tenet of the replication control model is that the blocks to re-replication in S, G2, and M phase use the same fundamental strategy of preventing pre-RC reassembly. Deregulating the mechanisms that prevent this reassembly in any of these cell cycle phases should thus lead to re-replication. Studies in human, *Drosophila* and *C. elegans* that deregulate geminin (Melixetian *et al.*, 2004), Cdt1 (Thomer *et al.*, 2004), and Cul-4 (which stabilizes Cdt1) (Zhong *et al.*, 2003), respectively, have inferred that re-replication can occur within S phase based on evidence of a prolonged S phase. In this study, we directly demonstrate that cells can re-initiate replication at multiple origins while the first round of replication is still ongoing. Thus, we establish that mechanisms used to prevent re-replication in G2/M phase also prevent re-replication within S phase.

Despite sharing common mechanisms to carry out the same fundamental strategy, the block to re-replication in S phase and G2/M phase are not identical. Two differences are readily apparent when comparing cells re-replicating through S phase during a G1 release with cells re-replicating at a G2/M phase arrest. The first difference is the bias toward re-initiation of early origins that is only observed in the G1 release experiment. The simplest explanation for this bias is suggested by the S phase re-replication profiles, which show re-initiation at early origins occurring before late origins have had a chance

to fire. These observations suggest that early origins clear their replication pre-RCs sooner and are more available for pre-RC reassembly during S phase, although other explanations for this bias cannot be ruled out.

The second difference between the G1 release and G2/M phase re-replication is that the amount of re-replication induced during the G1 release was greater than the amount induced in G2/M phase in both the OMC and OC strains. This difference can be observed by flow cytometry but is most striking when G1 release and G2/M phase re-replication profiles are compared. There are a growing number of examples of mechanisms that vary in their efficacy across the cell cycle, such as Cdc6 degradation in budding yeast (Perkins *et al.*, 2001), Cdt1 degradation in *Xenopus* and humans (Nishitani *et al.*, 2004; Arias and Walter, 2005; Li and Blow, 2005; Yoshida *et al.*, 2005), and geminin inhibition in human cells (Ballabeni *et al.*, 2004). Together these results indicate that the block to re-replication is dynamic with the number and relative contribution of regulatory mechanisms implementing the block changing during the cell cycle.

What is limiting re-replication?

A key difference between re-replication and replication in the OMC strain is that a significantly smaller number of origins initiate efficiently during re-replication (106 versus 193). This reduction in origin firing likely contributes to the limited re-replication observed in the OMC strain and suggests that additional mechanisms are still restraining re-initiation. Consistent with both notions, additional mechanisms inhibiting ORC (by CDK binding to Orc6 (Wilmes *et al.*, 2004)) and Cdc6 (by CDK binding to the N-terminus of phosphorylated Cdc6, (Mimura *et al.*, 2004)) have recently been identified in

budding yeast. The latter mechanism is already disrupted in the OMC strain because of the N-terminal deletion of Cdc6. Disrupting the former mechanism in the OMC background moderately enhances re-replication, but this re-replication is still restrained (Wilmes *et al.*, 2004; Tanny *et al.*, 2006), suggesting that still more re-replication controls remain to be identified.

The reduced number of re-initiating pro-ARSs, however, may not be the only factor limiting re-replication. Previous work suggests that a single replication fork should be able to replicate 100-200kb (Dershowitz and Newlon, 1993; van Brabant *et al.*, 2001). Our re-replicating profiles show that the amount of DNA synthesis associated with many re-initiating origins is significantly reduced 100-200 kb away from these origins (Figure S7). These data suggest that re-replicating forks may not be able to progress as far as replicating forks, although a more direct analysis of fork movement will be needed to confirm this hypothesis.

Multiple nonredundant mechanisms work in combination to reduce the probability of re-replication.

We previously showed that we could reliably detect G2/M phase re-replication by flow cytometry in the OMC strain when ORC, Mcm2-7, and Cdc6 are deregulated, but not when only two of the three proteins were deregulated (Nguyen *et al.*, 2001). Since then, there have been many other examples where multiple replication controls had to be disrupted to detect re-replication (reviewed in (Diffley, 2004; Blow and Dutta, 2005)). These observations have led to the presumption that the eukaryotic replication controls

are redundant. We favor an alternative view that replication controls are not redundant and that disruption of one or a few of controls can lead to low levels of re-replication.

Failure to detect this re-replication has been due to the insensitivity of standard replication assays. In support of the view, the more sensitive microarray CGH assay used in this study was able to detect G2/M phase re-replication in the OC and MC_{2A} strains. We did not detect re-replication when only a single mechanism was disrupted, but we note that the microarray CGH assay has its own detection limits and may have difficulty detecting rare or sporadic replication events. The development of even more sensitive single-cell assays that can detect these rare re-replication events may reveal that the chance of re-replication occuring is increased when ORC, Mcm2-7, or Cdc6 is individually deregulated.

Our findings support a model in which the block to re-replication is provided by a patchwork of many mechanisms, each of which contributes to a portion of the block by reducing the probability that re-replication will occur within a cell cycle. The combined action of all these mechanisms is needed to reduce the probability to such low levels that re-replication events become exceedingly rare and virtually prohibited. Successive disruption of these mechanisms does not lead to a sudden collapse of the block after a threshold of deregulation is reached, but instead results in a gradual erosion of the block manifested by incrementally higher frequencies and/or levels of limited re-replication. Because all mechanisms contribute in some way to the block, more than one mechanism or combination of mechanisms can be overridden to generate detectable re-replication. Hence, the fact that disruption of a mechanism is sufficient to induce limited re-

replication does not make it the critical or dominant mechanism in the block to re-replication.

Levels of re-replication likely to contribute to genomic instability and tumorigenesis may not be detectable by most currently available assays.

Because genomic instability is associated with, and possibly facilitates, tumorigenesis, there has been much interest in understanding the derangements in DNA metabolism and cell cycle control that can cause genomic instability. Re-replication is a potential source of genomic instability both because it produces extra copies of chromosomal segments and because it generates DNA damage and/or replication stress (Melixetian *et al.*, 2004; Zhu *et al.*, 2004; Archambault *et al.*, 2005; Green and Li, 2005). Re-replication has also been potentially linked to tumorigenesis by the observation that overexpression of Cdt1, which can contribute to re-replication (reviewed in (Blow and Dutta, 2005)), can transform NIH3T3 into tumorigenic cells (Arentson *et al.*, 2002). However, two considerations have raised concerns about the biological relevance of these potential connections. First, if replication controls are highly redundant, the probability that a cell will spontaneously acquire the multiple disruptions needed to induce re-replicate will be extremely small. Second, we and others have shown that cells undergoing overt re-replication experience extensive inviability (Jallepalli *et al.*, 1997; Yanow *et al.*, 2001; Wilmes *et al.*, 2004; Green and Li, 2005) or apoptosis (Vaziri *et al.*, 2003; Thomer *et al.*, 2004), making cell death a more likely outcome than genomic instability or tumorigenesis.

Our results in this study counter the first concern by challenging the concept of redundancy in replication control and showing that very low levels of re-replication can still be observed when fewer controls are disrupted. We also have evidence that lower levels of re-replication induce lower levels of inviability (data not shown), diminishing the second concern. Consequently, we suggest that re-replication at levels well below current detection limits may occur with greater frequency than previously anticipated and that genomic instability may arise from these low, non-lethal levels of re-replication.

ACKNOWLEDGEMENTS

We thank Adam Carroll, Emily Wang and Marian Tse for assistance in constructing the microarrays. We thank Hiten Madhani, Bruce Alberts, David Morgan, and David Toczyski for helpful discussions and comments on the manuscript and Steve Bell for discussion of results before publication. This work was supported by grants to J.J.L. from the Sandler Program in Biological Sciences, the ACS (RPG-99-169-01-CCG) and the NIH (RO1 GM59704). B.R.M. was supported by an NSF Predoctoral Fellowship (DGE-0202754) and a DOD Breast Cancer Predoctoral Fellowship (W81XWH-04-1-0409). R.J.M. was supported by an NIH Genetics and Cell Biology Training Grant (T32 GM07810).

REFERENCES

Archambault, V., Ikui, A.E., Drapkin, B.J., and Cross, F.R. (2005). Disruption of mechanisms that prevent rereplication triggers a DNA damage response. Mol Cell Biol *25*, 6707-6721.

Arentson, E., Faloon, P., Seo, J., Moon, E., Studts, J.M., Fremont, D.H., and Choi, K. (2002). Oncogenic potential of the DNA replication licensing protein CDT1. Oncogene *21*, 1150-1158.

Arias, E.E., and Walter, J.C. (2005). Replication-dependent destruction of Cdt1 limits DNA replication to a single round per cell cycle in Xenopus egg extracts. Genes Dev *19*, 114-126.

Balakrishnan, R., Christie, K. R., Costanzo, M. C., Dolinski, K., Dwight, S. S., Engel, S. R., Fisk, D. G., Hirschman, J. E., Hong, E. L., Nash, R., Oughtred, R., Skrzypek, M., Theesfeld, C. L., Binkley, G., Lane, C., Schroeder, M., Sethuraman, A., Dong, S., Weng, S., Miyasato, S., Andrada, R., Botstein, D., and Cherry, J. M. "Saccharomyces Genome Database".

Ballabeni, A., Melixetian, M., Zamponi, R., Masiero, L., Marinoni, F., and Helin, K. (2004). Human geminin promotes pre-RC formation and DNA replication by stabilizing CDT1 in mitosis. Embo J *23*, 3122-3132.

Bell, S.P., and Dutta, A. (2002). DNA replication in eukaryotic cells. Annu Rev Biochem *71*, 333-374.

Blow, J.J., and Dutta, A. (2005). Preventing re-replication of chromosomal DNA. Nat Rev Mol Cell Biol *6*, 476-486.

DeRisi, J.L., Iyer, V.R., and Brown, P.O. (1997). Exploring the metabolic and genetic control of gene expression on a genomic scale. Science *278*, 680-686.

Dershowitz, A., and Newlon, C.S. (1993). The effect on chromosome stability of deleting replication origins. Mol Cell Biol *13*, 391-398.

Diffley, J.F. (2004). Regulation of early events in chromosome replication. Curr Biol *14*, R778-786.

Drury, L.S., Perkins, G., and Diffley, J.F. (1997). The Cdc4/34/53 pathway targets Cdc6p for proteolysis in budding yeast. Embo J *16*, 5966-5976.

Drury, L.S., Perkins, G., and Diffley, J.F. (2000). The cyclin-dependent kinase Cdc28p regulates distinct modes of Cdc6p proteolysis during the budding yeast cell cycle. Curr Biol *10*, 231-240.

Elsasser, S., Chi, Y., Yang, P., and Campbell, J.L. (1999). Phosphorylation controls timing of Cdc6p destruction: A biochemical analysis. Mol Biol Cell *10*, 3263-3277.

Gopalakrishnan, V., Simancek, P., Houchens, C., Snaith, H.A., Frattini, M.G., Sazer, S., and Kelly, T.J. (2001). Redundant control of rereplication in fission yeast. Proc Natl Acad Sci U S A *98*, 13114-13119.

Green, B.M., and Li, J.J. (2005). Loss of rereplication control in Saccharomyces cerevisiae results in extensive DNA damage. Mol Biol Cell *16*, 421-432.

Guthrie, C., and Fink, G. (eds.) (1990). Guide to Yeast Genetics and Molecular Biology. Academic Press.

Haase, S.B., and Lew, D.J. (1997). Flow cytometric analysis of DNA content in budding yeast. Methods Enzymol *283*, 322-332.

Hennessy, K.M., and Botstein, D. (1991). Regulation of DNA replication during the yeast cell cycle. Cold Spring Harb Symp Quant Biol *56*, 279-284.

Huberman, J.A., Spotila, L.D., Nawotka, K.A., el-Assouli, S.M., and Davis, L.R. (1987). The in vivo replication origin of the yeast 2 microns plasmid. Cell *51*, 473-481.

Iyer, V.R., Horak, C.E., Scafe, C.S., Botstein, D., Snyder, M., and Brown, P.O. (2001). Genomic binding sites of the yeast cell-cycle transcription factors SBF and MBF. Nature *409*, 533-538.

Jallepalli, P.V., Brown, G.W., Muzi-Falconi, M., Tien, D., and Kelly, T.J. (1997). Regulation of the replication initiator protein p65cdc18 by CDK phosphorylation. Genes Dev *11*, 2767-2779.

Labib, K., Diffley, J.F., and Kearsey, S.E. (1999). G1-phase and B-type cyclins exclude the DNA-replication factor Mcm4 from the nucleus. Nat Cell Biol *1*, 415-422.

Li, A., and Blow, J.J. (2005). Cdt1 downregulation by proteolysis and geminin inhibition prevents DNA re-replication in Xenopus. Embo J *24*, 395-404.

Liku, M.E., Nguyen, V.Q., Rosales, A.W., Irie, K., and Li, J.J. (2005). CDK Phosphorylation of a Novel NLS-NES Module Distributed between Two Subunits of the Mcm2-7 Complex Prevents Chromosomal Rereplication. Mol Biol Cell *16*, 5026-5039.

Machida, Y.J., Hamlin, J.L., and Dutta, A. (2005). Right place, right time, and only once: replication initiation in metazoans. Cell *123*, 13-24.

McGarry, T.J., and Kirschner, M.W. (1998). Geminin, an inhibitor of DNA replication, is degraded during mitosis. Cell *93*, 1043-1053.

Melixetian, M., Ballabeni, A., Masiero, L., Gasparini, P., Zamponi, R., Bartek, J., Lukas, J., and Helin, K. (2004). Loss of Geminin induces rereplication in the presence of functional p53. J Cell Biol *165*, 473-482.

Mimura, S., Seki, T., Tanaka, S., and Diffley, J.F. (2004). Phosphorylation-dependent binding of mitotic cyclins to Cdc6 contributes to DNA replication control. Nature *431*, 1118-1123.

Moll, T., Tebb, G., Surana, U., Robitsch, H., and Nasmyth, K. (1991). The role of phosphorylation and the CDC28 protein kinase in cell cycle-regulated nuclear import of the S. cerevisiae transcription factor SWI5. Cell *66*, 743-758.

Nguyen, V.Q., Co, C., Irie, K., and Li, J.J. (2000). Clb/Cdc28 kinases promote nuclear export of the replication initiator proteins Mcm2-7. Curr Biol *10*, 195-205.

Nguyen, V.Q., Co, C., and Li, J.J. (2001). Cyclin-dependent kinases prevent DNA re-replication through multiple mechanisms. Nature *411*, 1068-1073.

Nishitani, H., Lygerou, Z., and Nishimoto, T. (2004). Proteolysis of DNA replication licensing factor Cdt1 in S-phase is performed independently of geminin through its N-terminal region. J Biol Chem *279*, 30807-30816.

Perkins, G., Drury, L.S., and Diffley, J.F. (2001). Separate SCF(CDC4) recognition elements target Cdc6 for proteolysis in S phase and mitosis. Embo J *20*, 4836-4845.

Raghuraman, M.K., Brewer, B.J., and Fangman, W.L. (1997). Cell cycle-dependent establishment of a late replication program. Science *276*, 806-809.

Raghuraman, M.K., Winzeler, E.A., Collingwood, D., Hunt, S., Wodicka, L., Conway, A., Lockhart, D.J., Davis, R.W., Brewer, B.J., and Fangman, W.L. (2001). Replication dynamics of the yeast genome. Science *294*, 115-121.

Tanaka, S., and Diffley, J.F. (2002). Interdependent nuclear accumulation of budding yeast Cdt1 and Mcm2-7 during G1 phase. Nat Cell Biol *4*, 198-207.

Tanny, R.E., MacAlpine, D.M., Blitzblau, H.G., and Bell, S.P. (2006). Genome-wide Analysis of Re-replication Reveals Inhibitory Controls that Target Multiple Stages of Replication Initiation. Mol Biol Cell, (under review).

Thomer, M., May, N.R., Aggarwal, B.D., Kwok, G., and Calvi, B.R. (2004). Drosophila double-parked is sufficient to induce re-replication during development and is regulated by cyclin E/CDK2. Development *131*, 4807-4818.

van Brabant, A.J., Buchanan, C.D., Charboneau, E., Fangman, W.L., and Brewer, B.J. (2001). An origin-deficient yeast artificial chromosome triggers a cell cycle checkpoint. Mol Cell *7*, 705-713.

Vas, A., Mok, W., and Leatherwood, J. (2001). Control of DNA rereplication via Cdc2 phosphorylation sites in the origin recognition complex. Mol Cell Biol *21*, 5767-5777.

Vaziri, C., Saxena, S., Jeon, Y., Lee, C., Murata, K., Machida, Y., Wagle, N., Hwang, D.S., and Dutta, A. (2003). A p53-dependent checkpoint pathway prevents rereplication. Mol Cell *11*, 997-1008.

Wilmes, G.M., Archambault, V., Austin, R.J., Jacobson, M.D., Bell, S.P., and Cross, F.R. (2004). Interaction of the S-phase cyclin Clb5 with an "RXL" docking sequence in the initiator protein Orc6 provides an origin-localized replication control switch. Genes Dev *18*, 981-991.

Wyrick, J.J., Aparicio, J.G., Chen, T., Barnett, J.D., Jennings, E.G., Young, R.A., Bell, S.P., and Aparicio, O.M. (2001). Genome-wide distribution of ORC and MCM proteins in S. cerevisiae: high-resolution mapping of replication origins. Science *294*, 2357-2360.

Yabuki, N., Terashima, H., and Kitada, K. (2002). Mapping of early firing origins on a replication profile of budding yeast. Genes Cells *7*, 781-789.

Yanow, S.K., Lygerou, Z., and Nurse, P. (2001). Expression of Cdc18/Cdc6 and Cdt1 during G2 phase induces initiation of DNA replication. Embo J *20*, 4648-4656.

Yoshida, K., Takisawa, H., and Kubota, Y. (2005). Intrinsic nuclear import activity of geminin is essential to prevent re-initiation of DNA replication in Xenopus eggs. Genes Cells *10*, 63-73.

Zhong, W., Feng, H., Santiago, F.E., and Kipreos, E.T. (2003). CUL-4 ubiquitin ligase maintains genome stability by restraining DNA-replication licensing. Nature *423*, 885-889.

Zhu, W., Chen, Y., and Dutta, A. (2004). Rereplication by depletion of geminin is seen regardless of p53 status and activates a G2/M checkpoint. Mol Cell Biol *24*, 7140-7150.

Table 1. Plasmids used in this study

Plasmid	Key Features	Source
pJL737	*ORC6 URA3*	Nguyen *et al.* 2001
pJL806	*pGAL1 URA3*	Nguyen *et al.* 2001
pJL1206	*MCM7-(NLS)2 URA3*	Nguyen *et al.* 2001
pJL1488	*pGAL1-Δntcdc6-cdk2A URA3*	This study
pJL1489	*pGAL1-Δntcdc6 URA3*	Nguyen *et al.* 2001
pKI1260	*MCM7-(svnls3A)2 URA3*	Nguyen *et al.* 2001
pMP933	*ORC2 URA3*	Nguyen *et al.* 2001
YIp22	*pMET3-HA3-CDC20 TRP1*	Uhlmann *et al.* 2000
pFA6a	*KanMX6*	Wach *et al.* 1994
pAG25	*NatMX4*	Goldstein *et al.* 1999
pPP117	*cdc7-1 URA3*	Hollingsworth *et al.* 1992

Table 2. Strains used in this study

Strain	Genotype	Source
YJL310	*leu2-3,112 ura3-52 trp1-289 bar1Δ::LEU2*	Detweiter and Li 1998
YJL3244	*orc2-cdk6A orc6-cdk4A leu2 ura3-52::{pGAL1, URA3} trp1-289 ade2 ade3 MCM7-2NLS bar1Δ::LEU2 cdc20::{pMET3-HA3-CDC20, TRP1}*	Nguyen *et al.* 2001
YJL3248	*orc2-cdk6A orc6-cdk4A ura3-52::{pGAL1-Δntcdc6, URA3} trp1-289 leu2 ade2 ade3 MCM7-2NLS bar1Δ::LEU2 cdc20::{pMET3-HA3-CDC20, TRP1}*	Nguyen *et al.* 2001
YJL3249	*orc2-cdk6A orc6-cdk4A ura3-52::{pGAL1-Δntcdc6, URA3} trp1-289 leu2 ade2 ade3 MCM7-2NLS bar1Δ::LEU2 cdc20::{pMET3-HA3-CDC20, TRP1}*	This study
YJL4486	*ORC2 ORC6 leu2 ura3-52::{pGAL1, URA3} trp1-289 ade2 ade3 MCM7-2NLS bar1Δ::LEU2 cdc20::{pMET3-HA3-CDC20, TRP1}*	This study
YJL4489	*ORC2 ORC6 ura3-52::{pGAL1-Δntcdc6-cdk2A, URA3} trp1-289 leu2 ade2 ade3 MCM7-2NLS bar1Δ::LEU2 cdc20::{pMET3-HA3-CDC20, TRP1}*	This study
YJL4832	*orc2-cdk6A orc6-cdk4A ura3-52::{pGAL1, URA3} trp1-289 leu2 ade2 ade3 MCM7-2nls3A bar1Δ::LEU2*	This study

	cdc20::{pMET3-HA3-CDC20, TRP1}	
YJL3240	*orc2-cdk6A orc6-cdk4A ura3-52::{pGAL1-Δntcdc6, URA3} trp1-289 leu2 ade2 ade3 MCM7-2nls3A bar1Δ::LEU2 cdc20::{pMET3-HA3-CDC20, TRP1}*	This study
YJL5038	*his3Δ::KanMX leu2Δ0 met15Δ0 ura3Δ0 bar1Δ::NatMX4 can1Δ::pMFA1-HIS3::pMFα1-LEU2*	This study
YJL5493	*orc2-cdk6A orc6-cdk4A leu2 ura3-52::{pGAL1, URA3} trp1-289 ade2 ade3 MCM7-2NLS bar1Δ::LEU2 cdc20::{pMET3-HA3-CDC20, TRP1}*	This study
YJL5834	*ORC2 ORC6 leu2 ura3-52::{pGAL1, URA3} trp1-289 ade2 ade3 MCM7 bar1::LEU2*	This study
YJL5787	*ORC2 ORC6 ura3-52::{pGAL1-Δntcdc6-cdk2A, URA3} trp1-289 leu2 ade2 ade3 MCM7-2NLS bar1Δ::LEU2 cdc20::{pMET3-HA3-CDC20, TRP1} Δars316::KanMX6*	This study
YJL5858	*ORC2 ORC6 ura3-52::{pGAL1-Δntcdc6-cdk2A, URA3} trp1-289 leu2 ade2 ade3 MCM7-2NLS bar1Δ::LEU2 cdc20::{pMET3-HA3-CDC20, TRP1} Δars317::KanMX6*	This study
YJL5861	*ORC2 ORC6 ura3-52::{pGAL1-Δntcdc6-cdk2A, URA3} trp1-289 leu2 ade2 ade3 MCM7-2NLS bar1Δ::LEU2 cdc20::{pMET3-HA3-CDC20, TRP1} Δars318::KanMX4*	This study

YJL5816	*ORC2 ORC6 leu2 ura3-52::{pGAL1, URA3} trp1-289 ade2 ade3 MCM7-2NLS bar1Δ::LEU2 cdc20::{pMET3-HA3-CDC20, TRP1} cdc7-1*	This study
YJL5822	*ORC2 ORC6 ura3-52::{pGAL1-Δntcdc6-cdk2A, URA3} trp1-289 leu2 ade2 ade3 MCM7-2NLS bar1Δ::LEU2 cdc20::{pMET3-HA3-CDC20, TRP1} cdc7-1*	This study

Table 3. Oligonucleotides used in this study

Oligo	Purpose	Sequence
OJL1596	Δ*ARS316*	5'-TTAACTGACAATTCTTTTGAACAAAATTTAC ACTTCATCAAGAAAGATGCCGGATCCCCGGGT TAATTAA-3'
OJL1597	Δ*ARS316*	5'-TGATGACGAAGGATTCGTTGAAGTTGAAT GCACACAAAAAAAGCTTGATACATCGATGAAT TCGAGCTCG-3'
OJL1639	Δ*ARS317*	5'-ATTAAACAATGTTTGATTTTTTAAATCGCA ATTTAATACCCGGATCCCCGGGTTAATTAA-3'
OJL1640	Δ*ARS317*	5'-ATTTTTATGGAAGATTAAGCTCATAACTTG GACGGGGATCCATCGATGAATTCGAGCTCG-3'
OJL1641	Δ*ARS318*	5'-CGATAAAGTTATTATTTAGATTACATGTCA CCAACATTTTCGGATCCCCGGGTTAATTAA-3'
OJL1642	Δ*ARS318*	5'-AGAGAAAATAGCTATTTACCTCAACATTTA AAGGTATTAACATCGATGAATTCGAGCTCG-3'
OJL1607	*ARS317 probe*	5'-ATCGATTATCTGTTTGGCAGG-3'
OJL1608	*ARS317 probe*	5'-GAATTCAAAGAAGTCAATCTTATG-3'
OJL1452	*bar1*Δ	5'-ATTAAAAATGACTATATATTTGATATTTAT ATGCTATAAAGAAATTGTACTCCAGATTTCCAT

		CGATGAATTCGAGCTCG-3'
OJL1454	*bar1*Δ	5’-AGTGGTTCGTATCGCCTAAAATCATACCA AAATAAAAAGAGTGTCTAGAAGGGTCATATAC GGATCCCCGGGTTAATTAA-3'

Figure 1 Use of comparative genomic hybridization (CGH) on spotted microarrays to assay DNA replication.

A) Schematic representation of the CGH replication assay. Genomic DNA is purified from non-replicating and replicating cells, differentially labeled with Cy3 and Cy5, and competitively hybridized to a microarray containing 12,034 ORF and intergenic PCR products. Cy5/Cy3 ratios are normalized so that the average ratio of all elements equals the DNA content of the cells (as determined by flow cytometry). Normalized ratios are plotted against chromosomal position and mathematically smoothed to generate a replication profile. In most cases, two hybridizations are performed from each of two independent experiments. The resulting four replication profiles are averaged into one composite profile, and the locations of origins are identified using a peak finding algorithm. Chromosomal regions lacking data of sufficient quality are represented as gaps in the profiles.

B) CGH replication assay described for Figure 1A was performed on YJL5038**,** a wild-type yeast strain in the S288c background. G1 phase genomic DNA was hybridized against S phase genomic DNA obtained 120 min after cells were released from G1 phase into media containing hydroxyurea (HU). The composite replication profile (blue line) plus and minus the "experiment variability" (light gray band, see Methods) is shown for Chromosome X. Positions of origins annotated in the Saccharomyces Genome Database (SGD, (Balakrishnan)) (red triangles) and the centromere (black circle) are marked along the X-axis. Replication profiles derived from Raghuraman *et al.* (Raghuraman *et al.*, 2001) (violet line) and Yabuki *et al.* (Yabuki *et al.*, 2002) (orange line) are shown for comparison.

C) S phase progression assayed by flow cytometry for experiment described in Figure 1B at the indicated times following release from G1 phase. DNA content of 1.4 C was used to normalize the S288c replication profile.

D) The S phase replication profile of the re-replication competent OMC strain and the congenic wild-type strain are similar. S phase replication profiles were generated for the OMC strain YJL3248 (*MCM7-2NLS orc2-cdk6A orc6-cdk4A pGAL1-*Δ*ntcdc6 pMET3-HA3-CDC20*) and a congenic wild-type A364a strain YJL5834 (*pGAL1*) essentially as described in Figure 1B except S phase cells were harvested, respectively, at 135 min and 180 min after alpha factor release. The S phase replication profile for the OMC strain (green line) and the A364a strain (black line) for chromosome X is shown. SGD annotated origins (red triangles) and the centromere (black circle) are marked along the X-axis.

E) S phase progression assayed by flow cytometry for experiment described in Figure 1D at the indicated times following release from G1 phase. DNA contents of 1.35 C and 1.4 C, respectively, were used to normalize the OMC and A364a replication profiles.

Figure 1

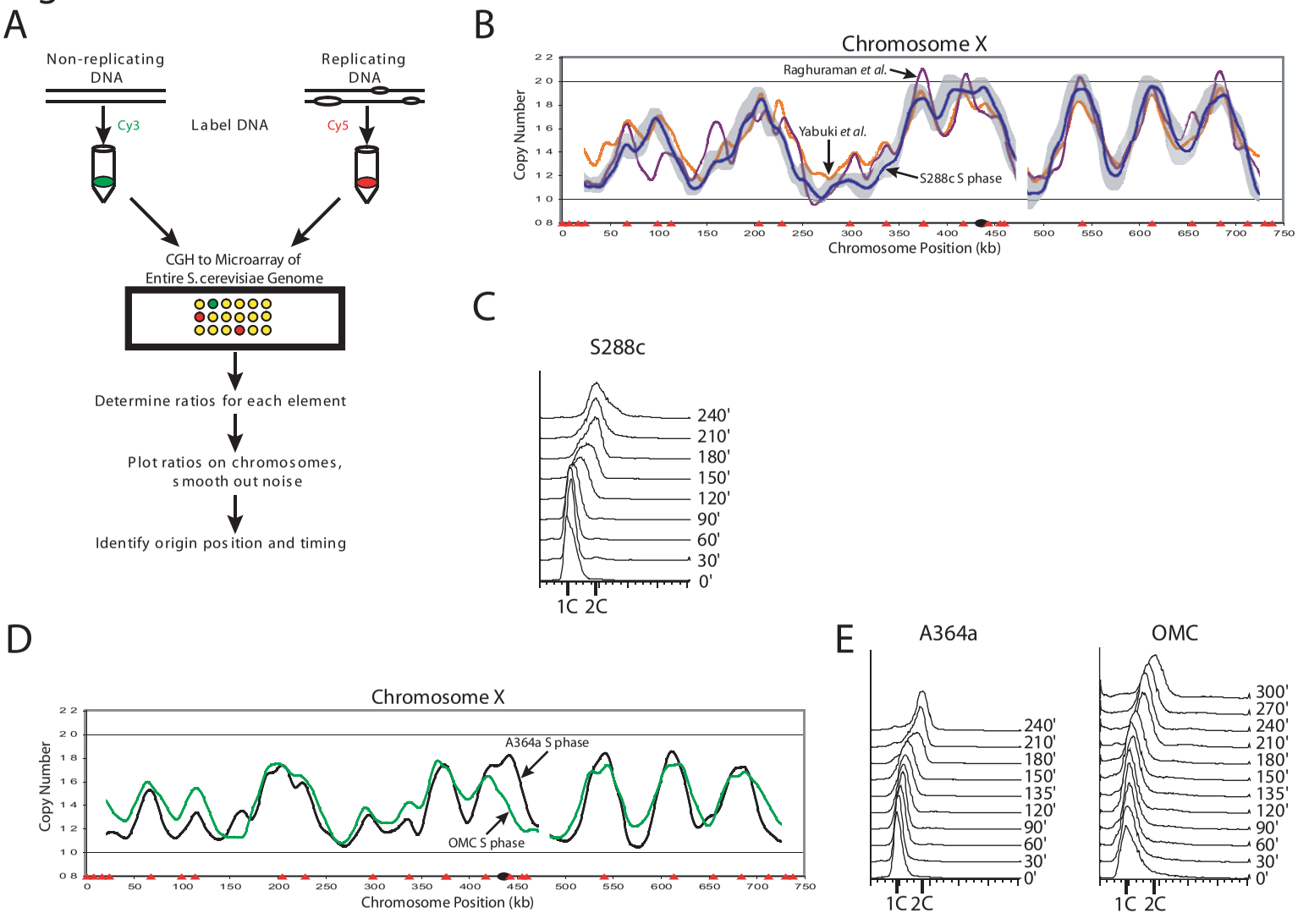
A
Non-replicating DNA
Replicating DNA
Cy3
Label DNA
Cy5
CGH to Microarray of Entire S. cerevisiae Genome
Determine ratios for each element
Plot ratios on chromosomes, smooth out noise
Identify origin position and timing
B
Chromosome X
Raghuraman et al.
Yabuki et al.
S288c S phase
Copy Number
Chromosome Position (kb)
C
S288c
240'
210'
180'
150'
120'
90'
60'
30'
0'
1C 2C
D
Chromosome X
A364a S phase
OMC S phase
Copy Number
Chromosome Position (kb)
E
A364a
OMC
240'
210'
180'
150'
135'
120'
90'
60'
30'
0'
300'
270'
1C 2C

Figure 2 Re-replication induced during G2/M phase when ORC, Mcm2-7 and Cdc6 are deregulated.

A) G2/M phase re-replication in the OMC strain is readily detectable by flow cytometry. The OMC strain YJL3248 (*orc2-cdk6A orc6-cdk4A MCM7-2NLS pGAL1-Δntcdc6 pMET3-HA3-CDC20)* and the control OM strain YJL3244 (*orc2-cdk6A orc6-cdk4A MCM7-2NLS pGAL1 pMET3-HA3-CDC20*) were arrested in G2/M phase. Once arrested, galactose was added, which induced re-replication in the OMC strain. Samples were taken for flow cytometry at the indicated points after galactose addition. The DNA content of 2.7 C at 3 hr was used to normalize the OMC re-replication profile in Figure 2B.

B) Genomic DNA was purified from the OMC strain and the control OM strain after 3 hr of galactose induction as described in Figure 2A and competitively hybridized against each other as described in Figure 1A. The OMC G2/M phase re-replication profiles (black lines, right axis), the OMC S phase replication profiles replotted from Figure 1D (gray lines, left axis), locations of pro-ARSs mapped by Wyrick *et al.* (Wyrick *et al.*, 2001) (gray triangles) and the centromeres (black circles) are shown for chromosomes III, VI, and XIV.

C) Each chromosome participates when OMC cells are induced to re-replicate in G2/M phase. The OMC strain and the control OM strain from the experiment presented in Figure 2A were harvested for pulsed field gel electrophoresis (PFGE) at the indicated times. Southern blots of the gel were probed with fragments containing ARS305 to detect chromosome III, ARS607 to detect chromosome VI, and ARS1413 to detect

chromosome XIV. For each chromosome the Southern signal for both the gel well and the normal chromosomal position are shown.

D) Replication timing does not correlate with efficiency of G2/M phase re-replication in the OMC strain. For each of the pro-ARSs defined by Wyrick *et al.* (Wyrick *et al.*, 2001), the DNA copy number from the OMC G2/M phase re-replication profile in Figure 2B was plotted versus the DNA copy number from the OMC S phase replication profile in Figure 2B. Line represents linear regression of plot.

Figure 2

A

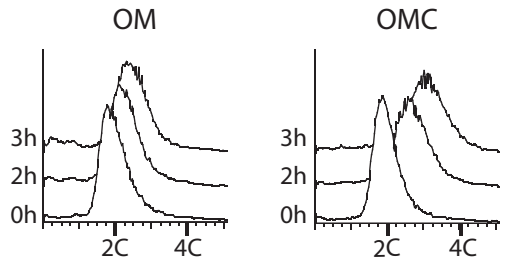

B

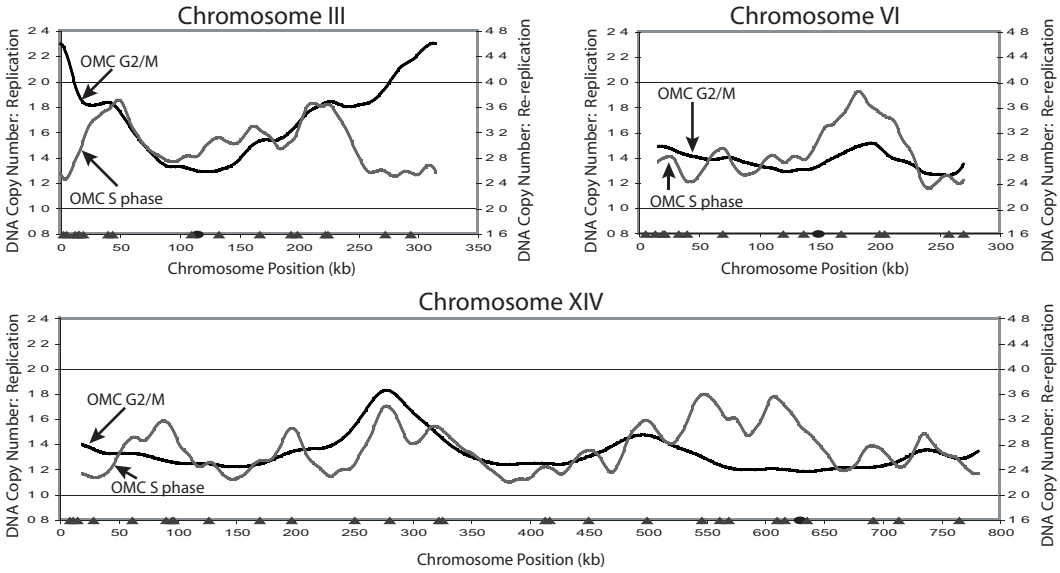

C

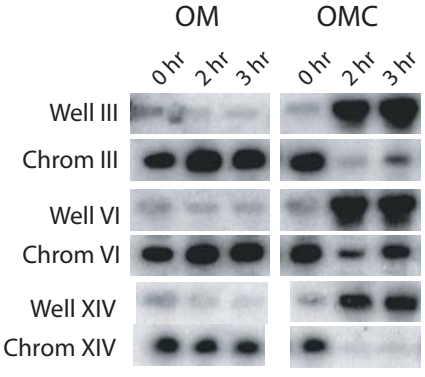

D

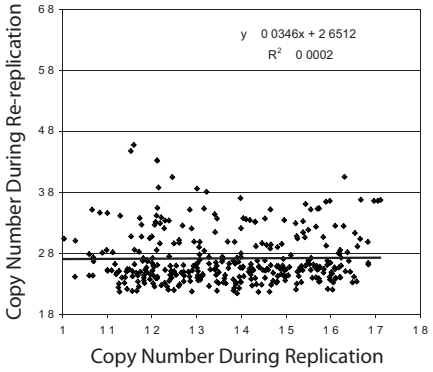

Figure 3 Deregulation of ORC, Mcm2-7 and Cdc6 can induce re-replication in S phase.

A) Flow cytometry of OMC cells induced to re-replicate in S phase. The OMC strain YJL3249 (*orc2-cdk6A orc6-cdk4A MCM7-2NLS pGAL1-*Δ*ntcdc6 pMET3-HA3-CDC20*) was arrested in G1 phase, induced to express Δntcdc6 by the addition of galactose, then released from the arrest into media containing HU to delay cells from exiting S phase. At 4 hr the cells were still in S phase with a DNA content of 1.4 C. This value was used to normalize the re-replication profile in 3B.

B) OMC cells can re-initiate and re-replicate within S phase. Genomic DNA was isolated at the 0 hr (G1 phase) and 4 hr (S phase) time points from the OMC strain YJL3249 as described in Figure 3A and competitively hybridized against each other. The resulting profiles shown for chromosomes III and X reflect copy number increases due to both replication and re-replication. Locations of pro-ARSs mapped by Wyrick *et al.* (Wyrick *et al.*, 2001) (gray triangles) and the centromeres (black circles) are plotted along the X-axis.

Figure 3

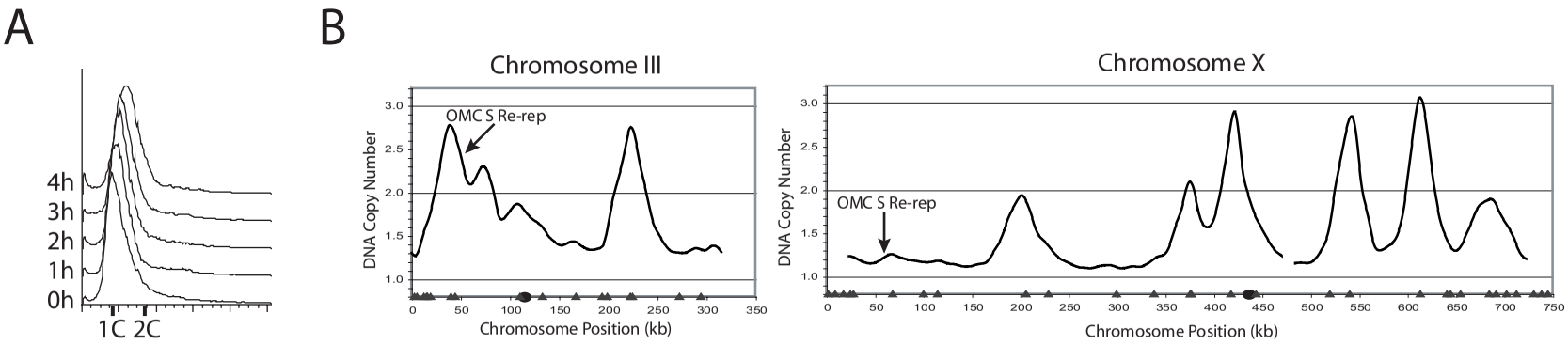
A
4h
3h
2h
1h
0h
1C 2C
B
Chromosome III
OMC S Re-rep
DNA Copy Number
Chromosome Position (kb)
Chromosome X
OMC S Re-rep
DNA Copy Number
Chromosome Position (kb)

Figure 4 Re-replication induced upon release from a G1 arrest when ORC, Mcm2-7 and Cdc6 are deregulated.

A) Robust re-replication of OMC cells following G1 release. The OMC strain YJL3248 (*orc2-cdk6A orc6-cdk4A MCM7-2NLS pGAL1-Δntcdc6 pMET3-HA3-CDC20)* and the control OM strain YJL3244 (*orc2-cdk6A orc6-cdk4A MCM7-2NLS pGAL1 pMET3-HA3-CDC20*) were arrested in G1 phase, exposed to galactose to induce Δntcdc6 in the OMC strain, then released from the arrest into G2/M phase. Samples were taken for flow cytometry at the indicated times after release from the alpha factor arrest. The OMC re-replication profile in Figure 4C was normalized to the 3 hr DNA content of 3.2 C.

B) Cells that were induced to re-replicate in Figure 4A were harvested for PFGE at the indicated times. Southern blots of the gel were probed for chromosomes III, VI, and XIV as described in Figure 2C.

C) Re-replication profile of the OMC strain following G1 release. Genomic DNA was purified from the OMC strain and the control OM strain 3 hr after G1 release. The two DNA preparations were labeled and competitively hybridized against each other to generate the G1 release re-replication profiles shown for chromosomes III, VI, and XIV. Locations of pro-ARSs mapped by Wyrick *et al.* (Wyrick *et al.*, 2001) (gray triangles) and the centromeres (black circles) are plotted along the X-axis.

D) Re-replication induced in the OMC strain following a G1 release is slightly biased toward early replicating pro-ARSs. For each of the pro-ARSs defined by Wyrick *et al.* (Wyrick *et al.*, 2001), the DNA copy number from the OMC G1 release re-replication

profile in Figure 4C was plotted versus the DNA copy number from the OMC S phase replication profile in Figure 2B. Line represents linear regression of plot.

Figure 4

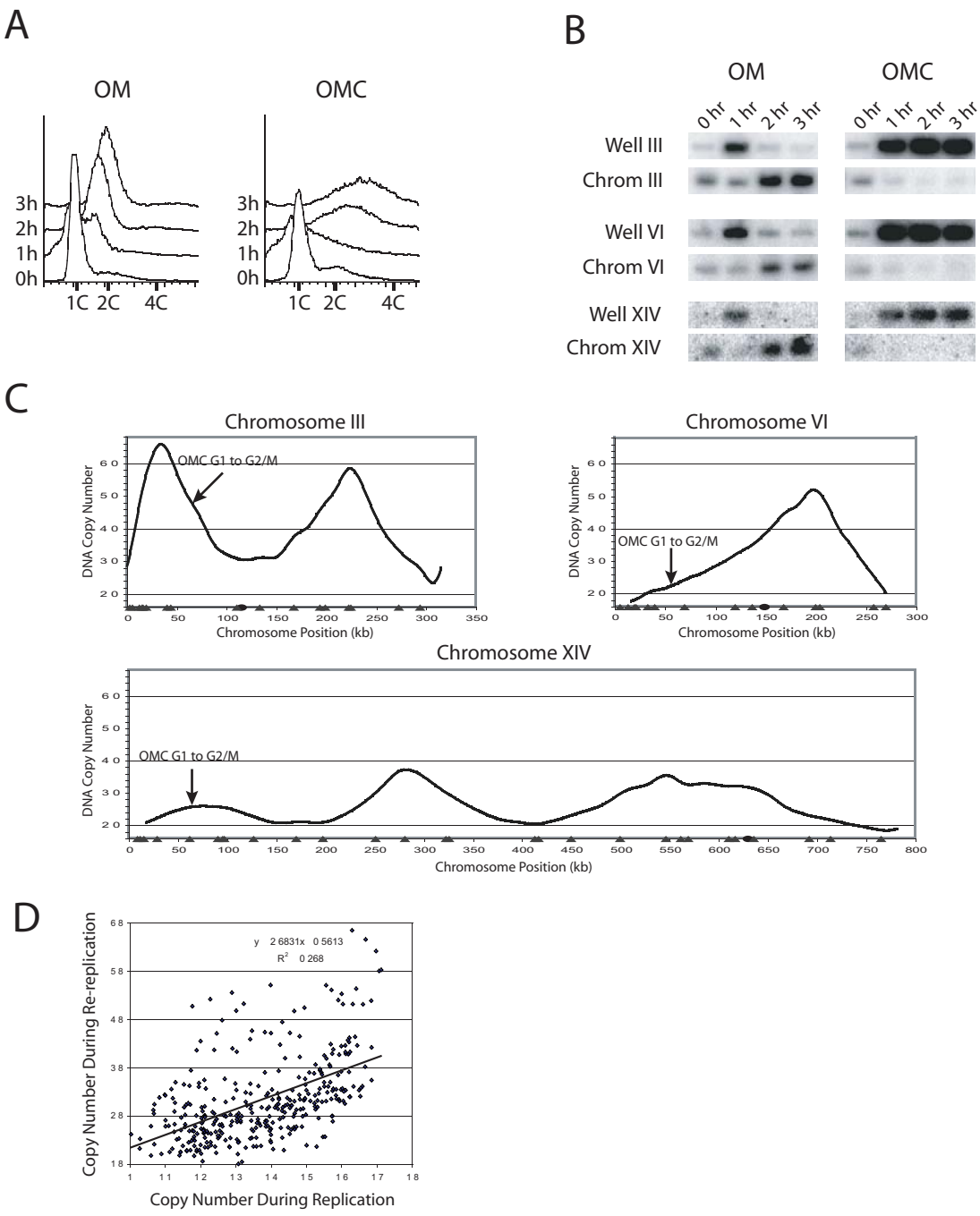
A
OM
OMC
3h
2h
1h
0h
1C 2C 4C
B
OM
OMC
0 hr
1 hr
2 hr
3 hr
Well III
Chrom III
Well VI
Chrom VI
Well XIV
Chrom XIV
C
Chromosome III
OMC G1 to G2/M
DNA Copy Number
Chromosome Position (kb)
Chromosome VI
OMC G1 to G2/M
DNA Copy Number
Chromosome Position (kb)
Chromosome XIV
OMC G1 to G2/M
DNA Copy Number
Chromosome Position (kb)
D
y 2 6831x 0 5613
R² 0 268
Copy Number During Re-replication
Copy Number During Replication

Figure 5 Re-replication can be induced when only ORC and Cdc6 are deregulated.

A) Re-replication is undetectable by flow cytometry in OC cells in G2/M phase. The OC strain YJL3240 (*orc2-cdk6A orc6-cdk4A pGAL1-Δntcdc6 pMET3-HA3-CDC20)* and the control O strain YJL4832 (*orc2-cdk6A orc6-cdk4A pGAL1 pMET3-HA3-CDC20*) were arrested in G2/M phase and induced with galactose as described in Figure 2A. Samples for flow cytometry were taken at the indicated times after galactose addition. The OC G2/M re-replication profile in Figure 5E was normalized to the 3 hr DNA content of 2.0 C.

B) Significant re-replication can be induced in OC cells during a G1 release. The OC strain and the control O strain were induced with galactose and released from a G1 arrest as described in Figure 4A. Samples for flow cytometry were taken at the indicated times after G1 release. The OC G1 release re-replication profile in Figure 5E was normalized to the 3 hr DNA content of 2.6 C.

C) Re-replication is not readily detected by PFGE in OC cells in G2/M phase. Strains that were induced to re-replicate in Figure 5A were harvested for PFGE at the indicated times. Southern blots of the gel were probed for chromosomes III, VI, and XIV as described in Figure 2C.

D) Some but not all copies of each chromosome participate when OC cells are induced to re-replicate in G2/M phase. Strains that were induced to re-replicate in Figure 5B were harvested for PFGE at the indicated times. Southern blots of the gel were probed for chromosomes III, VI, and XIV as described in Figure 2C.

E) Cell cycle position significantly affects the extent of re-replication in the OC strain. The OC strain and the control O strain were induced to re-replicate in G2/M phase

or during a G1 release as described, respectively, in Figures 5A and 5B. For each induction protocol, OC and O strain genomic DNA were prepared and competitively hybridized against each other. Shown for chromosomes III, VI, and XIV are OC G2/M phase re-replication profiles (black lines), OC G1 release re-replication profiles (gray lines), locations of pro-ARSs mapped by Wyrick *et al.* (Wyrick *et al.*, 2001) (gray triangles), and the centromeres (black circles).

Figure 5

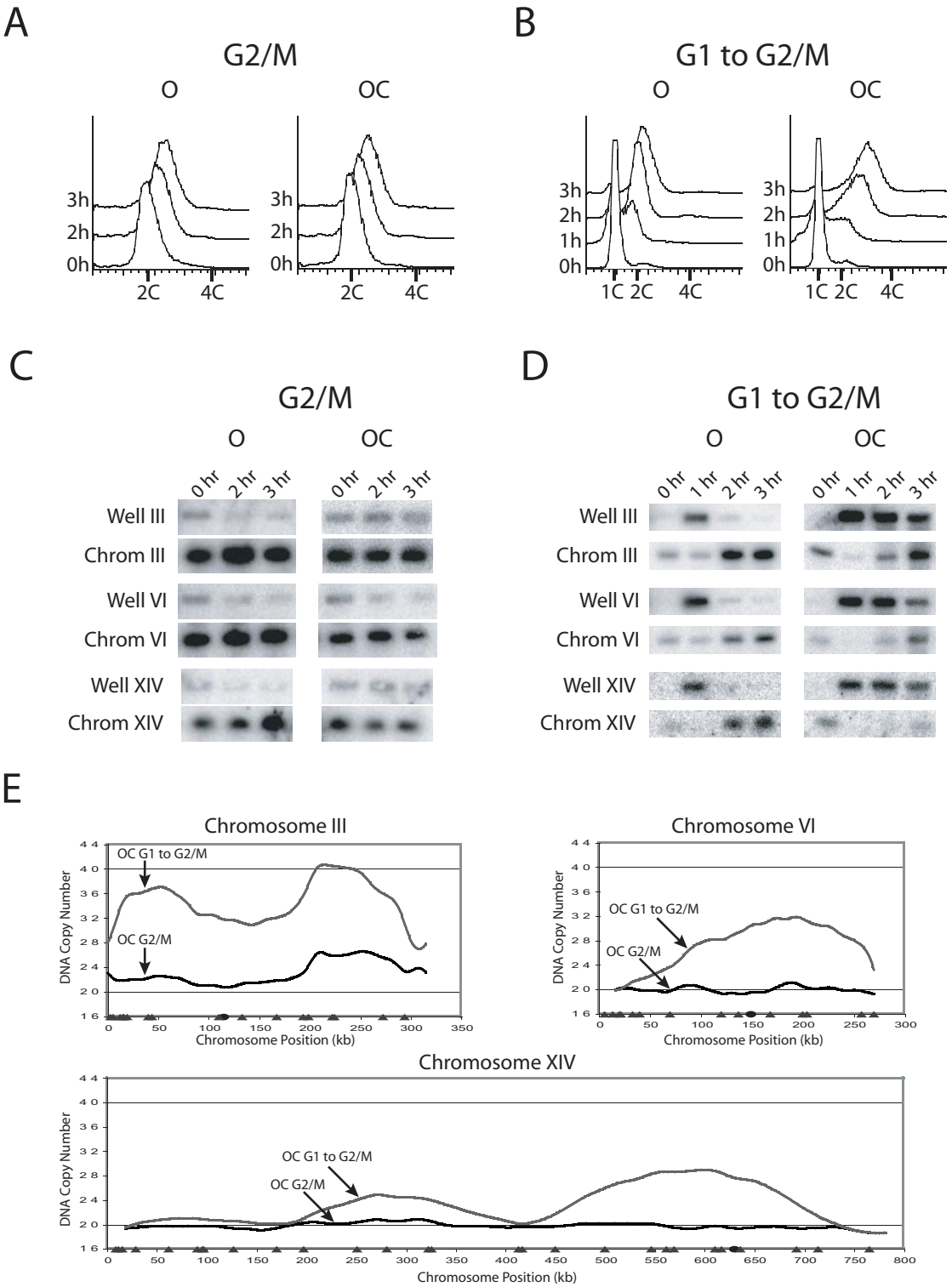
A
G2/M
O
OC
3h
2h
0h
2C
4C
B
G1 to G2/M
O
OC
3h
2h
1h
0h
1C 2C
4C
C
G2/M
O
OC
0 hr
2 hr
3 hr
Well III
Chrom III
Well VI
Chrom VI
Well XIV
Chrom XIV
D
G1 to G2/M
O
OC
0 hr
1 hr
2 hr
3 hr
Well III
Chrom III
Well VI
Chrom VI
Well XIV
Chrom XIV
E
Chromosome III
OC G1 to G2/M
OC G2/M
DNA Copy Number
Chromosome Position (kb)
Chromosome VI
OC G1 to G2/M
OC G2/M
DNA Copy Number
Chromosome Position (kb)
Chromosome XIV
OC G1 to G2/M
OC G2/M
DNA Copy Number
Chromosome Position (kb)

Figure 6 Re-replication occurs primarily on a single chromosome when Mcm2-7 and Cdc6 are deregulated

A) Re-replication is undetectable by flow cytometry in MC_{2A} cells in G2/M phase. The MC_{2A} strain YJL4489 (*MCM7-NLS pGAL1-Δntcdc6-cdk2A pMET3-HA3-CDC20*) and the control M strain YJL4486 (*MCM7-2NLS pGAL1 pMET3-HA3-CDC20*) were arrested in G2/M phase and induced with galactose as described in Figure 2A. Samples for flow cytometry were taken at the indicated times after galactose addition. The MC_{2A} G2/M re-replication profile in Figure 6E was normalized to the 3 hr DNA content of 2.0 C.

B) Re-replication is undetectable by flow cytometry in MC_{2A} cells during a G1 release. The MC_{2A} strain and the control M strain were induced with galactose and released from a G1 arrest as described in Figure 4A. Samples for flow cytometry were taken at the indicated times. The MC_{2A} G1 release re-replication profile in Figure 6E was normalized to the 3 hr DNA content of 2.0 C.

C) A portion of the population of chromosome III molecules participate when MC_{2A} cells are induced to re-replicate in G2/M phase. The strains that were induced to re-replicate in Figure 6A were harvested for PFGE at the indicated times. Southern blots of the gel were probed for chromosomes III, VI, and XIV as described in Figure 2C.

D) A portion of the population of chromosome III molecules participate when MC_{2A} cells are induced to re-replicate during a G1 release. The strains that were induced to re-replicate in Figure 6B were harvested for PFGE at the indicated times. Southern blots of the gel were probed for chromosomes III, VI, and XIV as described in Figure 2C.

E) Re-replication in the MC_{2A} strain occurs primarily on chromosome III. The MC_{2A} strain and the control M strain were induced to re-replicate in G2/M phase or during a G1 release as described, respectively, in Figures 6A and 6B. For each induction protocol, MC_{2A} and M strain genomic DNA were prepared and competitively hybridized against each other. Shown for chromosomes III, VI, and XIV are MC_{2A} G2/M phase re-replication profiles (black lines), MC_{2A} G1 release re-replication profiles (gray lines), locations of pro-ARSs mapped by Wyrick *et al.* (Wyrick *et al.*, 2001) (gray triangles) and the centromeres (black circles).

Figure 6

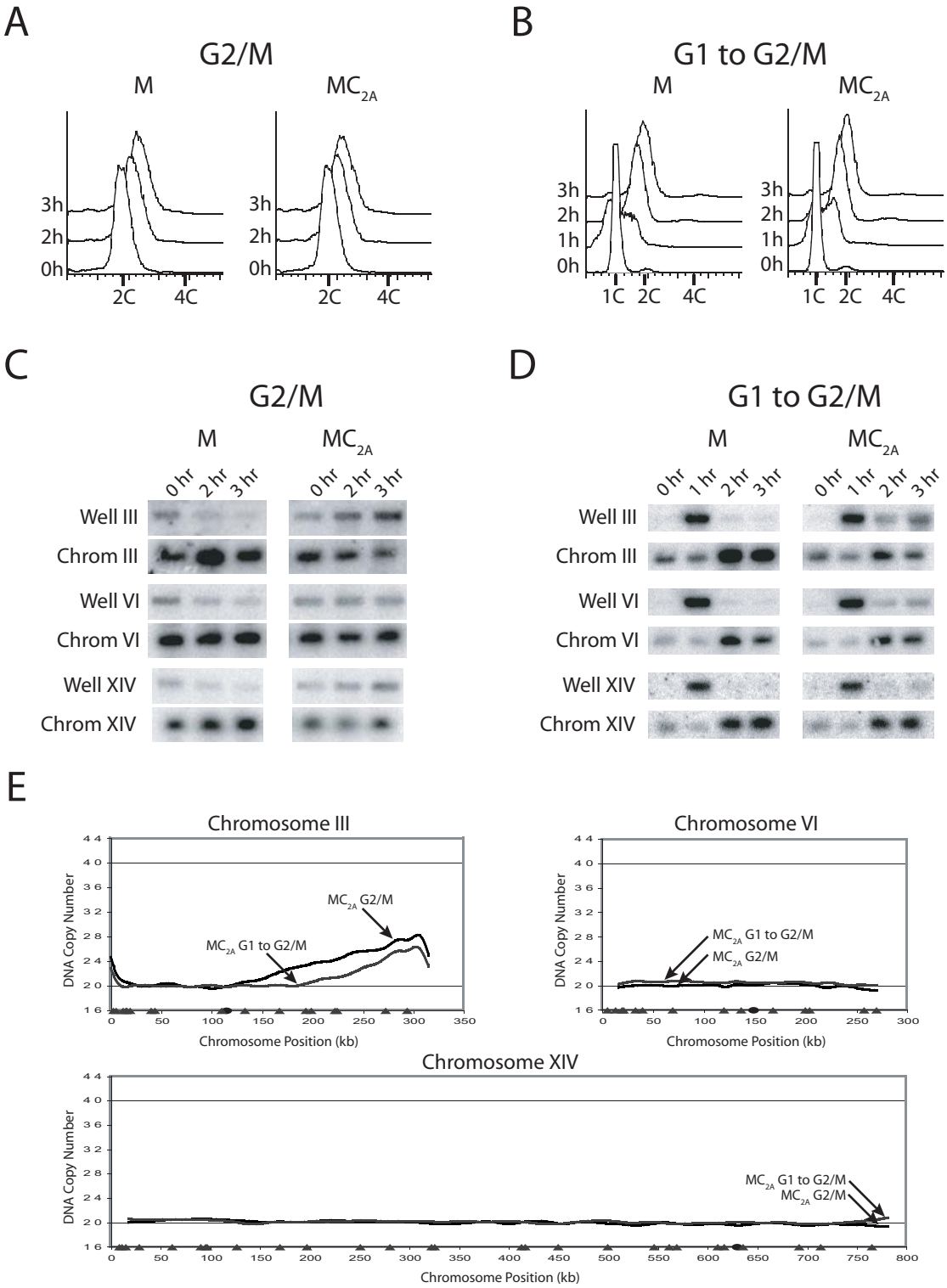
A
G2/M
M
MC2A
3h
2h
0h
2C
4C
B
G1 to G2/M
M
MC2A
3h
2h
1h
0h
1C
2C
4C
C
G2/M
M
MC2A
0 hr
2 hr
3 hr
Well III
Chrom III
Well VI
Chrom VI
Well XIV
Chrom XIV
D
G1 to G2/M
M
MC2A
0 hr
1 hr
2 hr
3 hr
Well III
Chrom III
Well VI
Chrom VI
Well XIV
Chrom XIV
E
Chromosome III
DNA Copy Number
MC2A G2/M
MC2A G1 to G2/M
Chromosome Position (kb)
Chromosome VI
DNA Copy Number
MC2A G1 to G2/M
MC2A G2/M
Chromosome Position (kb)
Chromosome XIV
DNA Copy Number
MC2A G1 to G2/M
MC2A G2/M
Chromosome Position (kb)

Figure 7 The re-replication arising from deregulation of both Mcm2-7 and Cdc6 depends on *ARS317* and Cdc7.

A) Re-initiation bubbles are induced at *ARS317* when MC_{2A} re-replicates in G2/M phase. The MC_{2A} strain YJL4489 (*MCM7-NLS pGAL1-*Δ*ntcdc6-cdk2A pMET3-HA3-CDC20*) and the control M strain YJL4486 (*MCM7-2NLS pGAL1 pMET3-HA3-CDC20*) were arrested in G2/M phase and induced with galactose as described in Figure 6A. Genomic DNA was purified from each strain at both 0 and 2 hr after induction and subjected to neutral-neutral 2-dimensional gel electrophoresis. Southern blots of the gels were probed with an *ARS317* fragment. Black arrow indicates re-replication bubbles.

B) *ARS317* sequence is required for the bulk of re-replication induced in MC_{2A} cells. The MC_{2A}-Δ*ars317* strain YJL5858 (*MCM7-NLS pGAL1-*Δ*ntcdc6-cdk2A pMET3-HA3-CDC20* Δ*ars317*) and the control M strain YJL4486 were arrested in G2/M phase and induced with galactose for 3 hours as described in Figure 6A. Genomic DNA from the two strains was competitively hybridized against each other to generate the MC_{2A}-Δ*ars317* G2/M phase re-replication profile shown for chromosome III (gray line). The MC_{2A} G2/M phase re-replication profile from Figure 5E is replotted for comparison (black line). The locations of pro-ARSs mapped by Wyrick *et al.* (Wyrick *et al.*, 2001) (gray triangles), and the centromere (black circle) are plotted along the X-axis.

C) Cdc7 kinase is required for re-replication induced in MC_{2A} cells. The MC_{2A} strain YJL4489, the congenic MC_{2A}-*cdc7* strain YJL5821 (*MCM7-2NLS pGAL1-*Δ*ntcdc6-2A pMET3-HA3-CDC20 cdc7-1*) and their respective controls, the M strain YJL4486 and the M-*cdc7* strain YJL5816 (*MCM7-2NLS pGAL1 pMET3-HA3-CDC20 cdc7-1*) were induced with galactose as described in Figure 6A, except the initial arrest

was performed at 23° C, and the arrested cells were shifted to 35° C for 1 hr, before the addition of galactose. Genomic DNA was isolated 4 hr after galactose addition and competitively hybridized (MC_{2A} versus M and MC_{2A}-*cdc7* versus M-*cdc7*) as described in Figure 1A. Re-replication profiles for the MC_{2A} (black line) and MC_{2A}-*cdc7* (gray line) strains are shown for chromosome III. Locations of pro-ARSs mapped by Wyrick *et al.* (Wyrick *et al.*, 2001) (gray triangles), and the centromere (black circle) are plotted along the X-axis.

Figure 7

A

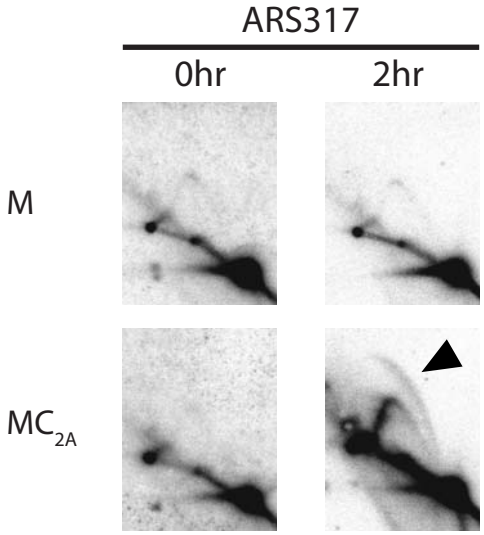
ARS317
0hr
2hr
M
MC2A

B

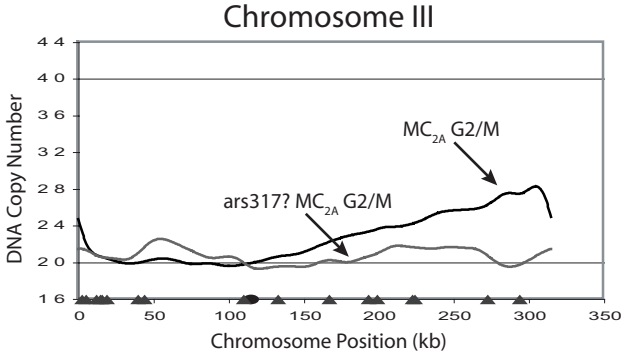
Chromosome III
DNA Copy Number
MC2A G2/M
ars317? MC2A G2/M
Chromosome Position (kb)

C

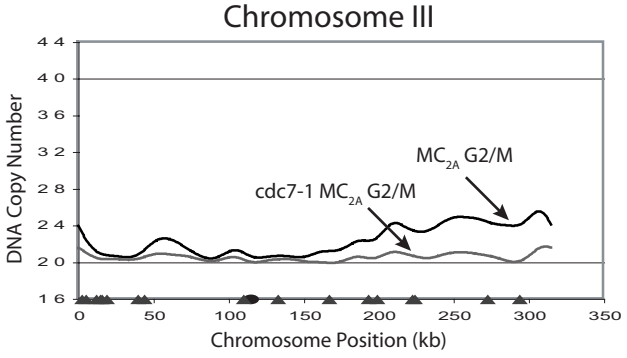
Chromosome III
DNA Copy Number
MC2A G2/M
cdc7-1 MC2A G2/M
Chromosome Position (kb)

CHAPTER 3

The progression of replication forks set up during inappropriate re-replication is impaired

ABSTRACT

Faithful duplication of the genome from one generation to the next is critical for the integrity of a cell's hereditary information. In eukaryotes replication is limited to once and only once per cell cycle through the combined action of multiple overlapping inhibitory mechanisms. Deregulation of these mechanisms leads to partial re-replication of the genome, activation of the DNA damage checkpoint, and double stranded breaks. Here we show using microarray comparative genomic hybridization (CGH) that the fork progression during re-replication is impaired across the entire yeast genome. Re-replication forks appear to travel at least five-fold slower than S phase forks and fail to bridge the inter-origin distance between re-initiating origins. We find that this impairment of fork progression is not due to lack of sufficient nucleotides. We also provide evidence that fork progression is impaired by a mechanism that is independent of fork head-to-tail collisions. These data are consistent with a model in which replication fork failure during re-replication causes DNA damage.

INTRODUCTION

Eukaryotic replication must be tightly controlled such that it only occurs once and only once per cell cycle. In order for large genomes be replicated in a timely manner DNA replication initiates at hundreds of different sites, called origins of replication, each S phase. This presents a challenge for a cell because the initiation at these origins must be coordinated such that each segment of the genome is duplicated precisely once each S phase. Any disruption can potentially result in the gain or loss of information and an unstable genome.

In order to achieve tight coordination of replication, the initiation reaction is compartmentalized into two stages. These stages occur in discrete phases of the cell cycle (reviewed in (Bell and Dutta, 2002; Diffley, 2004; Machida *et al.*, 2005)). During the first stage, which occurs in G1 phase when cyclin-dependent kinase (CDK) activity is low, origins of replication are selected by the assembly of the pre-replicative complex (pre-RC). A pre-RC is assembled at each origin by the sequential loading of the Origin Recognition Complex (ORC), Cdc6, Cdt1 and the MCM2-7 complex. As cells enter S phase the second stage of initiation, origin activation, is triggered by the activity of the CDK and the Cdc7-Dbf4 kinase (DDK). Upon origin activation additional components of the replisome, including the DNA polymerases are recruited, the DNA is unwound, bidirectional replication forks are setup, and the pre-RC is disassembled leaving only ORC at the origin. At the same time that the CDKs are promoting activation of origins their activity is simultaneously preventing the components of the pre-RC from re-assembling through the remainder of S, G2 and M phases.

The temporal separation of these two stages is insufficient by itself to achieve tight control of replication initiation. In order to prevent spurious re-initiation cells have multiple overlapping mechanisms to prevent reassembly of pre-RCs at origins of replication (reviewed in (Arias and Walter, 2007)). *Saccharomyces cerevisiae* has at least six separate mechanisms for inhibiting re-replication. Cdk1-Clb5 inactivates ORC by phosphorylation of Orc2 and Orc6 (Nguyen *et al.*, 2001) and by direct binding to Orc6 (Wilmes *et al.*, 2004). The MCM2-7 complex is phosphorylated by CDK and together with Cdt1, exported from the nucleus (Labib *et al.*, 1999; Nguyen *et al.*, 2000; Tanaka and Diffley, 2002; Liku *et al.*, 2005). CDKs inhibit Cdc6 by down regulating its transcription (Moll *et al.*, 1991), stimulating its ubiquitylation and degradation (Drury *et al.*, 1997; Elsasser *et al.*, 1999; Drury *et al.*, 2000), and by direct binding (Mimura *et al.*, 2004). CDKs use similar a mechanisms in fission yeast to promote destruction of Cdc6 homolog, Cdc18 (Jallepalli *et al.*, 1997). Each individual mechanism is quite potent at preventing re-replication. Disruption of mechanisms targeting ORC, Cdc6 and MCM2-7 are required in *S. cerevisiae* to observe massive re-replication (Nguyen *et al.*, 2001). A more sensitive assay, microarray CGH, demonstrated that deregulation of mechanisms targeting only ORC and Cdc6 or MCM2-7 and Cdc6 are sufficient to cause small amounts of re-replication. Thus cells require multiple overlapping mechanisms in order to maintain a tight block to re-replication.

Metazoan cells use similar strategies to preventing re-replication by regulating the stability, activity, and localization of pre-RC components (for review see (Arias and Walter, 2007)). Unlike in budding yeast, not all mechanisms are directly dependent upon CDK activity. These mechanisms include a protein called geminin that binds and inhibits

Cdt1, and a second mechanism of replication-coupled mechanism to degrade Cdt1 (Arias and Walter, 2005). Mammalian cells contain a G2 specific mechanism to degrade CDT1, which does require the activity of the CDK.

The loss of re-replication control has deleterious consequences to cells beyond extra DNA synthesis. In budding yeast, re-replication causes activation of the DNA damage checkpoint and cell inviability (Archambault *et al.*, 2005; Green and Li, 2005). Evidence of double strand breaks and chromosomal fragmentation are detected (Green and Li, 2005). In metazoans re-replication activates the DNA damage checkpoint and double stranded breaks are observed (Vaziri *et al.*, 2003; Melixetian *et al.*, 2004; Zhu *et al.*, 2004; Li and Blow, 2005; Lovejoy *et al.*, 2006; Zhu and Dutta, 2006). In mammalian cells re-replication caused severe DNA lesions that dramatically reduced cell viability (Melixetian *et al.*, 2004; Zhu *et al.*, 2004). Similar to yeast, the structure and origin of the DNA damage is unknown.

While there is evidence that it is the re-replication itself that causes the DNA lesions it is unknown why this occurs (Green and Li, 2005; Davidson *et al.*, 2006). Any model to explain this phenomenon must account for why re-replication is different from replication. One insight into this problem is the fact that DNA synthesis due to re-replication in budding yeast is limited relative to S phase replication. Flow cytometry indicates that re-replication does not result in a complete duplication of the genome (Nguyen *et al.*, 2001). Only about one-third of the genome is duplicated in three hours, which is at least five times longer than a normal budding yeast S phase. Microarray CGH analysis of yeast undergoing massive re-replication demonstrated that there are stark differences between normal S phase replication and re-replication induced in G2/M

phase. Approximately half the number origins had detectable initiation during re-replication as compared to S phase (Green *et al.*, 2006; Tanny *et al.*, 2006). Of those origins that re-initiate very few initiate efficiently in every cell. It has been shown that limiting the number of origins in that initiate in S phase can result in severe consequences to the cell (Shimada *et al.*, 2002) (Gibson *et al.*, 2004) (Lemoine *et al.*, 2005). Presumably if a limited number of origins re-initiate, then forks will need to replicate large stretches of DNA, increasing the odds they will collapse. Thus one potential explanation is that re-replication simply does not initiate sufficient origins to fully duplicate the genome.

A number of additional explanations for the re-replication induced DNA damage have been proposed. A lack of synthetic materials such as nucleotides in G2/M might cause re-replication to be incomplete. Alternatively, re-replication might improperly assemble the replication machinery thus resulting in slow or unstable forks. Another hypothesis is that re-replication might cause a single origin to initiate multiple times. A fork from a later round of re-replication could then in theory catch up to and collide with a fork from an earlier round causing collapse. Work in *Xenopus* indicates these collisions occur and result in DNA damage when massive re-replication is induced (Davidson *et al.*, 2006).

A better understanding of replication fork behavior during re-replication is critical in order to differentiate between these hypotheses and understand why re-replication so toxic to cells. We performed a kinetic analysis of re-replication using microarray CGH to evaluate fork progression during re-replication across the entire yeast genome. These studies indicated that re-replication fork movement progression is severely restricted

relative to S phase fork progression thus demonstrating that both origin initiation and fork progression are limited during re-replication. In addition, we found that the decreased fork progression is most consistent with forks irreversibly stalling or collapsing. We also showed that increasing available nucleotide pools did not restore the normal rate of DNA synthesis. In addition, we provide evidence that re-replication fork progression was defective even in the absence of fork head-to-tail collisions indicating that each individual re-replication fork progression was severely challenged.

MATERIALS AND METHODS

Plasmids and Strains

All plasmids used in this study are described in Table 1, all yeast strains are described in Table 2 and all oligonucleotides are described in Table 3. Details about strain construction can be found in Supplemental Methods.

Yeast media, growth and arrest

Cells were grown in YEP, synthetic complete (SC), or synthetic (S broth) medium (Guthrie and Fink, 1990) supplemented with 2% dextrose (wt/vol), 2% galactose (wt/vol), 3% raffinose (wt/vol), or 3% raffinose (wt/vol) + 0.05% dextrose (wt/vol). For S phase experiments cells were grown overnight in SDC-Met,Ura and arrested in G1 phase with 50 ng/ml alpha factor (all strains were *bar1*) at 30˚C. Cells were released from G1 phase arrest by filtering, washing, and then resuspending in prewarmed 30˚C YEPD containing 100 μg/ml pronase and 100 mM hydroxyurea (HU). Cells were released from

HU by filtering, washing, and then resuspending in prewarmed 30˚C YEPD containing 2 mM methionine and 15 µg/ml nocodazole.

To obtain reproducible induction of re-replication, cells were inoculated from a fresh unsaturated culture containing 2% dextrose into a culture containing 3% raffinose + 0.05% dextrose and grown for 12-15 h the night prior to the experiment. The *GAL1* promoter (*pGAL1*) was induced by addition of 2% galactose and repressed by addition of 2% dextrose. The *MET3* promoter (*pMET3*) was repressed by the addition of 2 mM methionine. All experiments were performed at 30˚C except where noted. For induction of re-replication in G2/M phase, cells grown overnight in SRaffC-Met,Ura + 0.05% dextrose were pelleted and resuspended in YEPRaff + 2 mM methionine and 15 µg/ml nocodazole. Once arrested (>90% large budded cells), galactose was added to a final concentration of 2%. In experiments in which the *GAL1* promoter was repressed dextrose was added to a final concentration of 2% at the indicated time.

For induction of a single round of re-replication using strains containing *cdc7-1*, cells were grown and arrested at 23˚C. Cultures were shifted to 35˚C by filtering and resuspending in prewarmed 35˚C YEPRaff + 2 mM methionine and 15 µg/ml nocodazole for 45 min followed by addition of 2% galactose. These cultures were split after 1 hour in galactose and either kept in galactose or dextrose was added to 2%. After 1 hour cells were released by rapidly shifting to 23˚C by the addition of the appropriate volume of 0.5˚C YEPGal + 2 mM methionine and 15 µg/ml nocodazole or 0.5˚C YEPDex + 2 mM methionine and 15 µg/ml nocodazole.

Flow cytometry

Cells were fixed with 70% ethanol and stained with 1 μM Sytox Green (Molecular Probes, Eugene, OR) as previously described (Haase and Lew, 1997).

Microarray CGH Assay

Microarrays containing 12,034 PCR products representing every ORF and intergenic region were prepared essentially as described (DeRisi *et al.*, 1997; Iyer *et al.*, 2001) (see Supplemental Methods). Genomic DNA was prepared, labeled and hybridized as described in Green *et al.* (Green *et al.*, 2006). Modifications to the previous protocols can be found in Supplemental Methods. For each replication or re-replication profile two hybridizations were performed from each of two independent experiments. The resulting four profiles were averaged into one composite profile.

Data analysis

Raw Cy5/Cy3 ratios from scanned arrays were normalized to the DNA content per cell based on the flow cytometry data to determine absolute copy number of each DNA segment. Raw values were then binned and smoothed using Fourier Convolution Smoothing essentially as described (Raghuraman *et al.*, 2001). The rate of replication fork progression "Peak Spread" was calculated using the smoothed data from two sequential replication profiles. The peak spread was determined at each origin for the indicated spatial and temporal intervals. Values in Tables IV and V are the average and standard error calculated from two independent replicate experiments. Individual measurements of peak spread can be found in Table S2. Details of normalization, data

analysis and fork progression rate determinations are described in Supplemental Methods. The data discussed in this publication have been deposited in NCBI's Gene Expression Omnibus (GEO, http:://www.ncbi.nlm.nih.gov/geo/) and are accessible through GEO Series accession number GSEXXXX.

Results

Microarray CGH can be used to measure replication fork progression

Re-replication causes DNA damage and chromosome fragmentation. The mechanism by which this occurs is unclear. We have previously shown that re-replication is limited in both its ability to duplicate the genome and in the modest number of origins which re-initiate. We hypothesized that additional constraints are imposed upon the ability of the cell to re-replicate its genome that could potentially explain the observed DNA damage. We decided to investigate whether replication forks setup during re-replication were able to progress with the speed and efficiency of S phase forks. We used a genome-wide approach to investigate whether there was a systematic defect in replication fork progression that could explain the limited re-replication and DNA damage.

We have previously used microarray comparative genomic hybridization (CGH) to monitor the number, location, and efficiency of replication initiation events during replication and re-replication (Green *et al.*, 2006). This assay measures the increase in DNA copy number that arises during replication or re-replication. During S phase, the average copy number of each DNA segment in a population is determined by the proportion of cells that have duplicated this segment. Since early replicating regions will

have duplicated in more cells than later replicating regions, the average copy number of each segment provides an indication of the time it replicates. Origins of replication, which replicate earlier than their neighboring segments, can thus be identified from the chromosomal position of peak maxima in the replication profile.

We have adapted this assay to monitor the average rate of fork progression during replication and re-replication in budding yeast. Microarrays have been successfully used to study replication fork progression from the *E. coli* origin of replication (Khodursky *et al.*, 2000; Simmons *et al.*, 2004). To study fork progression, microarray CGH replication profiles were generated at multiple time points. A peak in a given replication profile should widen at a rate determined by the fork progression rate as diagrammed in Figure 1A. The position of a peak corresponds to an origin's location and the height of a peak represents the proportion of cells in the population that have initiated at that origin. For any point along the side of a peak, the height represents the proportion of cells in which replication forks have traveled from the origin to this position. This "peak spread" is measured by the chromosomal distance from a position with a given copy number in the initial profile to the position with the same copy number in the subsequent profile. Dividing this peak spread by the time interval between profiles yields the rate of fork progression. For clarity we will describe a measured peak spread using three parameters: the origin from which the fork originated, the height at which the measurement was made, and the time interval over which the measurement was made.

We initially focused on fork progression from a specific origin on Chromosome XIV, ARS1414. ARS1414 initiates efficiently in during both S phase and re-replication induced in G2/M allowing direct comparison of forks from same origin (Green *et al.*,

2006). ARS1414 is well suited for competitive genomic hybridization analysis because the neighboring origins to the left are well characterized and have been mapped to relatively small regions (Friedman *et al.*, 1996). This allowed us to mutate the three closest origins to the left of ARS1414 to create a large origin-free region of approximately 153 kb. ARS1413 was inactivated by point mutation and ARS1412 and ARS1411 were deleted in a strain that is capable of inducing re-replication due to mutations in ORC, Mcm2-7 and Cdc6 (Friedman *et al.*, 1996; Nguyen *et al.*, 2001). The resulting strain will be referred to as the OMC ChrXIV-3arsΔ strain (*orc2-cdk6A orc6-cdk4A MCM7-2NLS pGAL1-Δntcdc6 ars1411Δ ars1412Δ ars1413*).

We first examined the rate of S phase replication fork progression in the OMC ChrXIV-3arsΔ strain. Measuring fork progression in S phase allowed us to determine what the normal fork progression rate was for this strain and allowed us to validate this approach for studying fork progression. To obtain a synchronous S phase population OMC ChrXIV-3arsΔ strains were first arrested in G1 phase. Cells were then released into a low concentration of hydroxyurea (HU) to allow origins to fire but to slow replication fork progression. After 180 min the HU was removed and the cells were released into a G2/M arrest. Cells were harvested for genomic DNA at 180 min, 200 min, and 220 min (0 min, 20 min, and 40 min following the release from HU). Flow cytometry analysis demonstrated that at 180 min cells had a DNA content of 1.3 C. Soon after, cells began to replicate rapidly and completed S phase within 70 min (Figure 1B).

Genomic DNA from each time point was purified and competitively hybridized against non-replicating G1 phase DNA. The replication profile for each time point was normalized to DNA content calculated from the flow cytometry data and plotted in

Figure 1C. The S phase replication profile shows that at 180 min many of the cells had initiated at ARS1414. Most of the cells had not elongated more than 30kb from ARS1414 at this time. We note that despite the disruption of the three known origins (ARS1411, ARS1412, and ARS1413) in this region, we still detected weak initiation activity due to an uncharacterized origin at approximately 70 kb from ARS1414. Because of its limited contribution to copy number increases in this region, the presence of this weak cryptic ARS does not have a significant impact on our measurements of fork progression from ARS1414.

From the replication profiles in Figure 1C we observe two important features of S phase replication. The first is that forks progress rapidly away from origins once HU is removed. Secondly, as cells progress through S phase there is a qualitative change in the shape of the profile as the cells complete replication of the chromosomes (Figure 1 and Supplemental Figure 1). For example, the valley between ARS1414 and the origin to the right ARS1415 is largely filled in by the 220 min (40 min) time point.

In order to more precisely the measure the rate of fork progression we used the data from the three profiles at 180, 200, and 220 min to determine the peak spread from forks originating from ARS1414. Two peak spread measurements were calculated for ARS1414. The first was calculated starting from the apex of the ARS1414 peak in the 0 min profile and ending at the equivalent height in the 20 min profile. The second was calculated for the time interval from 20 min to 40 min following release at the height of the ARS1414 peak in the 200 min profile. The fork progression rates were 0.91 +/- 0.06 kb/min and 1.28 +/- 0.13 kb/min, respectively (Table IV).

Microarray-based analysis of fork progression allows us to monitor fork movement as a function of time at multiple origins in the same experiment. We took advantage of this to confirm that the observed rate of fork progression from ARS1414 was similar to that of forks originating from other origins. We selected 24 additional origins for analysis that initiated with high efficiency and were a minimum of 50 kb from an adjacent origin. The peak spread from each of these origins was measured for the two time intervals in a similar manner to those measured for ARS1414. The average rate of fork progression was 0.87 +/- 0.04 kb/min for the 0 min to 20 min time interval and 1.31 +/- 0.07 kb/min for the 20 min to 40 min time interval (Table IV). These values are highly similar to those for ARS1414.

Our measured rate of S phase replication fork progression is similar to those previously published which range from 1.9 to 3.7 kb/min for yeast (Petes and Williamson, 1975; Rivin and Fangman, 1980; Ferguson *et al.*, 1991; Lengronne *et al.*, 2001) and 1.5 to 3 kb/min for mammalian cells (Scott *et al.*, 1997; Lebofsky *et al.*, 2006). Our value is somewhat lower than previously published data. One likely explanation is incomplete recovery from hydroxyurea since the measured rate was reproducibly slower for the first 20 min relative to that in the second 20 min. An alternative explanation is that the mutations that permit induction of re-replication also effect fork progression. These mutations do slightly negatively effect initiation (Green *et al.*, 2006). Nonetheless, these values are in agreement with previously reported measurements of fork progression and support validation of this assay as a measure of replication fork progression.

Restrained fork progression during G2/M phase re-replication

We next wanted to measure the rate of fork progression during re-replication to compare it against the rate in replication. We arrested OMC ChrXIV-3arsΔ cells in G2/M phase by depletion of CDC20 and addition of nocodazole. Re-replication was induced by addition of galactose. Flow cytometry shows that the cells increased their DNA content at a constant rate (Figure 2A). Following induction of re-replication cells were collected for analysis by microarray CGH at 60 min intervals starting at 180 min. These time points were selected because cells had re-initiated sufficiently to generate peaks of comparable height to those observed in the S phase experiment. Genomic DNA from each time point was purified and competitively hybridized against non-replicating G1 phase DNA. The re-replication profile for each time point was normalized to DNA content calculated from the flow cytometry and plotted in Figure 2B. The re-replication profile at 180 min shows significant reinitiation at a number of origins on Chromosome XIV, including ARS1414 (Figure 2B).

Given that S phase replication forks in this strain travel at approximately 1 kb/min we predicted that unimpaired re-replication forks should be able to travel at least 60 kb each hour. From the re-replication profiles in Figure 2B we observed that replication forks were unable to elongate that far. We measured the three peak spreads at ARS1414. Two were calculated at the height of the ARS1414 peak in the 180 min profile, from 180 min to 240 min and from 240 min to 300 min. The third peak spread was calculated at the height of the ARS1414 peak in the 240 min time point from 240 min to 300 min (Table V). In each case, we observed that re-replication was severely limited ranging from 3 to 5 fold slower than fork progression in S phase.

We also observed that re-replication fork progression became progressively slower as the distance from the origin increased. Re-replication forks beginning at ARS1414 progressed at a rate of 0.37 +/- 0.02 kb/min from 180 min to 240 min. Those same forks progressed at a rate of 0.15 +/- 0.01 kb/min from 240 min to 300 min. The window of time in which forks elongated did not seem to affect the rate of fork progression. Re-replication forks starting at ARS1414 progressed at a rate of 0.31 +/- 0.02 kb/min from 240 min to 300 min. This suggests that existing forks are slowing the further they get from the origin, but that newly generated forks close to the origin are not becoming slower over the course of the experiment.

To test if these findings could be generalized we measured re-replication fork progression from 16 origins across the genome. Similar to the S phase analysis we required that each origin be separated by at least 50 kb and re-initiate at least as efficiently as the adjacent origins. Three peak spreads from each of these origins was measured in the same manner similar as those measured for ARS1414 re-replication. These values are highly similar to those measured for ARS1414 and confirm our findings that re-replication fork progression is severely restrained (Table V).

Impaired fork progression when new re-initiation events are limited

The defect in re-replication fork progression could be explained by forks traveling unusually slowly, forks traveling at normal rate but stalling or collapsing at a high frequency or both. Under conditions of constant galactose induction, new replication forks will be established throughout the experiment, complicating the analysis. To limit the influence of new initiation events on the analysis of fork progression, we subjected

cells to pulse of re-replication. OMC ChrXIV-3arsΔ cells were arrested in G2/M and Δ*ntcdc6* expression was induced by galactose. After 90 min of induction, dextrose was added to repress the *pGAL1* promoter driving Δ*ntcdc6* expression. The Δntcdc6 mutant is not completely refractory to CDK stimulated degradation and protein levels drop below detection approximately 1 hour after its transcription is repressed (Drury *et al.*, 2000). The addition of dextrose reduced the increase in DNA content by flow cytometry demonstrating that the repression was effective in curbing DNA synthesis (Compare Figure 2A and Figure 3A.)

Replication fork progression was analyzed by microarray CGH 90 min after dextrose addition. Cells were harvested for genomic DNA at 180 min (90 min after dextrose addition), 240 min and 300 min. The microarray CGH re-replication profiles show that far less reinitiation at re-replicating origins indicating that we were successful in limiting new initiation events (Figure 3B and Supplemental Figure 3 and 4). Importantly, we observed that progression from existing forks was severely impaired. The total population of replication forks did not progress as well when new initiation events were reduced (Table V). In contrast to the profiles in the S phase experiment, the re-replication profiles showed little evidence of filling in the valleys between peaks. This suggests that the majority of forks setup during re-replication did not complete replication of the chromosomes.

Nucleotides are not limiting fork progression during re-replication in G2/M phase

One potential explanation for impaired replication fork progression during re-replication in G2/M phase is that there are insufficient nucleotides to complete DNA

synthesis. We hypothesized that if nucleotide pools were limiting then upregulation of nucleotide synthesis should enhance the bulk DNA synthesis during re-replication. Nucleotide synthesis is regulated such that levels peak at the start of S phase and are maintained at low levels during the other stages of the cell cycle (Nordlund and Reichard, 2006). Key regulators modulate the activity of the ribonucleotide reductase complex, RNR1-4. To increase nucleotide levels we inactivated two mechanisms that downregulate RNR in a cell cycle-dependent manner. We inactivated the first mechanism by deleting *SML*1. Sml1 binds and inhibits RNR1 when cells are not in S phase (Zhao *et al.*, 1998; Chabes *et al.*, 1999). We also deleted a second protein, Wtm1 which downregulates nucleotides synthesis by sequestering a subcomplex of RNR2/RNR4 in the nucleus when the cells are not in S phase (Lee and Elledge, 2006; Zhang *et al.*, 2006). Importantly, deregulating both mechanisms has an additive effect on RNR activity (Lee and Elledge, 2006).

We examined re-replication by flow cytometry in a *wtm1*Δ *sml1*Δ OMC strain and compared its ability to re-replicate with that of the OMC strain. Cells were arrested in G2/M phase and were induced to re-replicate by galactose addition as described in Figure 2. Flow cytometry indicates that strains with OMC *wtm1*Δ *sml1*Δ re-replicated to an identical extent as strains with wild type SML1 and WTM1 (Figure 4). This demonstrates that re-replication is not limited simply by insufficient nucleotides and this is unlikely to explain the observed defect in fork progression.

Fork progression is inhibited during a single round of re-replication

Recent works in *Xenopus* suggests a mechanism through which high levels of Cdt1 are able to cause DNA damage (Davidson *et al.*, 2006). The authors proposed that multiple rounds of re-initiation could have generated successive re-replication forks that chased each other down the chromosome. The second fork could potentially catch up to the first fork causing a fork head-to-tail collision. The authors argued that this resulted in extrusion of the newly synthesized DNA from the replication bubble, which resulted in activation of the damage checkpoint. We were interested in whether fork head-to-tail collisions were responsible for the impaired fork progression during re-replication that we observe in yeast.

To test this idea we examined re-replication elongation when only a single round of re-replication was permitted. To do this we made use of a system in which we could stage re-replication pre-RC assembly and reinitiation. We made use a strain, MC_{2A} cdc7-1 (*MCM7-2NLS Δntcdc6-cdk2A cdc7-1*), which re-initiates primarily from a single origin, ARS317, in a manner dependent on the kinase CDC7 (Green *et al.*, 2006). We used the galactose inducible/dextrose repressible transcriptional control of *pGAL1-Δntcdc6-cdk2A* to control the re-assembly of pre-RCs. The conditional temperature-sensitive allele cdc7-1 was used to regulate the ability of origins to initiate.

MC2A cdc7-1 cells were arrested in G2/M by depletion of CDC20 and addition of nocodazole. The ability of cells to initiate was then turned off by raising the temperature to 35˚C to inactivate cdc7-1 (Figure 5A). Galactose was added to induce expression of pGAL-Δntcdc6-2A to allow pre-RC complexes to assemble on the chromatin. Dextrose was then added to transcriptionally repress pGAL-Δntcdc6-2A.

After one hour, the temperature was then lowered to reactivate cdc7-1 and allow origins to initiate. A parallel culture in which dextrose was not added underwent continuous reinitiation (Figure 5B).

When new initiation events were suppressed by the addition of dextrose, re-replication initiates at ARS317 at a low level (Figure 5C). New initiations events were not detected after 2 hours demonstrating that turning off initiation was effective. Interestingly, when only a single round of re-replication occurred cells still showed severely impaired fork progression. The replication profiles remained nearly entirely static after 2 hours. One would expect that any forks still able to elongate after 2 hours would cause an increase in copy number to the right of the profile. The lack of any change in the profile shows that the vast majority of the forks that were established were unable to progress. This suggests that even when a single round of re-replication occurs, fork progression was still impaired. While this does not rule out fork head-to-tail collisions as an important aspect of impaired elongation it suggests that there are additional barriers to fork progression during re-replication.

DISCUSSION

Microarray CGH can be used to monitor replication fork progression across the entire genome

We have demonstrated a method to monitor genome-wide replication fork progression in budding yeast. This assay allows the direct comparison of fork progression

at specific loci under different conditions while at the same time monitoring fork progression globally. Using this method we measured rates of replication fork progression that are in accordance with previously published estimates of replication elongation.

We applied this microarray CGH assay to study the fork progression from origins induced to re-initiate in G2/M, outside of the normal cell cycle regulated time of initiation. We observe that forks setup during re-replication are severely impaired in fork progression and cannot complete a single round of DNA synthesis. The population average rate of fork progression is at least five fold slower than normal S phase fork progression.

Replication forks are irreversibly stalling or collapsing during re-replication

It has been postulated that re-replication forks might stall or collapse more frequently if they are forced to travel longer distances than forks need to in S phase (Arias and Walter, 2007). Such longer distances are indeed required during re-replication because we have shown previously that far fewer origins re-initiate with high efficiency during re-replication when compared with S phase ((Green *et al.*, 2006), Supplemental Figure 1, Supplemental Figure 2). However, re-replication forks appear to have difficulty simply matching the performance of S phase forks. During S phase, replication forks can travel up to 100-200 kb ((Dershowitz and Newlon, 1993), (van Brabant *et al.*, 2001)). When re-replication is induced however the vast majority of forks seem to be far more limited with very few making it 100kb from the origin (Supplementary Fig 2). Thus it

appears that re-replication forks are not only forced to travel further than they would need to in S phase but are also less capable of traveling such distances.

The impaired fork progression that we observe during re-replication could be due to forks that elongate at slow rate or to forks that stall or collapse at high frequency. The data we have presented here is most consistent with a model in which forks emanating from origins are either irreversibly stalling or collapsing at a high frequency. Unlike in S phase replication, re-replication forks did not fill the valleys between the peaks and the shape of the profile did not flatten with increasing time. This was observed both when three mechanisms where deregulated (*orc2-cdk6A orc6-cdk4A MCM7-SVNLS$_2$ pGAL1-*Δ*ntcdc6*, Figure 3) and when two mechanisms were deregulated (*MCM7-SVNLS$_2$ pGAL1-*Δ*ntcdc6-cdk2A*, Figure 6B). These results indicate that existing replication forks do not progress significantly and are unable to finish replicating the chromosomes, i.e. they have irreversibly stalled and/or collapsed.

While our data is most consistent with replication forks stalling or collapsing, it does not exclude the possibility that re-replication forks are also traveling more slowly than S phase forks before they actually stop. Determining the rate of movement of individual forks during re-replication will require pulse-chase analysis of single re-replicating chromosomes through molecular combing. If such an analysis detects slower re-replication fork rates, it would raise the possibility that the stalling or collapse of these forks is the culmination of their exposure to continual stress.

Impaired fork progression may lead to DNA damage

Re-replication results in activation of the DNA damage response, double stranded breaks, chromosomal fragmentation and lethality (Green and Li, 2005), (Archambault *et al.*, 2005), (Vaziri *et al.*, 2003), (Melixetian *et al.*, 2004), (Zhu *et al.*, 2004), (Jin *et al.*, 2006), (Lovejoy *et al.*, 2006), (Zhu and Dutta, 2006). Such dire consequences suggest a rationale for why cells have evolved so many overlapping mechanisms to inhibit re-replication and raises the possibility that disruptions in the control of replication could be an underappreciated cause of genomic instability. However, there is no a priori reason why re-replication should lead to DNA damage. Our observation of impaired re-replication fork progression provides an experimental clue to why re-replication is so strongly associated with DNA damage.

The data we have presented suggest a model in which re-replication sets up impaired replication forks. These forks are unable to progress normally and may be poorly stabilized, resulting in a permanently stalled or collapsed fork. Such disrupted forks could then lead to DNA lesions, triggering the DNA damage response that we and others have observed (Archambault *et al.*, 2005; Green and Li, 2005). Importantly, while a large number of such lesions results in lethality, reduced levels of re-replication may produce a survivable amount of DNA damage that could lead to heritable genetic alterations. We have observed that limited re-replication can indeed promote genomic instability (unpublished data, B. Green). Our results here suggest that impaired re-replication fork progression may ultimately be responsible for this instability. Thus it is important to understand why the forks generated during re-replication behave so differently than the forks assembled during normal S phase replication.

What is causing impaired fork progression during re-replication?

Potential causes of impaired fork progression impaired can be broadly classified into two categories. In the first category, the replication fork is improperly assembled and thus fails to progress normally. This may be manifested as stochastic halting or failing to withstand challenges that S phase forks normally face, such as protein complexes bound to chromosomes. The second class of models are those in which the replication fork machinery itself is normal but the forks are confronted with challenges that do not exist in normal S phase and that they are not equipped to handle. For example, there may be differences between S and G2/M phase chromatin. Alternatively, forks from one round of replication could catch up and displace forks from the previous round. In both case the forks are challenged by something that is unique to the cell cycle position or to re-replication. We have addressed two of the most prominent of this second class of models.

Are nucleotides a limiting factor in re-replication fork progression

One appealing explanation for the impaired fork progression during G2/M re-replication is a lack of the nucleotide precursors needed for DNA synthesis. Since ribonucleotide reductase, which mediates a key step in deoxyribonucleotide synthesis, is down-regulated in a cell cycle dependent manner, we tested whether this enzyme was limiting during G2/M phase re-replication. We found, however, that removing two inhibitory controls on the cell cycle regulation of ribonucleotide reductase had no effect

on bulk DNA synthesis during re-replication. Thus it is unlikely that the defect in fork progression is due to a simple lack of nucleotides.

S phase replication forks stalled by hydroxyurea (HU) activate the replication stress checkpoint and cause phosphorylation of Rad53 in a manner dependent on the protein Mrc1 (Alcasabas *et al.*, 2001; Osborn and Elledge, 2003). Consistent with the idea that forks are not stalling due to insufficient nucleotides, we have previously shown that re-replication activates the DNA damage checkpoint and causes Rad53 phosphorylation in a Rad9 dependent and Mrc1 independent manner (Green and Li, 2005). This suggests that the defect in re-replication fork progression is different from that of S phase forks stalling from insufficient nucleotides. In addition, re-replication forks are capable of signaling through Mrc1 when they are stalled with HU. Thus re-replication forks are capable of responding to depleted nucleotides but normally do not. This strongly suggests that impaired fork progression during re-replication cannot be explained by insufficient nucleotides.

Finally, we also observed a defect in fork progression when only very limited re-replication occurs. The MC_{2A} strain, which has only two replication proteins deregulated, re-replicates most readily from one origin in Chromosome III. Despite this greatly reduced demand for dNTPs, fork progression from this origin is still severely impaired. Together, our results strongly suggests that insufficient nucleotides cannot account for the impaired fork progression observed during re-replication in G2/M phase.

Do fork head-to-tail collisions limit re-replication fork progression

It has recently been reported that multiple rounds of re-replication in *Xenopus* extracts causes DNA fragments to be extruded from the re-replicating template when a fork from one round catches up and collides with a fork from the preceding round. In fact, it was concluded that these head-to-tail fork collisions were the primary cause of DNA fragmentation and the DNA damage response observed in these extracts. We were thus interested in whether such head-to-tail collisions were essential for the defective re-replication fork progression we observed in budding yeast.

To address this question we examined fork progression in the MC2A strain, where re-initiation is already very limited. We staged the induction of re-initiation so as to further limit it to a single round at the beginning of the induction period, thereby discouraging head-to-tail fork collisions. Re-initiation was significantly curtailed, and the residual increase in origin copy number that did occur cannot be readily attributed to multiple rounds of initiation on individual chromosomes. Nonetheless, fork progression in this experiment was still severely impaired. This result suggests that in budding yeast impaired fork progression during re-replication is not solely caused by head-to-tail fork collisions. We suspect instead that the stalling or collapse of re-replication forks can directly lead to DNA breaks in the parental DNA. Such parental DNA breaks were not detected in the re-replicating Xenopus extracts. However, we note that any large fragments that might have resulted from such breaks would not have been resolvable with the assays that were used to characterize the small extruded DNA fragments.

Importantly, our experiments do not rule out a role for head-to-tail fork collisions in impairing fork progression during re-replication in budding yeast. In fact, we

speculate that in certain cases head-to-tail fork collisions do have a role. For example, when re-replication is induced during S phase the peaks tend to reach a higher average copy number but attain a narrower shape than in re-replication induced in G2/M ((Green *et al.*, 2006), data not shown). In these cases we suspect that increased re-initiation (higher peaks) could further impair fork progression (narrower peaks) through head-to-tail fork collisions.

Is the replication fork machinery assembled properly

Another possibility that we have not directly addressed here is there may be limited amounts of a critical component of the replication fork. It has been shown that limiting amounts of replication proteins can cause DNA damage and genomic instability in cells that are still able to complete replication (Gibson *et al.*, 2004). In addition, re-replication initiation is impaired relative to S phase because far fewer origins fire during re-replication. This reduced initiation is the result of reduced origin activation rather than defective pre-RC assembly (Tanny *et al.*, 2006). One possibility is that defective origin activation during re-replication results in forks that are missing critical components. It will be important to determine whether forks established during re-replication contain all the components of the S phase replication machinery.

REFERENCES

Alcasabas, A.A., Osborn, A.J., Bachant, J., Hu, F., Werler, P.J., Bousset, K., Furuya, K., Diffley, J.F., Carr, A.M., and Elledge, S.J. (2001). Mrc1 transduces signals of DNA replication stress to activate Rad53. Nat Cell Biol *3*, 958-965.

Archambault, V., Ikui, A.E., Drapkin, B.J., and Cross, F.R. (2005). Disruption of mechanisms that prevent rereplication triggers a DNA damage response. Mol Cell Biol *25*, 6707-6721.

Arias, E.E., and Walter, J.C. (2005). Replication-dependent destruction of Cdt1 limits DNA replication to a single round per cell cycle in Xenopus egg extracts. Genes Dev *19*, 114-126.

Arias, E.E., and Walter, J.C. (2007). Strength in numbers: preventing rereplication via multiple mechanisms in eukaryotic cells. Genes Dev *21*, 497-518.

Bell, S.P., and Dutta, A. (2002). DNA replication in eukaryotic cells. Annu Rev Biochem *71*, 333-374.

Chabes, A., Domkin, V., and Thelander, L. (1999). Yeast Sml1, a protein inhibitor of ribonucleotide reductase. J Biol Chem *274*, 36679-36683.

Davidson, I.F., Li, A., and Blow, J.J. (2006). Deregulated replication licensing causes DNA fragmentation consistent with head-to-tail fork collision. Mol Cell *24*, 433-443.

DeRisi, J.L., Iyer, V.R., and Brown, P.O. (1997). Exploring the metabolic and genetic control of gene expression on a genomic scale. Science *278*, 680-686.

Dershowitz, A., and Newlon, C.S. (1993). The effect on chromosome stability of deleting replication origins. Mol Cell Biol *13*, 391-398.

Diffley, J.F. (2004). Regulation of early events in chromosome replication. Curr Biol *14*, R778-786.

Drury, L.S., Perkins, G., and Diffley, J.F. (1997). The Cdc4/34/53 pathway targets Cdc6p for proteolysis in budding yeast. Embo J *16*, 5966-5976.

Drury, L.S., Perkins, G., and Diffley, J.F. (2000). The cyclin-dependent kinase Cdc28p regulates distinct modes of Cdc6p proteolysis during the budding yeast cell cycle. Curr Biol *10*, 231-240.

Elsasser, S., Chi, Y., Yang, P., and Campbell, J.L. (1999). Phosphorylation controls timing of Cdc6p destruction: A biochemical analysis. Mol Biol Cell *10*, 3263-3277.

Ferguson, B.M., Brewer, B.J., Reynolds, A.E., and Fangman, W.L. (1991). A yeast origin of replication is activated late in S phase. Cell *65*, 507-515.

Friedman, K.L., Diller, J.D., Ferguson, B.M., Nyland, S.V., Brewer, B.J., and Fangman, W.L. (1996). Multiple determinants controlling activation of yeast replication origins late in S phase. Genes Dev *10*, 1595-1607.

Gibson, D.G., Aparicio, J.G., Hu, F., and Aparicio, O.M. (2004). Diminished S-phase cyclin-dependent kinase function elicits vital Rad53-dependent checkpoint responses in Saccharomyces cerevisiae. Mol Cell Biol *24*, 10208-10222.

Green, B.M., and Li, J.J. (2005). Loss of rereplication control in Saccharomyces cerevisiae results in extensive DNA damage. Mol Biol Cell *16*, 421-432.

Green, B.M., Morreale, R.J., Ozaydin, B., Derisi, J.L., and Li, J.J. (2006). Genome-wide mapping of DNA synthesis in Saccharomyces cerevisiae reveals that mechanisms

preventing reinitiation of DNA replication are not redundant. Mol Biol Cell *17*, 2401-2414.

Guthrie, C., and Fink, G. (eds.) (1990). Guide to Yeast Genetics and Molecular Biology. Academic Press.

Haase, S.B., and Lew, D.J. (1997). Flow cytometric analysis of DNA content in budding yeast. Methods Enzymol *283*, 322-332.

Iyer, V.R., Horak, C.E., Scafe, C.S., Botstein, D., Snyder, M., and Brown, P.O. (2001). Genomic binding sites of the yeast cell-cycle transcription factors SBF and MBF. Nature *409*, 533-538.

Jallepalli, P.V., Brown, G.W., Muzi-Falconi, M., Tien, D., and Kelly, T.J. (1997). Regulation of the replication initiator protein p65cdc18 by CDK phosphorylation. Genes Dev *11*, 2767-2779.

Jin, J., Arias, E.E., Chen, J., Harper, J.W., and Walter, J.C. (2006). A family of diverse Cul4-Ddb1-interacting proteins includes Cdt2, which is required for S phase destruction of the replication factor Cdt1. Mol Cell *23*, 709-721.

Khodursky, A.B., Peter, B.J., Schmid, M.B., DeRisi, J., Botstein, D., Brown, P.O., and Cozzarelli, N.R. (2000). Analysis of topoisomerase function in bacterial replication fork movement: use of DNA microarrays. Proc Natl Acad Sci U S A *97*, 9419-9424.

Labib, K., Diffley, J.F., and Kearsey, S.E. (1999). G1-phase and B-type cyclins exclude the DNA-replication factor Mcm4 from the nucleus. Nat Cell Biol *1*, 415-422.

Lebofsky, R., Heilig, R., Sonnleitner, M., Weissenbach, J., and Bensimon, A. (2006). DNA replication origin interference increases the spacing between initiation events in human cells. Mol Biol Cell *17*, 5337-5345.

Lee, Y.D., and Elledge, S.J. (2006). Control of ribonucleotide reductase localization through an anchoring mechanism involving Wtm1. Genes Dev *20*, 334-344.

Lemoine, F.J., Degtyareva, N.P., Lobachev, K., and Petes, T.D. (2005). Chromosomal translocations in yeast induced by low levels of DNA polymerase a model for chromosome fragile sites. Cell *120*, 587-598.

Lengronne, A., Pasero, P., Bensimon, A., and Schwob, E. (2001). Monitoring S phase progression globally and locally using BrdU incorporation in TK(+) yeast strains. Nucleic Acids Res *29*, 1433-1442.

Li, A., and Blow, J.J. (2005). Cdt1 downregulation by proteolysis and geminin inhibition prevents DNA re-replication in Xenopus. Embo J *24*, 395-404.

Liku, M.E., Nguyen, V.Q., Rosales, A.W., Irie, K., and Li, J.J. (2005). CDK Phosphorylation of a Novel NLS-NES Module Distributed between Two Subunits of the Mcm2-7 Complex Prevents Chromosomal Rereplication. Mol Biol Cell *16*, 5026-5039.

Lovejoy, C.A., Lock, K., Yenamandra, A., and Cortez, D. (2006). DDB1 maintains genome integrity through regulation of Cdt1. Mol Cell Biol *26*, 7977-7990.

Machida, Y.J., Hamlin, J.L., and Dutta, A. (2005). Right place, right time, and only once: replication initiation in metazoans. Cell *123*, 13-24.

Melixetian, M., Ballabeni, A., Masiero, L., Gasparini, P., Zamponi, R., Bartek, J., Lukas, J., and Helin, K. (2004). Loss of Geminin induces rereplication in the presence of functional p53. J Cell Biol *165*, 473-482.

Mimura, S., Seki, T., Tanaka, S., and Diffley, J.F. (2004). Phosphorylation-dependent binding of mitotic cyclins to Cdc6 contributes to DNA replication control. Nature *431*, 1118-1123.

Moll, T., Tebb, G., Surana, U., Robitsch, H., and Nasmyth, K. (1991). The role of phosphorylation and the CDC28 protein kinase in cell cycle-regulated nuclear import of the S. cerevisiae transcription factor SWI5. Cell *66*, 743-758.

Nguyen, V.Q., Co, C., Irie, K., and Li, J.J. (2000). Clb/Cdc28 kinases promote nuclear export of the replication initiator proteins Mcm2-7. Curr Biol *10*, 195-205.

Nguyen, V.Q., Co, C., and Li, J.J. (2001). Cyclin-dependent kinases prevent DNA re-replication through multiple mechanisms. Nature *411*, 1068-1073.

Nordlund, P., and Reichard, P. (2006). Ribonucleotide reductases. Annu Rev Biochem *75*, 681-706.

Osborn, A.J., and Elledge, S.J. (2003). Mrc1 is a replication fork component whose phosphorylation in response to DNA replication stress activates Rad53. Genes Dev *17*, 1755-1767.

Petes, T.D., and Williamson, D.H. (1975). Fiber autoradiography of replicating yeast DNA. Exp Cell Res *95*, 103-110.

Raghuraman, M.K., Winzeler, E.A., Collingwood, D., Hunt, S., Wodicka, L., Conway, A., Lockhart, D.J., Davis, R.W., Brewer, B.J., and Fangman, W.L. (2001). Replication dynamics of the yeast genome. Science *294*, 115-121.

Rivin, C.J., and Fangman, W.L. (1980). Replication fork rate and origin activation during the S phase of Saccharomyces cerevisiae. J Cell Biol *85*, 108-115.

Scott, R.S., Truong, K.Y., and Vos, J.M. (1997). Replication initiation and elongation fork rates within a differentially expressed human multicopy locus in early S phase. Nucleic Acids Res *25*, 4505-4512.

Shimada, K., Pasero, P., and Gasser, S.M. (2002). ORC and the intra-S-phase checkpoint: a threshold regulates Rad53p activation in S phase. Genes Dev *16*, 3236-3252.

Simmons, L.A., Breier, A.M., Cozzarelli, N.R., and Kaguni, J.M. (2004). Hyperinitiation of DNA replication in Escherichia coli leads to replication fork collapse and inviability. Mol Microbiol *51*, 349-358.

Tanaka, S., and Diffley, J.F. (2002). Interdependent nuclear accumulation of budding yeast Cdt1 and Mcm2-7 during G1 phase. Nat Cell Biol *4*, 198-207.

Tanny, R.E., MacAlpine, D.M., Blitzblau, H.G., and Bell, S.P. (2006). Genome-wide Analysis of Re-replication Reveals Inhibitory Controls that Target Multiple Stages of Replication Initiation. Mol Biol Cell, (under review).

van Brabant, A.J., Buchanan, C.D., Charboneau, E., Fangman, W.L., and Brewer, B.J. (2001). An origin-deficient yeast artificial chromosome triggers a cell cycle checkpoint. Mol Cell *7*, 705-713.

Vaziri, C., Saxena, S., Jeon, Y., Lee, C., Murata, K., Machida, Y., Wagle, N., Hwang, D.S., and Dutta, A. (2003). A p53-dependent checkpoint pathway prevents rereplication. Mol Cell *11*, 997-1008.

Wilmes, G.M., Archambault, V., Austin, R.J., Jacobson, M.D., Bell, S.P., and Cross, F.R. (2004). Interaction of the S-phase cyclin Clb5 with an "RXL" docking sequence

in the initiator protein Orc6 provides an origin-localized replication control switch. Genes Dev *18*, 981-991.

Xu, W., Aparicio, J.G., Aparicio, O.M., and Tavare, S. (2006). Genome-wide mapping of ORC and Mcm2p binding sites on tiling arrays and identification of essential ARS consensus sequences in S. cerevisiae. BMC Genomics *7*, 276.

Zhang, Z., An, X., Yang, K., Perlstein, D.L., Hicks, L., Kelleher, N., Stubbe, J., and Huang, M. (2006). Nuclear localization of the Saccharomyces cerevisiae ribonucleotide reductase small subunit requires a karyopherin and a WD40 repeat protein. Proc Natl Acad Sci U S A *103*, 1422-1427.

Zhao, X., Muller, E.G., and Rothstein, R. (1998). A suppressor of two essential checkpoint genes identifies a novel protein that negatively affects dNTP pools. Mol Cell *2*, 329-340.

Zhu, W., Chen, Y., and Dutta, A. (2004). Rereplication by depletion of geminin is seen regardless of p53 status and activates a G2/M checkpoint. Mol Cell Biol *24*, 7140-7150.

Zhu, W., and Dutta, A. (2006). An ATR- and BRCA1-mediated Fanconi anemia pathway is required for activating the G2/M checkpoint and DNA damage repair upon rereplication. Mol Cell Biol *26*, 4601-4611.

TABLES

Table I. Plasmids used in this study

Plasmid	Key Features	Source
pJL806	*pGAL1 URA3*	Nguyen *et al.* 2001
pJL1489	*pGAL1-Δntcdc6 URA3*	Nguyen *et al.* 2001
YIp22	*pMET3-HA3-CDC20 TRP1*	Uhlmann *et al.* 2000
pBO1555	*pMET3-HA3-CDC20 NatMX4*	Green *et al.* 2005
pR306-ARS-ACS2	*ars1413-ACS2 URA3*	Friedman *et al.* 1996
pAG25	*NatMX4*	Goldstein *et al.* 1999
pUG6	*loxP–kanMX–loxP*	Guldener *et al.* 1996

Table II. Strains used in this study

Strain	Genotype	Source
YJL5493	*orc2-cdk6A orc6-cdk4A leu2 ura3-52::{pGAL1, URA3} trp1-289 ade2 ade3 MCM7-2NLS bar1Δ::LEU2 cdc20::{pMET3-HA3-CDC20, TRP1}*	(Green *et al.*, 2006)
YJL3249	*orc2-cdk6A orc6-cdk4A ura3-52::{pGAL1-Δntcdc6, URA3} trp1-289 leu2 ade2 ade3 MCM7-2NLS bar1Δ::LEU2 cdc20::{pMET3-HA3-CDC20, TRP1}*	(Green *et al.*, 2006)
YJL5821	*ORC2 ORC6 ura3-52::{pGAL1-Δntcdc6-cdk2A, URA3} trp1-289 leu2 ade2 ade3 MCM7-2NLS bar1Δ::LEU2 cdc20::{pMET3-HA3-CDC20, TRP1} cdc7-1*	(Green *et al.*, 2006)
YJL6180	*orc2-cdk6A orc6-cdk4A ura3-52::{pGAL1, URA3} trp1-289 leu2 ade2 ade3 MCM7-2NLS bar1Δ::LEU2 cdc20::{pMET3-HA3-CDC20, TRP1} ars1413-ACS ars1412Δ::loxp-KanMX4-loxp ars1411Δ::NatMX4*	This study
YJL6185	*orc2-cdk6A orc6-cdk4A ura3-52::{pGAL1-Δntcdc6, URA3} trp1-289 leu2 ade2 ade3 MCM7-2NLS bar1Δ::LEU2 cdc20::{pMET3-HA3-CDC20, TRP1} ars1413-ACS ars1412Δ::loxp-KanMX4-loxp ars1411Δ::NatMX4*	This study
YJL6844	*orc2-cdk6A orc6-cdk4A ura3-52::{pGAL1, URA3} trp1-289 leu2 ade2 ade3 MCM7-2NLS bar1Δ::LEU2 cdc20::{pMET3-HA3-CDC20, NatMX4} wtm1Δ::KanMX4 sml1Δ::TRP1*	This study
YJL6841	*orc2-cdk6A orc6-cdk4A ura3-52::{pGAL1-Δntcdc6, URA3} trp1-289 leu2 ade2 ade3 MCM7-2NLS bar1Δ::LEU2 cdc20::{pMET3-HA3-CDC20, NatMX4} wtm1Δ::KanMX4 sml1Δ::TRP1*	This study

Table III. Oligonucleotides used in this study

Oligo	Purpose	Sequence
OJL1717	*ars1411*Δ	5'-CAATCGAATTGCCATTTTTTTCCTGCTTACGTTCGATAGATAGCCAAATGCAGCTGAAGCTTCGTACGC-3'
OJL1718	*ars1411*Δ	5'-TACACCAATCAAACCTCAATGAGTGAAGCTTTGTACGTAGAAATACTGAAGCATAGGCCACTAGTGGATCTG-3'
OJL1719	*ars1412*Δ	5'-CGAGCAAATCAATGATAAGTACAAGTCCAATCGGACTGATTCGTAAAAATCAGCTGAAGCTTCGTACGC-3'
OJL1720	*ars1412*Δ	5'-CCACCAACTCCTCTCTACTTGCGTGTGTATTTGTTTGTATACATGTGTAAGCATAGGCCACTAGTGGATCTG-3'
OJL1732	*ars1413-ACS confirmation*	5'-TTCTGTCGTGGAGTTGGCTT-3'
OJL1733	*ars1413-ACS confirmation*	5'-AAAATGGCTGAGGGCTGTGT-3'
OJL1912	*wtm1*Δ	5'-TTTCCTAACATACGGTGGTTTATGT-3'
OJL1915	*wtm1*Δ	5'-ATAGAACTTCCTTATTCTGAGCCGT-3'

Table IV. The average rate of fork progression in S phase

	Fork rate during 0 min to 20 min kb/min	Fork rate during 20 min to 40 min kb/min
ARS1414	0.91 +/- 0.06	1.28 +/- 0.13
Other origins*	0.87 +/- 0.04	1.31 +/- 0.07

- Other origins is the average rate of fork progression measured at 24 origins

Table V. The average rate of fork progression during re-replication

Origin	Δntcdc6 expression (Gal/Dex) at 90min	Fork rate during 180 min - 240 min at 180 min peak height kb/min	Fork rate during 240 min - 300 min at 180 min peak height kb/min	Fork rate during 240 min - 300 min at 240 min peak height kb/min
ARS1414	Galactose	0.37 +/- 0.02	0.15 +/- 0.01	0.31 +/- 0.02
Other origins	Galactose	0.36 +/- 0.03	0.21 +/- 0.01	0.32+/- 0.02
ARS1414	Dextrose	0.26 +/- 0.09	0.11 +/- 0.02	0.27 +/- 0.05
Other origins	Dextrose	0.22 +/- 0.02	0.09 +/- 0.01	0.26 +/- 0.03

* 'Other origins' is the average rate of fork progression measured at 16 origins

Figure Legends

Figure 1 Use of microarray comparative genomic hybridization (CGH) to assay replication fork progression in S phase

A) Principle of using microarray CGH to monitor replication fork progression. Peaks in the replication profile correspond to sites of replication initiation. In this simplified schematic, there is no additional initiation after time zero. As replication proceeds and the forks move away from the origins the width of the peaks should spread at a rate determined by the average fork elongation rate of the population, estimated to be between 1 and 3 kb/min in budding yeast.

B) S phase progression of cells allowed to partially replicate in low concentrations of hydroxyurea (HU) followed by release into media lacking HU. The re-replication competent strain YJL6185 (*orc2-cdk6A orc6-cdk4A MCM7-SVNLS$_2$ pGAL1-*Δ*ntcdc6 pMET3-HA3-CDC20 ars1411*Δ *ars1412*Δ *ars1413-ACS)* containing deregulations of ORC, Mcm2-7 and Cdc6 and deletion of three origins on Chromosome XIV (*OMC ChrXIVars*Δ) was arrested in G1 phase with alpha factor and then released into S phase in the presence of HU for 180 min. Cells were then released into a G2/M arrest in absence of HU. Cells were sampled for flow cytometry every 60 min following release from alpha factor arrest and every 10 min following release from HU. The DNA content of the replicating cells calculated from the flow cytometry is indicated to the right of each time point.

C) Microarray CGH was performed on *OMC ChrXIV-3ars*Δ cells in the experiment described in Figure 1B. G1 phase genomic DNA was hybridized against S phase genomic DNA obtained 180 min after cells were released from G1 phase into media containing hydroxyurea (HU) and 20 min and 40 min following release from HU. The DNA content of the replicating cells at each time point, determined by flow cytometry from Figure 1B, was used as a normalization factor for the Cy5/Cy3 ratios. Normalized ratios representing the average DNA copy number of replicating cells were plotted against chromosomal position and mathematically smoothed to generate a replication profile. The replication profiles at 180 min, 200 min, and 220 min are shown for chromosome XIV. Chromosomal regions lacking data of sufficient quality are represented as gaps in the profiles. Positions of nim-ARSs mapped by Xu *et al.* (Xu *et al.*, 2006) (gray triangles), deleted origins (gray triangles marked with an X), a weak cryptic origin (open triangle) and the centromere (black circle) are plotted along the X-axis. The distance an S phase replication fork moving at a rate 1 kb/min would be able to travel in 40 min (40 kb) is indicated by a black bar.

Figure 1

A

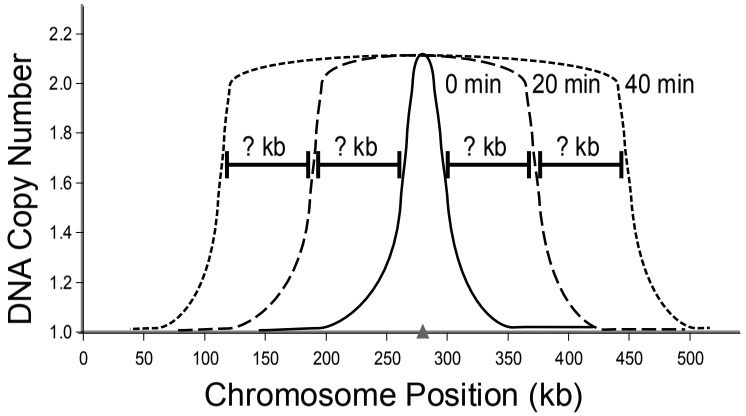
DNA Copy Number
Chromosome Position (kb)
0 min
20 min
40 min
? kb
? kb
? kb
? kb

B

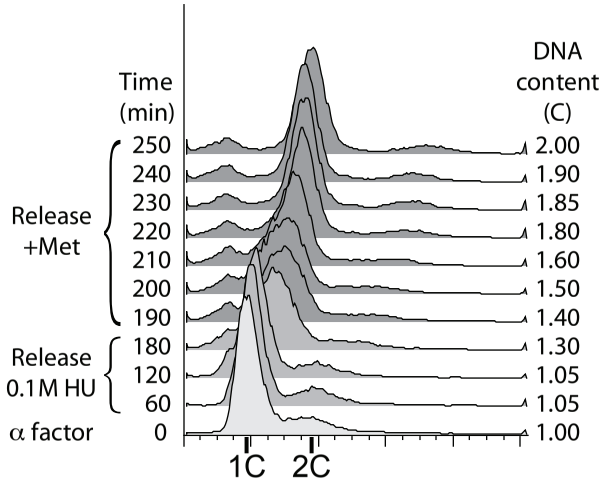
Time (min)
DNA content (C)
Release +Met
Release 0.1M HU
α factor
250 2.00
240 1.90
230 1.85
220 1.80
210 1.60
200 1.50
190 1.40
180 1.30
120 1.05
60 1.05
0 1.00
1C
2C

C

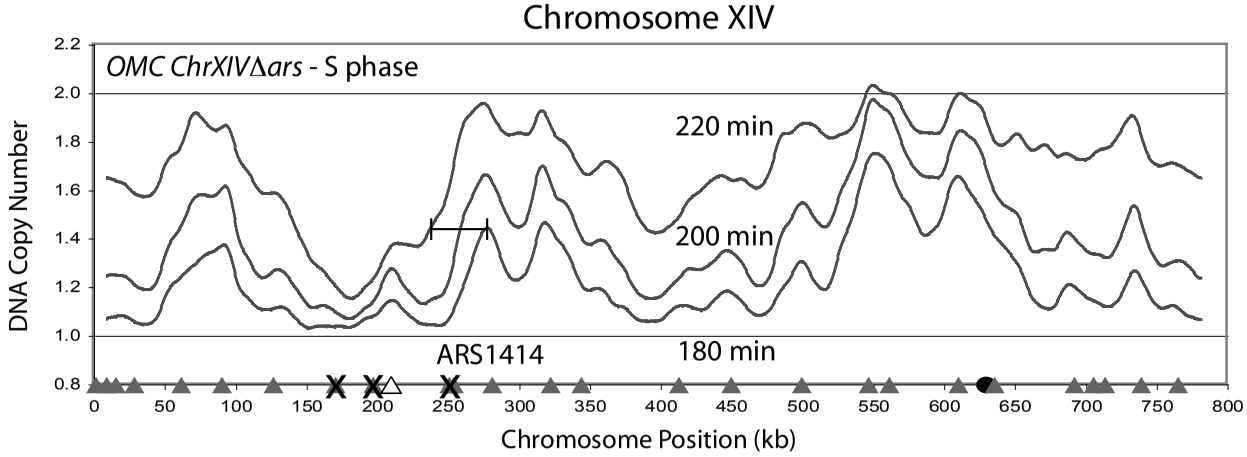
Chromosome XIV
OMC ChrXIVΔars - S phase
DNA Copy Number
220 min
200 min
180 min
ARS1414
Chromosome Position (kb)

Figure 2 Replication Fork progression is impaired during re-replication induced in G2/M phase.

A) Re-replication causes a slow continual increase in bulk DNA synthesis in G2/M phase cells. The *OMC ChrXIV-3ars*Δ strain YJL6185 (*orc2-cdk6A orc6-cdk4A MCM7-SVNLS$_2$ pGAL1-*Δ*ntcdc6 pMET3-HA3-CDC20 ars1411*Δ *ars1412*Δ *ars1413-ACS))* and the control *OM* strain YJL5493 (*orc2-cdk6A orc6-cdk4A MCM7-2NLS pGAL1 pMET3-HA3-CDC20*) were arrested in G2/M phase. Once arrested, galactose was added, which induced re-replication in the OMC strain. Samples were taken for flow cytometry at the indicated points after galactose addition. The DNA content of the re-replicating *OMC ChrXIV-3ars*Δ cells, calculated from the flow cytometry, is indicated to the right of each time point.

B) Genomic DNA was purified from the *OMC ChrXIV-3ars*Δ strain after 180 min, 240 min, and 300 min of galactose induction as described in Figure 2A and competitively hybridized against *OMC ChrXIV-3ars*Δ G1 phase genomic DNA. The *OMC ChrXIV-3ars*Δ G2/M phase re-replication profiles, positions of nim-ARSs mapped by Xu *et al.* (Xu *et al.*, 2006) (gray triangles), deleted origins (gray triangles marked with an X), a weak cryptic origin (open triangle), and the centromere (black circle) are shown for Chromosomes XIV. The distance an S phase replication fork moving at a rate 1 kb/min would be able to travel in 2 hour, 120 kb, is indicated by a black bar.

Figure 2

A

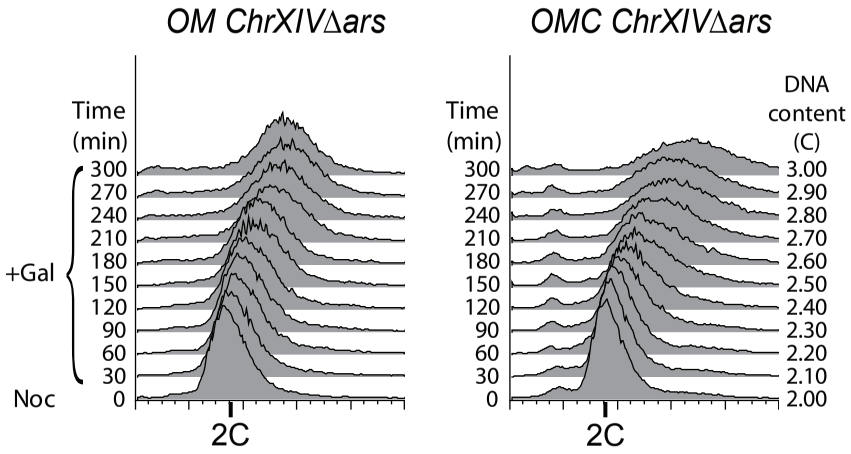
OM ChrXIVΔars
OMC ChrXIVΔars
Time (min)
DNA content (C)
+Gal
Noc
300
270
240
210
180
150
120
90
60
30
0
3.00
2.90
2.80
2.70
2.60
2.50
2.40
2.30
2.20
2.10
2.00
2C
2C

B

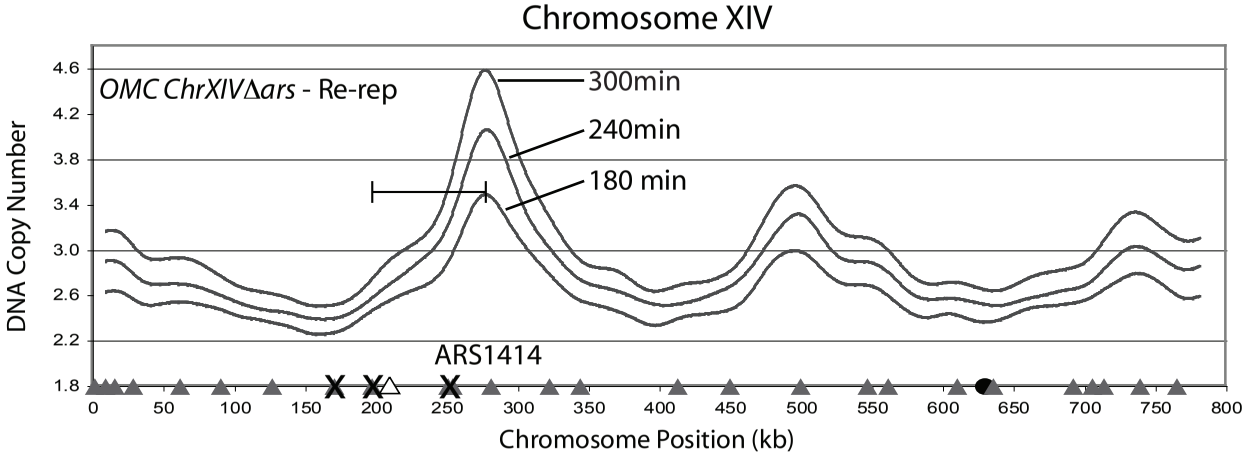
Chromosome XIV
OMC ChrXIVΔars - Re-rep
300min
240min
180 min
DNA Copy Number
4.6
4.2
3.8
3.4
3.0
2.6
2.2
1.8
ARS1414
0
50
100
150
200
250
300
350
400
450
500
550
600
650
700
750
800
Chromosome Position (kb)

Figure 3 Re-replication forks fail to complete replication of chromosomes following a pulse of re-replication.

A) Addition of dextrose reduces bulk DNA synthesis due to re-replication. The *OMC ChrXIV-3ars*Δ strain YJL6185 (*orc2-cdk6A orc6-cdk4A MCM7-SVNLS$_2$ pGAL1-*Δ*ntcdc6 pMET3-HA3-CDC20 ars1411*Δ *ars1412*Δ *ars1413-ACS))* and the control *OM* strain YJL5493 (*orc2-cdk6A orc6-cdk4A MCM7-2NLS pGAL1 pMET3-HA3-CDC20*) were arrested in G2/M phase. Once arrested, galactose was added, which induced re-replication in the OMC strain. After 90 min of galactose induction, dextrose was added to repress transcription of Δ*ntcdc6*. Samples were taken for flow cytometry at the indicated points. The DNA content of the re-replicating *OMC ChrXIV-3ars*Δ cells, calculated from the flow cytometry, is indicated to the right of each time point.

B) Genomic DNA was purified from the *OMC ChrXIV-3ars*Δ strain after 180 min, 240 min, and 300 min in the experiment described in Figure 2A and competitively hybridized against *OMC ChrXIV-3ars*Δ G1 phase genomic DNA. The *OMC ChrXIV-3ars*Δ G2/M phase re-replication profiles, positions of nim-ARSs mapped by Xu *et al.* (Xu *et al.*, 2006) (gray triangles), deleted origins (gray triangles marked with an X), a weak cryptic origin (open triangle), and the centromere (black circle) are shown for Chromosomes XIV. The distance an S phase replication fork moving at a rate 1 kb/min would be able to travel in 2 hour, 120 kb, is indicated by a black bar.

Figure 3

A

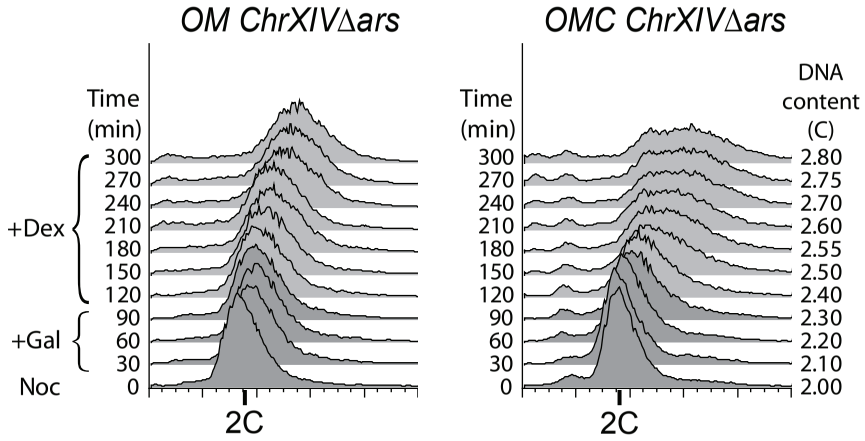
OM ChrXIVΔars
OMC ChrXIVΔars
Time (min)
DNA content (C)
+Dex
+Gal
Noc
300
270
240
210
180
150
120
90
60
30
0
2.80
2.75
2.70
2.60
2.55
2.50
2.40
2.30
2.20
2.10
2.00
2C
2C

B

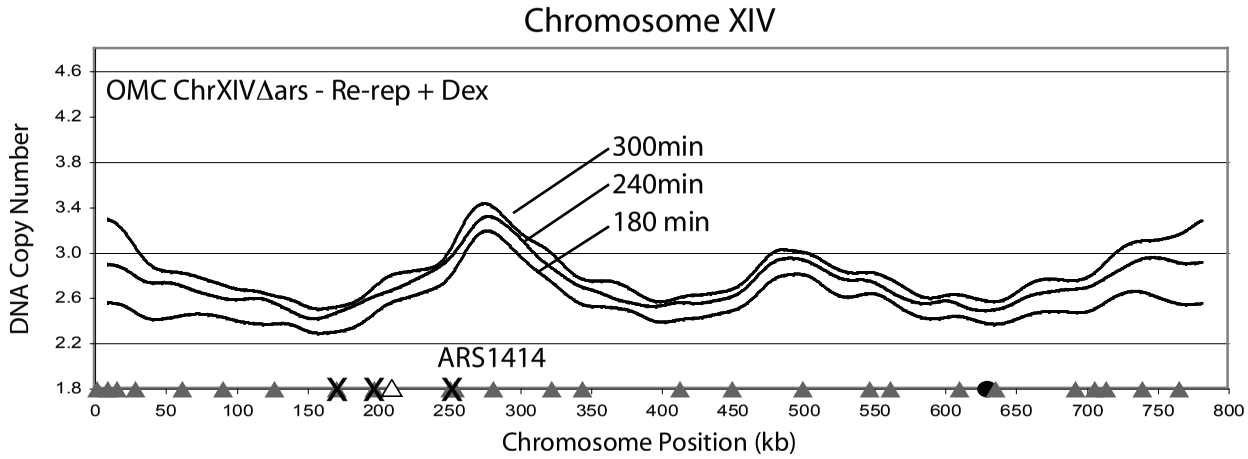
Chromosome XIV
OMC ChrXIVΔars - Re-rep + Dex
300min
240min
180 min
ARS1414
DNA Copy Number
4.6
4.2
3.8
3.4
3.0
2.6
2.2
1.8
0
50
100
150
200
250
300
350
400
450
500
550
600
650
700
750
800
Chromosome Position (kb)

Figure 4 Increasing nucleotide pools does not increase the amount of bulk DNA synthesis due to re-replication

The *OMC* strain YJL3249 (*orc2-cdk6A orc6-cdk4A MCM7-2NLS pGAL1-*Δ*ntcdc6 pMET3-HA3-CDC20)*, the control OM strain YJL5493 (*orc2-cdk6A orc6-cdk4A MCM7-2NLS pGAL1 pMET3-HA3-CDC20*), the *OMC sml1*Δ *wtm1*Δ strain YJL6841 (*orc2-cdk6A orc6-cdk4A MCM7-2NLS pGAL1-*Δ*ntcdc6 pMET3-HA3-CDC20 sml1*Δ *wtm1*Δ*)*, and the control *OM sml1*Δ *wtm1*Δ strain YJL6844 (*orc2-cdk6A orc6-cdk4A MCM7-2NLS pGAL1 pMET3-HA3-CDC20 sml1*Δ *wtm1*Δ) were arrested in G2/M phase. Once arrested, galactose was added, which induced re-replication in the *OMC* and *OMC sml1*Δ *wtm1*Δ strains. Samples were taken for flow cytometry at the indicated points after galactose addition.

Figure 4

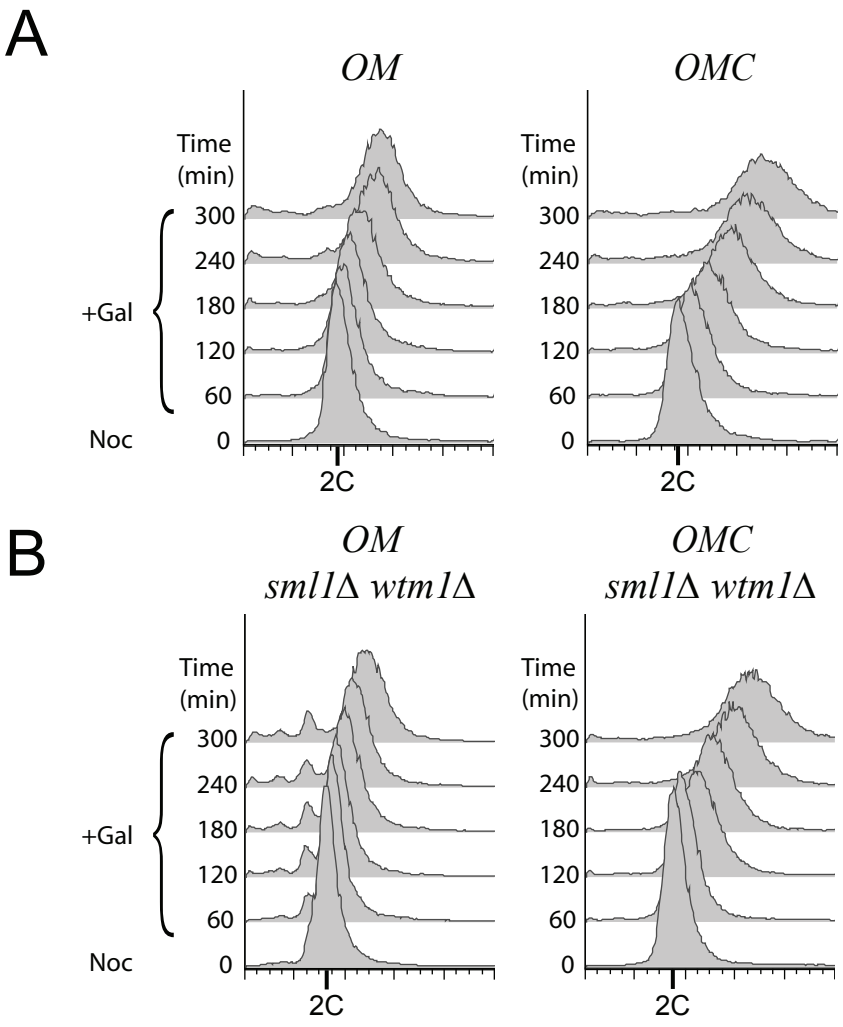
A
OM
OMC
Time (min)
300
240
180
120
60
0
+Gal
Noc
2C
B
OM
sml1Δ wtm1Δ
OMC
sml1Δ wtm1Δ

Figure 5 Replication fork progression is impaired after a single round of re-replication

A) Outline of experiment used to monitor fork progression after a single round of re-replication. The MC_{2A}-*cdc7* strain YJL5821 (*MCM7-2NLS pGAL1-*Δ*ntcdc6-2A pMET3-HA3-CDC20 cdc7-1*) was arrested at the permissive temperature in G2/M. The temperature was raised to the restrictive temperature, 35˚C, for 45 min to inactivate cdc7-1. Galactose was then added to induce expression of Δ*ntcdc6*, while maintaining cells at the restrictive temperature. After 1 hour the cells were split. One culture was maintained in galactose while dextrose was added to the other to suppress Δ*ntcdc6* transcription. After 1 hour the temperature was lowered to 23˚C to re-activate cdc7-1.

B and C) Genomic DNA was purified from the MC_{2A}-*cdc7* strain under conditions of continuous galactose induction (B) and dextrose repression (C) at 0 min, 120 min, and 240 min after lowering to the restrictive temperature in the experiment described in Figure 5A. Genomic DNA for each sample was competitively hybridized against MC_{2A}-*cdc7* G1 phase genomic DNA. The MC_{2A}-*cdc7* re-replication profiles, positions of nim-ARSs mapped by Xu *et al.* (Xu *et al.*, 2006) (gray triangles), and the centromere (black circle) are shown for Chromosomes III for both continuous galactose induction (B) and dextrose repression (C).

Figure 5

A

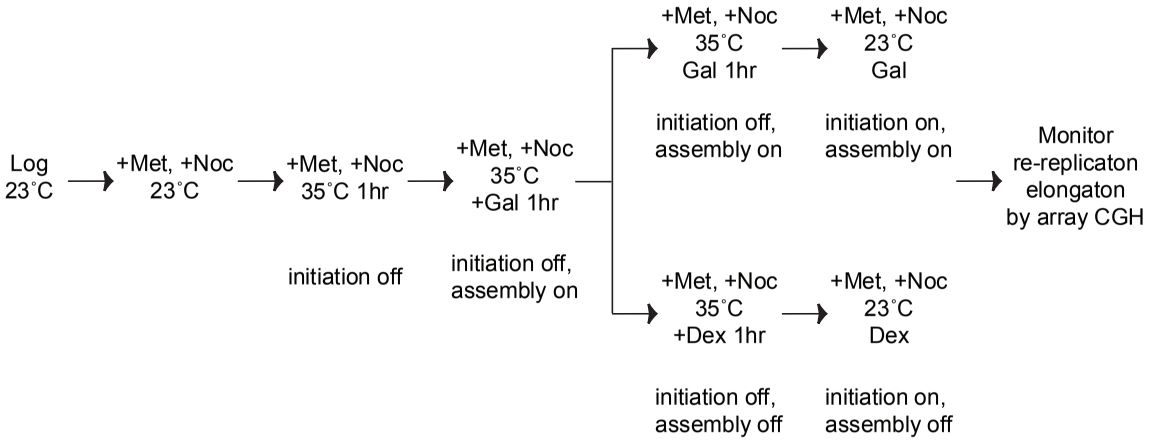
Log
23˚C
+Met, +Noc
23˚C
+Met, +Noc
35˚C 1hr
initiation off
+Met, +Noc
35˚C
+Gal 1hr
initiation off,
assembly on
+Met, +Noc
35˚C
Gal 1hr
initiation off,
assembly on
+Met, +Noc
23˚C
Gal
initiation on,
assembly on
+Met, +Noc
35˚C
+Dex 1hr
initiation off,
assembly off
+Met, +Noc
23˚C
Dex
initiation on,
assembly off
Monitor
re-replicaton
elongaton
by array CGH

B

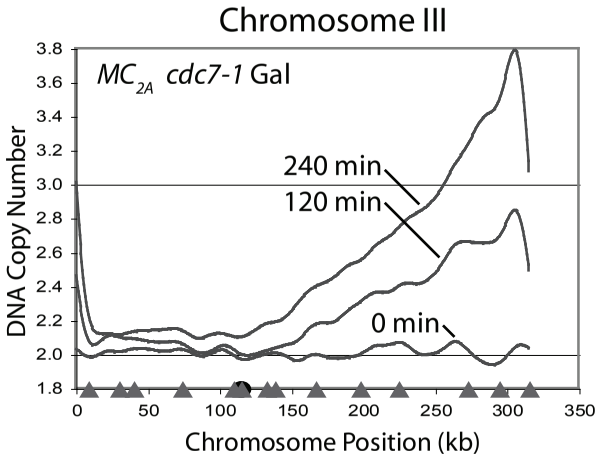
Chromosome III
MC2A cdc7-1 Gal
240 min
120 min
0 min
DNA Copy Number
Chromosome Position (kb)

C

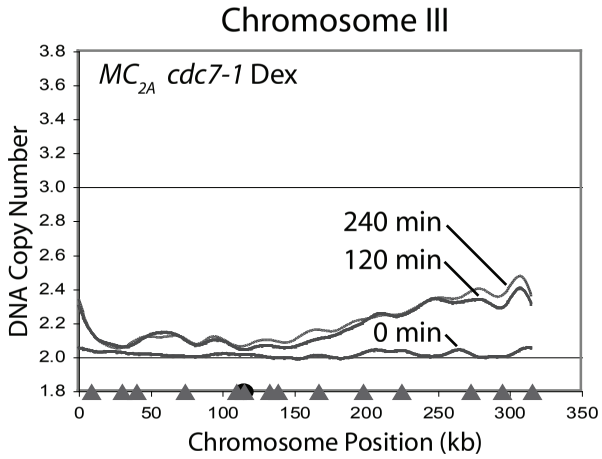
Chromosome III
MC2A cdc7-1 Dex
240 min
120 min
0 min
DNA Copy Number
Chromosome Position (kb)

CHAPTER 4

Conclusions

Eukaryotic cells orchestrate the initiation of DNA replication from hundreds of origins while at the same preventing reinitiation from any origin. Cells accomplish this with incredible fidelity allowing them to rapidly and accurately copying millions of base pairs each cell cycle. How cells accomplish this complex task has been a long-standing question. Recently, many of the mechanisms that prevent re-replication have been identified. When I began the research in this dissertation, it was not understood how these mechanisms interface with each other to achieve precise control of replication. In addition, very little was known about the nature of the DNA synthesis that occurred during re-replication. In Chapter 2, published in *Molecular Biology of the Cell* (Green *et al.*, 2006), we identified the locations of origins that reinitiated during different phases of the cell cycle, the origins that reinitiated when fewer mechanisms were disrupted, and the combinations of mechanisms whose loss resulted in re-replication. Chapter 3 (submitted) focused on research showing that re-replication fork progression was impaired and suggested a possible cause of re-replication induced DNA lesions.

In Chapter 2, I described our research on re-replication using a microarray based comparative genomic hybridization (CGH) assay, which I refined and streamlined. Improving the purity of the DNA preparation and optimization of the labeling protocol were critical to make this technology reliable and routine. Previous work in our lab had shown that several known S phase origins were able to reinitiate (Nguyen *et al.*, 2001). Using the comprehensive nature of this assay we were able to definitively show that the vast majority of re-initiation events were occurring from the normal S phase replication origins. Thus re-replication uses the same rules that govern which DNA sequences are capable of forming a pre-replicative complex (pre-RC) in S phase.

In contrast, the determinants that control replication timing in S phase do not appear to govern the efficiency of re-replication in G2/M. Several origins that replicate early in S phase do not detectably reinitiate during re-replication in G2/M whereas some late replicating origins such as *ARS317* do efficiently re-replicate. Identifying potential determinants of re-replication efficiency is a significant challenge. Aligning the location of efficient re-replication origins with existing genomic data sets does not immediately suggest a reason why some origins preferentially reinitiate in G2/M. Alignment of ARS sequences has been stymied because few origins have been mapped with sufficient resolution. Recently higher resolution identification of yeast origin locations have been published with many potential ACS sequences identified (Nieduszynski *et al.*, 2006; Xu *et al.*, 2006). The enhanced resolution of this data will greatly facilitate sequence alignments of origins making it feasible to identify sequence motifs that can predict if an origin is likely to reinitiate. Alternatively, deletion mapping of efficiently re-replicating origins such as *ARS317*, may yield insight into the determinants that sensitize certain origins to re-replication.

Deregulation of the mechanisms that prevent re-replication in S phase also caused significant re-replication. This demonstrated that these mechanisms function in both S and G2 phases of the cell cycle. A surprising result of our genome-wide analysis of S phase induced re-replication was that re-initiating origins were highly correlated with early replicating S phase origins. This is likely because these origins become available to reinitiate first since late initiating origins are still bound by the original pre-RC. It remains uncertain from our data whether normal S phase was completed when re-replication was induced. It is likely that the DNA damage induced by re-replication

activated the intra-S phase checkpoint, which inhibited the initiation of any unfired origins. Thus it would be interesting to know whether the existing S phase forks are disrupted by the re-replication.

Another major conclusion from the work presented in Chapter 2 was that re-replication can be detected after the deregulation of only two inhibitory mechanisms. Previous work in our lab (Nguyen *et al.*, 2001) had suggested that re-replication could only be observed after deregulation of three separate mechanisms. This led many in the field to assume that the mechanisms that prevent re-replication are redundant. We re-examined this issue and found that re-replication does occur when only two mechanisms were deregulated. Use of microarray CGH was critical to detect the re-replication because the amount of re-replication is reduced when fewer mechanisms are deregulated. This demonstrated that each mechanism acts to reduce the probability of re-replication. In addition, this clarifies how multiple mechanisms to prevent re-replication could be continually selected for and maintained during evolution.

An important implication of this work is that that very minor deregulations of re-replication could cause very low levels of sporadic re-replication. Re-replication leads to DNA damage and cell inviability (discussed below). Work in our lab has demonstrated that the lower amounts of re-replication are more survivable by the cell. This raises the possibility that rather than terminally arresting or undergoing apoptosis a cell might repair the damage and survive which could potentially lead to genomic instability. Genomic instability is a hallmark of cancer cells and is thought to be a driving force in tumorigenesis (Michor *et al.*, 2005; Coleman and Tsongalis, 2006; Jefford and Irminger-Finger, 2006; Raptis and Bapat, 2006). Recent work from our lab (Green, B unpublished

data) has demonstrated that re-replication can cause genomic instability in budding yeast. If this is also true in mammalian cells, then this raises the possibility that re-replication is an important causative agent of human disease.

Re-replication results in a DNA damage response, loss of viability, double strand breaks and chromosomal fragmentation (Vaziri *et al.*, 2003; Melixetian *et al.*, 2004; Archambault *et al.*, 2005; Green and Li, 2005; Lovejoy *et al.*, 2006; Zhu and Dutta, 2006). It was unclear in these experiments why re-replication resulted in DNA damage. One important finding was that re-replication triggered a DNA damage response rather than a replication stress response suggesting that replication forks were collapsing rather than stalling (Archambault *et al.*, 2005; Green and Li, 2005). Secondly, bulk DNA synthesis due to re-replication appeared more limited than could be accounted for by the number of origins that fired (Chapter 2, Figure 2).

In Chapter 3, I discuss research in which we demonstrate that replication fork progression is severely impaired during re-replication. Using microarray CGH, we demonstrate that this is a global phenomenon that occurs throughout the genome. We found that when new re-initiation events were limited re-replication forks were unable to complete replication of the chromosomes. These results were best explained by forks irreversible collapsing as there was little evidence of fork progression once new initiation events were repressed. When replication forks stall in S phase, a number of mechanisms exist to stabilize them, restart them, and aid their progression through certain chromosomal barriers (Tercero and Diffley, 2001; Cha and Kleckner, 2002; Pasero *et al.*, 2003; Calzada *et al.*, 2005; Szyjka *et al.*, 2005; Tourriere *et al.*, 2005; Azvolinsky *et al.*, 2006; Branzei and Foiani, 2006). Our results, however, suggest that the majority of re-

replication forks were not efficiently restarted since they never completed replication of the chromosomes.

Potential causes of impaired fork progression can be broadly classified into two categories. In the first category, the replication fork is improperly assembled and thus fails to progress normally. This may be manifested as stochastic halting or failing to withstand challenges that S phase forks are able to withstand. In the second class of models, the composition of the fork machinery is identical those in S phase but are confronted with challenges that do not exist during S phase and that they are not equipped to handle. For example, there could be differences in the cellular environment or chromatin structure in G2/M.

We initially ruled out one of the simplest models: that insufficient nucleotide pools in G2/M were causing replication forks to arrest. This was not unexpected since re-replication forks, despite being capable, do not activate the replication stress response (Green and Li, 2005). Another model that has been proposed is that defective chromatin assembly behind the replication fork, possibly because of insufficient free histones, could be responsible for the DNA damage. There is evidence in S phase that mutations in chromatin assembly genes can cause DNA damage and may disrupt the replication fork (Hoek and Stillman, 2003; Ye *et al.*, 2003; Franco *et al.*, 2005). Preliminary evidence suggests that re-replication causes upregulation of histone expression (Green, B unpublished data), however we cannot rule out a defect in the process of chromatin assembly.

One mechanism through which re-replication is able to cause DNA damage has been demonstrated in *Xenopus* (Davidson *et al.*, 2006). When high levels of Cdt1

induced massive re-replication, fragmented DNA that appeared to be extruded from the chromosome was observed. The authors proposed that the excessive Cdt1 levels induced multiple rounds of re-initiation, generating successive re-replication forks that followed each other down the chromosome. The second fork could potentially catch the first fork causing a collision. This would then cause extrusion of the DNA from the replication bubble, leaving the parental template DNA intact. In Chapter 3, I describe results that indicate that when only a single round of re-replication is permitted replication fork progression was still severely impaired. Thus, impaired re-replication forks are likely to be individually causing the DNA damage through an unknown mechanism. This is corroborated by evidence from our lab that re-replication generated subchromosomal fragments whose size was more consistent with broken chromosomes than extruded DNA molecules.

This does not rule out the possibility of that fork head-to-tail collisions are occurring at some origins in our experiments. At the most efficiently re-initiating origins we observed DNA copy number increases that indicate that multiple rounds of re-initiation must have occurred in some cells. In particular, re-replication induced during S phase generates significant DNA copy number increases at several origins (Chapter 2, Figure 4). It will be important to determine the relative contribution to the generation of DNA lesions by fork head-to-tail collisions and the impaired fork progression we have described.

The work presented here is an important step in understanding how cells achieve tight control to prevent re-replication and why this is essential for genomic integrity. This work established that each individual control mechanism has an overlapping but

nonredundant role in reducing the probability of a reinitiation event. I helped identify two constraints upon re-replication: limited origin initiation and impaired replication fork progression. This provided an important insight into how re-replication causes DNA lesions, which could potentially result in genomic instability. It will be important to extend this work to human cells to determine if re-replication initiation and fork progression are subject to the same constraints that we observed in yeast.

References

Archambault, V., Ikui, A.E., Drapkin, B.J., and Cross, F.R. (2005). Disruption of mechanisms that prevent rereplication triggers a DNA damage response. Mol Cell Biol *25*, 6707-6721.

Azvolinsky, A., Dunaway, S., Torres, J.Z., Bessler, J.B., and Zakian, V.A. (2006). The S. cerevisiae Rrm3p DNA helicase moves with the replication fork and affects replication of all yeast chromosomes. Genes Dev *20*, 3104-3116.

Branzei, D., and Foiani, M. (2006). The Rad53 signal transduction pathway: Replication fork stabilization, DNA repair, and adaptation. Exp Cell Res *312*, 2654-2659.

Calzada, A., Hodgson, B., Kanemaki, M., Bueno, A., and Labib, K. (2005). Molecular anatomy and regulation of a stable replisome at a paused eukaryotic DNA replication fork. Genes Dev *19*, 1905-1919.

Cha, R.S., and Kleckner, N. (2002). ATR homolog Mec1 promotes fork progression, thus averting breaks in replication slow zones. Science *297*, 602-606.

Coleman, W.B., and Tsongalis, G.J. (2006). Molecular mechanisms of human carcinogenesis. Exs, 321-349.

Davidson, I.F., Li, A., and Blow, J.J. (2006). Deregulated replication licensing causes DNA fragmentation consistent with head-to-tail fork collision. Mol Cell *24*, 433-443.

Franco, A.A., Lam, W.M., Burgers, P.M., and Kaufman, P.D. (2005). Histone deposition protein Asf1 maintains DNA replisome integrity and interacts with replication factor C. Genes Dev *19*, 1365-1375.

Green, B.M., and Li, J.J. (2005). Loss of rereplication control in Saccharomyces cerevisiae results in extensive DNA damage. Mol Biol Cell *16*, 421-432.

Green, B.M., Morreale, R.J., Ozaydin, B., Derisi, J.L., and Li, J.J. (2006). Genome-wide mapping of DNA synthesis in Saccharomyces cerevisiae reveals that mechanisms preventing reinitiation of DNA replication are not redundant. Mol Biol Cell *17*, 2401-2414.

Hoek, M., and Stillman, B. (2003). Chromatin assembly factor 1 is essential and couples chromatin assembly to DNA replication in vivo. Proc Natl Acad Sci U S A *100*, 12183-12188.

Jefford, C.E., and Irminger-Finger, I. (2006). Mechanisms of chromosome instability in cancers. Crit Rev Oncol Hematol *59*, 1-14.

Lovejoy, C.A., Lock, K., Yenamandra, A., and Cortez, D. (2006). DDB1 maintains genome integrity through regulation of Cdt1. Mol Cell Biol *26*, 7977-7990.

Melixetian, M., Ballabeni, A., Masiero, L., Gasparini, P., Zamponi, R., Bartek, J., Lukas, J., and Helin, K. (2004). Loss of Geminin induces rereplication in the presence of functional p53. J Cell Biol *165*, 473-482.

Michor, F., Iwasa, Y., Vogelstein, B., Lengauer, C., and Nowak, M.A. (2005). Can chromosomal instability initiate tumorigenesis? Semin Cancer Biol *15*, 43-49.

Nguyen, V.Q., Co, C., and Li, J.J. (2001). Cyclin-dependent kinases prevent DNA re-replication through multiple mechanisms. Nature *411*, 1068-1073.

Nieduszynski, C.A., Knox, Y., and Donaldson, A.D. (2006). Genome-wide identification of replication origins in yeast by comparative genomics. Genes Dev *20*, 1874-1879.

Pasero, P., Shimada, K., and Duncker, B.P. (2003). Multiple roles of replication forks in S phase checkpoints: sensors, effectors and targets. Cell Cycle *2*, 568-572.

Raptis, S., and Bapat, B. (2006). Genetic instability in human tumors. Exs, 303-320.

Szyjka, S.J., Viggiani, C.J., and Aparicio, O.M. (2005). Mrc1 is required for normal progression of replication forks throughout chromatin in S. cerevisiae. Mol Cell *19*, 691-697.

Tercero, J.A., and Diffley, J.F. (2001). Regulation of DNA replication fork progression through damaged DNA by the Mec1/Rad53 checkpoint. Nature *412*, 553-557.

Tourriere, H., Versini, G., Cordon-Preciado, V., Alabert, C., and Pasero, P. (2005). Mrc1 and Tof1 promote replication fork progression and recovery independently of Rad53. Mol Cell *19*, 699-706.

Vaziri, C., Saxena, S., Jeon, Y., Lee, C., Murata, K., Machida, Y., Wagle, N., Hwang, D.S., and Dutta, A. (2003). A p53-dependent checkpoint pathway prevents rereplication. Mol Cell *11*, 997-1008.

Xu, W., Aparicio, J.G., Aparicio, O.M., and Tavare, S. (2006). Genome-wide mapping of ORC and Mcm2p binding sites on tiling arrays and identification of essential ARS consensus sequences in S. cerevisiae. BMC Genomics *7*, 276.

Ye, X., Franco, A.A., Santos, H., Nelson, D.M., Kaufman, P.D., and Adams, P.D. (2003). Defective S phase chromatin assembly causes DNA damage, activation of the S phase checkpoint, and S phase arrest. Mol Cell *11*, 341-351.

Zhu, W., and Dutta, A. (2006). An ATR- and BRCA1-mediated Fanconi anemia pathway is required for activating the G2/M checkpoint and DNA damage repair upon rereplication. Mol Cell Biol *26*, 4601-4611.

APPENDIX 1

Supplemental data for Chapter 2

SUPPLEMENTAL MATERIALS AND METHODS

Plasmids

All plasmids are described in Table 1. Only pJL1488 (*pGAL1-*Δ*ntcdc6-cdk2A*) was constructed in this study. It contains the sequence 5'-TATGAGCGGCCGC-3' followed by *CDC6* from +139 to +1983 inserted in the *Sma*I site of pJL806 downstream of the *GAL1* promoter. This plasmid expresses a truncated Cdc6 with amino acids 2-47 replaced by amino acids S-G-R and with S354A and S372A alanine substitutions at the two remaining CDK consensus phosphorylation sites (S/T-P-X-K/R). The S354A mutation was marked with an *Nhe*I restriction site by introducing silent nucleotide substitutions T1059a and T1060g. The S372A mutation was marked with a *Nar*I restriction site by introducing silent nucleotide substitutions T1113g, T1114g, and T1116g. Amino acid and base substitutions are listed relative to the first amino acid and nucleotide, respectively, of the wild type *CDC6* ORF (+1); the starting amino acid or nucleotide is on the left, and the substitution is on the right.

Strain construction

All strains (Table 2) with the exception of YJL5038 were derived from YJL1737 (*MAT*a *orc2-cdk6A orc6-cdk4A leu2 ura3-52 trp1-289 ade2 ade3 bar1*Δ*::LEU2*) (Nguyen *et al.*, 2001). The *orc2-cdk6A* and *orc6-cdk4A* alleles encode mutant proteins in which alanine is substituted for the phosphoacceptor serines or threonines at all full CDK consensus phosphorylation sites (residues 16, 24, 70, 174, 188, and 206 for *orc2-cdk6A*, and residues 106, 116, 123, and 146 *orc6-cdk4A*). Plasmids pMP933 (*ORC2,*

URA3/EcoNI), pJL737 (*ORC6, URA3*/SphI), pJL1206 (*MCM7-2NLS, URA3*/AspI), pKI1260 (*MCM7-2nls3A*/AspI) (Nguyen *et al.*, 2001) and pPP117 *(cdc7-1, URA3*/ClaI) (Hollingsworth *et al.*, 1992) were used in 2-step gene replacements at their respective chromosomal loci. YIp22 (*pMET3-HA3-CDC20, TRP1*/MscI) (Uhlmann *et al.*, 2000) was used in a one-step gene replacement at the CDC20 locus. Plasmids pJL806 (*pGAL1, URA3*/StuI), pJL1488 (*pGAL1-*Δ*ntcdc6-cdk2A, URA3*/StuI), and pJL1489 (*pGAL1-*Δ*ntcdc6, URA3*/StuI) (Nguyen *et al.*, 2001) were inserted at the *URA3* locus by one step integration.

ARS316, *ARS317* and *ARS318* were deleted using PCR fragments containing KanMX6 or NatMX4 that were amplified, respectively, from pFA6a (Wach *et al.*, 1994)) or pAG25 (Goldstein and McCusker, 1999) using oligonucleotide primers shown in Table 3. The *ars316*Δ removes a 1.19 kb sequence containing *ARS316* and replaces it with a KanMX6 cassette (Poloumienko *et al.*, 2001). The *ars317*Δ removes a 99 bp sequence containing the ARS consensus sequence (ACS) and the ABF1 binding site and replaces it with a KanMX6 cassette. The *ars318*Δ removes an 89 bp sequence containing the ARS consensus sequence (ACS) and the ABF1 binding site and replaces it with a NatMX6 cassette.

YJL5038 (*MAT*a *his3*Δ*::KanMX leu2*Δ*0 met15*Δ*0 ura3*Δ*0 bar1*Δ*::NatMX4 can1*Δ*::pMFA1-HIS3::pMF*α*1-LEU2*) was derived from a cross between YJL4161 (YD02458, *MAT*a *his3*Δ*::KanMX4 leu2*Δ*0 met15*Δ*0 ura3*Δ*0*, from the Saccharomyces Genome Deletion Project) (Winzeler *et al.*, 1999) and YJL4954 (*MAT*α *bar1*Δ*::NatMX4 can1*Δ*::pMFA1-HIS3::pMF*α*1-LEU2 his3*Δ*1 leu2*Δ*0 lys2*Δ*0 ura3*Δ*0 met15*Δ*0*). YJL4954 was generated by deleting *BAR1* in Y3655 (*MAT*α *can1*Δ*::pMFA1-HIS3::pMF*α*1-LEU2*

his3Δ1 leu2Δ0 lys2Δ0 ura3Δ0 met15Δ0) (Tong *et al.*, 2004) using a PCR fragment containing NatMX4 amplified from pAG25 (Goldstein and McCusker, 1999) using oligonucleotide primers shown in Table 3.

2-D Gel Electrophoresis

Neutral-neutral two-dimensional (2D) gel analysis was performed essentially as described at http://fangman-brewer.genetics.washington.edu. The DNA preparation described there is a slight modification of the one used in Huberman *et al.* (Huberman *et al.*, 1987). The following modifications to the previous protocols were made. Thirty micrograms of DNA was digested with *Cla*I and *Bgl*II for analysis of ARS317. Digested DNA was then enriched for replication intermediates with BND cellulose as follows. 4 g BND cellulose (Sigma B6385) was boiled in 20 ml water in a 50 ml conical tube for 5 min then spun at 2,000 rpm for 2 min in a SX4750 rotor using a GS-6 centrifuge (Beckman). The BND cellulose was washed once with 20 ml water and twice with NET (1 M NaCl, 1 mM EDTA, 10 mM Tris, pH 8.0) buffer. 1 ml packed column volume of BND cellulose suspension was placed in a disposable chromatography column (BioRad 731-1550) for each sample and washed with 5 ml of NET buffer. 5 M NaCl was added to each DNA digest to a final concentration of 1 M and the DNA was loaded on the column by passing the sample through twice. The column was washed with 5 ml NET and eluted with 3 ml 50 ˚C NET plus 1.8% caffeine. 3 ml isopropanol was added to the eluate, mixed by inversion and placed on ice for 30 min. The samples were spun for 30 min at 10,000 rpm at 4 ˚C, and the pellet was washed with ice cold 70% ethanol before being air-dried and resuspended in 40 µl TE. Loading dye (final concentrations: 2% w/v Ficoll

400, 0.01 M EDTA, 2% w/v SDS, 0.025% w/v bromophenol blue, 0.025% xylene cyanol) was added to the pellet and the entire sample was loaded on the gel.

For direct comparison, up to four samples were electrophoresed in the second dimension in quadrants of a single large gel and transferred using the high-salt downward capillary transfer method (Ausubel *et al.*, 2000) together to a single membrane GeneScreen Plus nitrocellulose membrane (NEN) and cross-linked with 0.12 J of UV light in a UV Stratalinker 1800 (Stratagene). The ARS317 probe was generated by PCR amplification of yeast genomic DNA using primers OJL1607 and OJL1608 (Table 3). This probe was labeled with the MegaPrime DNA labeling kit (Amersham Pharmacia), hybridized with ExpressHyb (Clontech) per the manufacturer's instructions and detected on a Storm 860 PhosphorImager (Molecular Dynamics).

Array Design and Fabrication

PCR products representing every ORF and intergenic region were designed and amplified as previously described (DeRisi *et al.*, 1997; Iyer *et al.*, 2001). Intergenic regions larger than 1.5 kb were amplified in segments of at most 1.5 kb. Each of the PCR products was resuspended in 3X SSC and robotically arrayed onto poly-L-lysine coated glass slides as previously described (DeRisi *et al.*, 1997). The remaining poly-L-lysine was then blocked as previously described (DeRisi *et al.*, 1997) (protocol is available at http://derisilab.ucsf.edu/core/resources/index.html) with the following modifications. The hydration step was omitted and instead slides were incubated in 3X SSC 0.2% SDS at 65˚C for 5 min. Slides were washed successively with H_2O and 95% ethanol, and then

dried by centrifugation for 2 min at 500 rpm in a SX4750 rotor using a GS-6 centrifuge (Beckman) and processed as described previously.

Genomic DNA preparation for CGH

450 ml of culture was mixed with 2.25 ml of 20% sodium azide and added to 50 ml of frozen, –80 ˚C, 0.2 M EDTA, 0.1% sodium azide. Cells were pelleted, washed with 50 ml 4 ˚C TE (10 mM TrisCl 1 mM EDTA pH 7.5) and stored frozen at –80˚C. Pellets were resuspended in 4 ml Lysis buffer (2% Triton X-100, 1% SDS, 100 mM NaCl, 10 mM Tris-Cl, 1 mM EDTA pH8.0) and mixed with 4 ml of phenol:$CHCl_3$:isoamyl alcohol (25:25:1) and 8 ml 0.5 mm glass beads (BioSpec Products, Inc., Bartlesville, OK). The suspension was vortexed seven times for 2 min separated by 2 min intervals at room temperature until greater than 95% of the cells lysed. The lysate was diluted with 8 ml phenol:$CHCl_3$:isoamyl alcohol and 8 ml TE, and then centrifuged at 18,500 x g for 15 min at RT. After collecting the aqueous phase, the interphase was re-extracted with 8 ml TE, and the second aqueous phase from this re-extraction pooled with the first. The combined aqueous phases were extracted with an equal volume of $CHCl_3$. The bulk of the RNA in the extract was selectively precipitated by addition of 0.01 volume 5 M NaCl to 50 mM and 0.4 volumes isopropanol and centrifugation at 12,000 x g for 15 min at RT. The RNA pellet was discarded and an additional 0.4 volumes of isopropanol was added to the supernatant. The sample was pelleted, washed with 70% ethanol, dried, and resuspended with 5.3 ml 10 mM Tris-Cl, (pH 8) 1 mM EDTA 1 M NaCl. RNase A (Qiagen, Valencia, CA) was added to 225 µg/ml followed by incubation at 37ºC for 30 min. Proteinase K was then added to 350

µg/ml followed by incubation at 55 ˚C for 30 min. Finally, 0.6 ml of 10% (w/v) Cetyltrimethylammonium Bromide (CTAB) in 1 M NaCl (prewarmed to 65 °C) was added and the sample was incubated for 20 min at 65 ˚C before being extracted with 8 ml $CHCl_3$ and centrifuged at 6000 x g for 15 min at RT. The DNA in the aqueous phase was precipitated with 0.8 volumes isopropanol at RT, washed with 70% ethanol, dried, and resuspended in 10 ml Qiagen buffer QBT. DNA was loaded and purified on a Qiagen Genomic-tip 100/G column as per the manufacturer's instructions (Qiagen, Valencia, CA). The eluted DNA was precipitated with 0.8 volumes isopropanol at 4 ˚C, washed with 70% ethanol, dried, and resuspended in 250 µl 2 mM Tris pH 7.5. This highly purified genomic DNA (OD 260/280 1.82-1.86) was sheared by sonication with a Branson Sonifier 450 to an average fragment size of 500 bp. Isolating DNA of this purity is important for generating reproducible replication profiles.

Labeling and Hybridization

5 µg of sheared genomic DNA was randomly primed with 10 µg of N_9 nonomer by boiling for 5 min, then cooling on ice for 5 min. 5-(3-Aminoallyl)-2'-deoxyuridine 5'-triphosphate (Sigma A0410, St. Louis, MO) was incorporated into the primed genomic DNA in a 50 µl reaction containing 10 mM TrisHCl pH 7.5, 5 mM MgCl2, 7.5 mM dithiothreitol, 120 µM dATP, 120 µM dCTP, 120 µM dGTP, 20 µM dTTP, 100 µM 5-(3-Aminoallyl)-2'-deoxyuridine 5'-triphosphate, and 5 U Klenow fragment. The reaction was incubated at 37˚C for 4 hr, and the DNA was purified using the DNA Clean and Concentrator kit (Zymo Research, Orange, California). 15-40 nmol of Cy3 and Cy5 (Amersham, Piscataway, NJ) were then separately coupled to the appropriate DNA with

0.1 M $NAHCO_3$, pH 9.0 for 1 hr (Bozdech *et al.*, 2003), and the fluorescently labeled DNA purified using the DNA Clean and Concentrator kit (Zymo Research, Orange, California). For most hybridizations, the replicating or re-replicating DNA was labeled with Cy5 and the non-replicating control DNA was labeled with Cy3.

Cy3 and Cy5 labeled DNA were pooled in a 40 µl mixture containing 3X SSC, 25 mM HEPES pH 7.0, and 0.25% SDS. Samples denatured for 2 min at 100˚C and hybridized under a glass mSeries Lifterslip (Erie Scientific 25x40I-M-5227, Portsmouth, NH) to a microarray for 18-24 hours at 63˚C. Microarrays were washed successively in 0.85X SSC, 0.02%SDS and 0.035X SSC immediately before scanning. The microarrays were spun dry and scanned with a GenePix 4000B scanner (Axon Instruments Union City, California) in an enclosed chamber where atmospheric ozone was maintained below 10 ppb using two OI-45 Ozone Interceptors (Ozone solutions, Sioux Center, Iowa). Reducing Cy5 exposure to atmospheric ozone during the final drying and scanning is essential for obtaining reproducible replication profiles.

Data analysis

Genepix Pro 4.0 software (Axon Instruments, Union City, CA) was used for micorarray image analysis and quantification. Data were filtered to remove features that had (1) obvious defects, (2) saturated pixels, (3) regression R^2 values less than 0.5, or (4) fewer than 55% of their pixels with fluorescence intensity greater than 2 standard deviations above background. Data was also filtered to remove 1572 features that contain repetitive sequences from the analysis. The median of the ratios for each element was used for the raw Cy5/Cy3 value.

The raw ratios were normalized by multiplying each value by a scalar normalization factor chosen so that the average of the normalized values was equal to the DNA content of the cells. DNA content was calculated from the median of the flow cytometry profile after correcting for signal increase due to mitochondrial replication (detailed information on the calculation of DNA content is provided below). The raw data were then binned and smoothed essentially as described (Raghuraman *et al.*, 2001). In short, a moving median was calculated over a 10 kb window for every 0.5 kb location along the genome. If a given 10 kb window did not contain any raw data points after filtering it was defined as a no data zone and the binned value from the previous window was used for smoothing purposes. The binned data were then smoothed using Fourier Convolution Smoothing essentially as described (Raghuraman *et al.*, 2001). However, the equation for k(S) was incorrectly provided in part II.3 of the supplemental information of that paper. The correct equation is as follows (personal communication, Collingwood D.):

$$k(S) = \{\exp(-2^{-S} n^2) : \text{n is an integer satisfying } -\left[\frac{T}{2}\right] \le n \le T - 1 - \left[\frac{T}{2}\right]\}$$

In Raghuraman *et al.* (Raghuraman *et al.*, 2001) the optimal value for S was computationally determined for each chromosome for each experiment. While this was effective for replication profiles, we found that predetermined values for S resulted in better re-replication profiles. Thus, for all G2/M and G1 release re-replication profiles, the following values for S were used for each chromosome: I: 8, II: 9.75, III: 8.25, IV: 12, V: 9, VI: 8, VII: 10.5, VIII: 9, IX: 8.75, X: 9.5, XI: 9.25, XII: 10.5, XIII: 10.25, XIV: 9.75, XV: 10.75, XVI: 10.25.

In most cases, two hybridizations were performed from each of two independent genomic DNA preparations. For presentation purposes, the resulting four replication profiles were averaged into one composite profile. Table S2 contains the value at each chromosomal locus for each of the composite profiles in this manuscript. In the final replication profiles, no data regions as described above are presented as gaps in the profiles.

Peak Finding

In order to identify potential origins, all local maxima in the smoothed data were identified and filtered based on two parameters, slide and drop. The maxima that satisfy our slide and drop parameters define the origin list. Due to the very different nature of replication and re-replication, some peak finding parameters were different between the two types of profiles. Solely for peak finding purposes, the re-replication data were normalized to half of their DNA content, in order to use the same range of parameters as are used during replication.

The drop value is a semi global measure of peak height. For each maximum, drop is the difference between the Cy5/Cy3 ratio of that maximum and the lowest Cy5/Cy3 value within 15kb (replication) or 200kb (re-replication) on either side of that maximum. The slide value (Glynn *et al.*, 2004) is a local measure of peak height and is the difference between the Cy5/Cy3 ratio of the maxima being considered and the closest local minima on either side of the maxima. The total slide is the sum of the left slide and the right slide. For replication profiles, a local maxima was identified as a potential origin if the following conditions all apply: 1) the drop value was greater than 0.05, 2) the

left slide was greater than 0.005, 3) the right slide was greater than 0.005 and 4) the total slide was greater than 0.05 (replication) or 0.02 (re-replication). .

To identify a list of origins for a given experimental condition, duplicate microarrays were performed for each of two independent genomic DNA preparations, and the sets of potential origins from the four individual microarrays were merged as follows. Hierarchical clustering (average linkage) was used to identify locations where several individual microarray experiments had potential origins. If three of the four microarray experiments recorded a potential origin in a 15 kb region (replication) or two of the four within 20 kb (re-replication), the locations of those potential origins were averaged and reported as the origin position for the merged dataset. Table S3 contains the list of identified origins for all experiments for which peak finding was performed.

Scatter Plot

The locations of 351 pro-ARSs from all the budding yeast chromosomes except chromosomes IV and XI were obtained from Wyrick *et al.* (Wyrick *et al.*, 2001). These chromosomes were excluded because some of the strains used in our study have duplications of portions of these chromosomes. These genomic alterations do not have any effect on the extent or origin usage of either replication or re-replication (data not shown). For each pro-ARS, the normalized Cy5/Cy3 ratio of that chromosomal locus for replication or re-replication was plotted against the ratio at that locus of the other profile being compared. The linear regression formula and R^2 value are shown on the plot.

Normalization of Replication and Re-replication Profiles by Quantification of Flow Cytometry Data

Flow cytometry was used to calculate the DNA content in each experiment. The genomic replication profiles and re-replication profiles were then normalized to the calculated DNA content. Quantification of absolute DNA content in *Saccharomyces cerevisiae* is complicated by fact that roughly 10% of the total DNA in a yeast cell is mitochondrial. Furthermore, cell cycle independent mitochondrial DNA replication causes the peak of flow cytometry profile to gradually increases in cell cycle arrested yeast (Pichler *et al.*, 1997). This complicates the quantification of the absolute DNA content by flow cytometry in synchronized yeast cultures. The following calculations were used to correct for the increase in the flow cytometry peak due to mitochondrial replication and thus determine the actual DNA content from the observed flow cytometry peak.

Replication: G1 into 0.1M HU

First, the absolute increase in fluorescent intensity due to the duplication of the yeast genome was calculated for each strain. The fluorescence intensity for the G1 peak (p_{Asyn}^{1C}) and the G2 peak (p_{Asyn}^{2C}) were determined from the asynchronous sample collected for each strain at the beginning of each experiment. The values for the G1 and G2 peaks in asynchronous samples were determined by applying the cell cycle model described by Watson *et al*. (Watson *et al.*, 1987) using the computer software FlowJo (Tree Star, Inc., Ashland, OR). The peak value for cell cycle synchronized samples was determined by

taking the median of the flow cytometry graph. The difference (Δp) between these two peaks was the signal increase due to a single round of replication.

$$\Delta p = p_{Asyn}^{2C} - p_{Asyn}^{1C} \quad (1)$$

When cells are cell cycle arrested, mitochondria continue to replicate their DNA. Thus, the fluorescent intensity continues to increase in the absence of ongoing genomic DNA replication. Thus, the peak of the G1 synchronized cells (p_0^{1C}) is greater than the G1 peak in the asynchronous population (p_{Asyn}^{1C}). Therefore, when all the cells in a population reach the G1 arrest, the subsequent G2 peak will no longer be twice value of the G1 peak. The subsequent G2 peak will be G1 plus the increase due to duplication of the genomic DNA (Δp). For cells arrested in G1 with □ factor the calculated 2C value at time 0 (c_0^{2C}) was:

$$c_0^{2C} = p_0^{1C} + \Delta p \quad (2)$$

Cells were subsequently released from the G1 arrest into G2 in the presence of hydroxyurea to slow S phase and nocodazole to arrest cells in the subsequent G2. The calculated value of the G2 peak was confirmed by the measured position of peak when the cells reached the nocodazole arrest. The rightward shift in the flow cytometry peak due to genomic independent (mitochondrial) replication was reduced in the presence of hydroxyurea. It has previously been shown that mitochondrial DNA copy number is

sensitive to nucleotide levels, which could explain the lack of further shift (Taylor *et al.*, 2005).

To calculate the extent of replication following synchronous release from factor an equation relating DNA content to the flow cytometry peak was generated using the measured G1 peak (p_0^{1C}) and calculated G2 peak (c_0^{2C}) as endpoints. In other words, since it is possible to correlate flow cytometry peak value to DNA content at 1C and 2C, a line connecting those points would enable us to determine the DNA content represented by any measured flow cytometry peak value between those two points. Thus, a linear regression line of the form $d = mp + b$ was generated where d is the DNA content, p is the median of the flow cytometry peak for a sample, m is the slope and b is the intercept. For a given time point (t) the median of the flow cytometry data (p_t) was used to calculate the DNA content (d_t). This value was then used as the normalization factor for the corresponding genomic replication profile. The DNA content of the G1 peak (d_{1C}) was one and the G2 peak (d_{2C}) was two.

$$d_t = \overbrace{\left(\frac{d_{2C} - d_{1C}}{c_0^{2C} - p_0^{1C}}\right)}^{m} p_t + \overbrace{\left[d_{1C} - \left(\frac{d_{2C} - d_{1C}}{c_0^{2C} - p_0^{1C}}\right) p_0^{1C}\right]}^{b} \qquad (3)$$

Re-replication: G2/M

A similar approach was used to correct for the shift in the flow cytometry peak due to mitochondrial replication during G2 arrest and induction of re-replication. For each re-replicating strain containing *pGAL1*-Δ*ntcdc6* there was a complementary *pGAL1* control strain. This *pGAL1* control did not re-replicate but did experience the genomic re-

replication independent shifting of the flow cytometry peak. Thus, its shift could be used to correct for re-replication independent shift in the re-replicating strain. At a given time point this shift (s_t^{pGAL1}) was the difference of the median of the flow cytometry data of the *pGAL1* control at the start the experiment ($p_0^{2C,pGAL1}$) and the median at the time of interest (p_t^{pGAL1}):

$$s_t^{pGAL1} = p_t^{pGAL1} - p_0^{2C,pGAL1} \quad (4)$$

The corrected value of the re-replicating strain's flow cytometry peak (f_t^{rerep}) at a given time was calculated by subtracting s_t^{pGAL1} from the median of the measured flow cytometry peak in the re-replicating strain (p_t^{rerep}).

$$f_t^{rerep} = p_t^{rerep} - s_t^{pGAL1} \quad (5)$$

As in the S phase experiments, the absolute increase in fluorescent intensity due to the duplication of the genome (Δp^{rerep}) was calculated using the G1 peak ($p_{Asyn}^{1C,rerep}$) and G2 peak ($p_{Asyn}^{2C,rerep}$) from the asynchronous sample of the *pGAL1*-Δ*ntcdc6* re-replicating strains.

$$\Delta p^{rerep} = p_{Asyn}^{2C,rerep} - p_{Asyn}^{1C,rerep} \quad (6)$$

Next, the value of a hypothetical 4C peak ($c_0^{4C,rerep}$) was calculated by adding twice Δp^{rerep} to the measured value of the G2/M arrested peak ($p_0^{2C,rerep}$).

$$c_0^{4C,rerep} = p_0^{2C,rerep} + 2(\Delta p^{rerep}) \tag{7}$$

A linear regression line $d = mf + b$ was generated similar to the S phase experiment above where d is the DNA content, f is the corrected median of the FACS peak for a sample, m is the slope and b is the intercept. For a given time point (t) the corrected median of the flow cytometry data (f_t^{rerep}) was used to calculate the DNA content (d_t). This value was then used as the normalization factor for the corresponding genomic re-replication profile. The DNA content of the G2 peak (d_{2C}) was two and the hypothetical 4C peak (d_{4C}) was four.

$$d_t = \overbrace{\left(\frac{d_{4C} - d_{2C}}{c_0^{4C,rerep} - p_0^{2C,rerep}}\right)}^{m} f_t^{rerep} + \overbrace{\left[d_{2C} - \left(\frac{d_{4C} - d_{2C}}{c_0^{4C,rerep} - p_0^{2C,rerep}}\right) p_0^{2C,rerep}\right]}^{b} \tag{8}$$

Re-replication: G1 into G2/M

As in the S phase experiments, the absolute increase in fluorescent intensity due to the duplication of the genome (Δp) was calculated using the G1 peak (p_{Asyn}^{1C}) and G2 peak (p_{Asyn}^{2C}) from asynchronous samples of both the *pGAL1* control and *pGAL1-*Δ*ntcdc6* re-replicating strains.

$$\Delta p^{pGAL1} = p_{Asyn}^{2C,pGAL1} - p_{Asyn}^{1C,pGAL1} \quad (9)$$

$$\Delta p^{rerep} = p_{Asyn}^{2C,rerep} - p_{Asyn}^{1C,rerep} \quad (10)$$

In this type of experiment the flow cytometry peak for the *pGAL1* control will increase for two reasons: genomic replication and genomic independent (mitochondrial) replication. The flow cytometry peaks in the *pGAL1*-Δ*ntcdc6* re-replicating strains will increase for up to three reasons: genomic replication, genomic independent (mitochondrial) replication and potentially re-replication. The value of the subsequent G2 peak ($c_0^{2C,pGAL1}$), which accounts for genomic replication, was calculated for the *pGAL1* control and *pGAL1*-Δ*ntcdc6* re-replicating strain.

$$c_0^{2C,pGAL1} = p_0^{1C,pGAL1} + \Delta p^{pGAL1} \quad (11)$$

$$c_0^{2C,rerep} = p_0^{1C,rerep} + \Delta p^{rerep} \quad (12)$$

The value of the fluorescence increase due to genomic replication independent (mitochondrial) shifting (s_t^{pGAL1}) was calculated from the *pGAL1* control strain by subtracting the calculated value of G2 peak ($c_0^{2C,pGAL1}$) from the median of the flow cytometry data at the cells were harvested (p_t^{pGAL1}).

$$s_t^{pGAL1} = p_t^{pGAL1} - c_0^{2C,pGAL1} \quad (13)$$

The shift (s_t^{pGAL1}) was then used to correct the observed flow cytometry peak of the re-replicating strain such that the peak value would reflect only the increases due to genomic replication and re-replication. The corrected value of the flow cytometry peak (f_t^{rerep}) was determined by subtracting s_t^{pGAL1} from the measured median of the flow cytometry data in the re-replicating strain (p_t^{rerep}).

$$f_t^{rerep} = p_t^{rerep} - s_t^{pGAL1} \tag{14}$$

Next, the value of a hypothetical 4C peak ($c_0^{4C,rerep}$) was calculated by adding three times Δp^{rerep} to the measured value of the G1 arrested peak ($p_0^{1C,rerep}$).

$$c_0^{4C,rerep} = p_0^{1C,rerep} + 3(\Delta p^{rerep}) \tag{15}$$

Finally, a linear regression line $d = mf + b$ was generated similar to the above experiments where d is the DNA content, f is the corrected median of the FACS peak for a sample, m is the slope and b is the intercept. For a given time point (t) the corrected median of the flow cytometry data (f_t^{rerep}) was used to calculate the DNA content (d_t). This value was then used as the normalization factor for the corresponding genomic re-replication profile. The DNA content of the G2 peak (d_{2C}) was two and the hypothetical 4C peak (d_{4C}) was four.

$$d_t = \overbrace{\left(\frac{d_{4C} - d_{2C}}{c_0^{4C,rerep} - c_0^{2C,rerep}}\right)}^{m} f_t^{rerep} + \overbrace{\left[d_{2C} - \left(\frac{d_{4C} - d_{2C}}{c_0^{4C,rerep} - c_0^{2C,rerep}}\right) c_0^{2C,rerep}\right]}^{b} \quad (16)$$

Re-replication: G1 into HU

The DNA content for re-replication induced from G1 into hydroxyurea was calculated as in the S phase experiments (Replication: G1 into HU) in the absence of induction of re-replication.

REFERENCES

Ausubel, F.M., Brent, R., Kinsgbury, R.E., Moore, D.D., Seidman, J.G., Smith, J.A., and Struhl, K. (2000). Current Protocols in Molecular Biology. John Wiley & Soncs, Inc.: New York.

Bozdech, Z., Zhu, J., Joachimiak, M.P., Cohen, F.E., Pulliam, B., and DeRisi, J.L. (2003). Expression profiling of the schizont and trophozoite stages of Plasmodium falciparum with a long-oligonucleotide microarray. Genome Biol *4*, R9.

DeRisi, J.L., Iyer, V.R., and Brown, P.O. (1997). Exploring the metabolic and genetic control of gene expression on a genomic scale. Science *278*, 680-686.

Glynn, E.F., Megee, P.C., Yu, H.G., Mistrot, C., Unal, E., Koshland, D.E., DeRisi, J.L., and Gerton, J.L. (2004). Genome-wide mapping of the cohesin complex in the yeast Saccharomyces cerevisiae. PLoS Biol *2*, E259.

Goldstein, A.L., and McCusker, J.H. (1999). Three new dominant drug resistance cassettes for gene disruption in Saccharomyces cerevisiae. Yeast *15*, 1541-1553.

Hollingsworth, R.E., Jr., Ostroff, R.M., Klein, M.B., Niswander, L.A., and Sclafani, R.A. (1992). Molecular genetic studies of the Cdc7 protein kinase and induced mutagenesis in yeast. Genetics *132*, 53-62.

Huberman, J.A., Spotila, L.D., Nawotka, K.A., el-Assouli, S.M., and Davis, L.R. (1987). The in vivo replication origin of the yeast 2 microns plasmid. Cell *51*, 473-481.

Iyer, V.R., Horak, C.E., Scafe, C.S., Botstein, D., Snyder, M., and Brown, P.O. (2001). Genomic binding sites of the yeast cell-cycle transcription factors SBF and MBF. Nature *409*, 533-538.

Nguyen, V.Q., Co, C., and Li, J.J. (2001). Cyclin-dependent kinases prevent DNA re-replication through multiple mechanisms. Nature *411*, 1068-1073.

Pichler, S., Piatti, S., and Nasmyth, K. (1997). Is the yeast anaphase promoting complex needed to prevent re-replication during G2 and M phases? Embo J *16*, 5988-5997.

Poloumienko, A., Dershowitz, A., De, J., and Newlon, C.S. (2001). Completion of replication map of Saccharomyces cerevisiae chromosome III. Mol Biol Cell *12*, 3317-3327.

Raghuraman, M.K., Winzeler, E.A., Collingwood, D., Hunt, S., Wodicka, L., Conway, A., Lockhart, D.J., Davis, R.W., Brewer, B.J., and Fangman, W.L. (2001). Replication dynamics of the yeast genome. Science *294*, 115-121.

Taylor, S.D., Zhang, H., Eaton, J.S., Rodeheffer, M.S., Lebedeva, M.A., O'Rourke T, W., Siede, W., and Shadel, G.S. (2005). The conserved Mec1/Rad53 nuclear checkpoint pathway regulates mitochondrial DNA copy number in Saccharomyces cerevisiae. Mol Biol Cell *16*, 3010-3018.

Tong, A.H., Lesage, G., Bader, G.D., Ding, H., Xu, H., Xin, X., Young, J., Berriz, G.F., Brost, R.L., Chang, M., Chen, Y., Cheng, X., Chua, G., Friesen, H., Goldberg, D.S., Haynes, J., Humphries, C., He, G., Hussein, S., Ke, L., Krogan, N., Li, Z., Levinson, J.N., Lu, H., Menard, P., Munyana, C., Parsons, A.B., Ryan, O., Tonikian, R., Roberts, T., Sdicu, A.M., Shapiro, J., Sheikh, B., Suter, B., Wong, S.L., Zhang, L.V., Zhu, H., Burd, C.G., Munro, S., Sander, C., Rine, J., Greenblatt, J., Peter, M., Bretscher, A., Bell, G., Roth, F.P., Brown, G.W., Andrews, B., Bussey, H., and Boone, C. (2004). Global mapping of the yeast genetic interaction network. Science *303*, 808-813.

Uhlmann, F., Wernic, D., Poupart, M.A., Koonin, E.V., and Nasmyth, K. (2000). Cleavage of cohesin by the CD clan protease separin triggers anaphase in yeast. Cell *103*, 375-386.

Wach, A., Brachat, A., Pohlmann, R., and Philippsen, P. (1994). New heterologous modules for classical or PCR-based gene disruptions in Saccharomyces cerevisiae. Yeast *10*, 1793-1808.

Watson, J.V., Chambers, S.H., and Smith, P.J. (1987). A pragmatic approach to the analysis of DNA histograms with a definable G1 peak. Cytometry *8*, 1-8.

Winzeler, E.A., Shoemaker, D.D., Astromoff, A., Liang, H., Anderson, K., Andre, B., Bangham, R., Benito, R., Boeke, J.D., Bussey, H., Chu, A.M., Connelly, C.,

Davis, K., Dietrich, F., Dow, S.W., El Bakkoury, M., Foury, F., Friend, S.H., Gentalen, E., Giaever, G., Hegemann, J.H., Jones, T., Laub, M., Liao, H., Liebundguth, N., Lockhart, D.J., Lucau-Danila, A., Lussier, M., M'Rabet, N., Menard, P., Mittmann, M., Pai, C., Rebischung, C., Revuelta, J.L., Riles, L., Roberts, C.J., Ross-MacDonald, P., Scherens, B., Snyder, M., Sookhai-Mahadeo, S., Storms, R.K., Veronneau, S., Voet, M., Volckaert, G., Ward, T.R., Wysocki, R., Yen, G.S., Yu, K., Zimmermann, K., Philippsen, P., Johnston, M., and Davis, R.W. (1999). Functional characterization of the S. cerevisiae genome by gene deletion and parallel analysis. Science *285*, 901-906.

Wyrick, J.J., Aparicio, J.G., Chen, T., Barnett, J.D., Jennings, E.G., Young, R.A., Bell, S.P., and Aparicio, O.M. (2001). Genome-wide distribution of ORC and MCM proteins in S. cerevisiae: high-resolution mapping of replication origins. Science *294*, 2357-2360.

Table S1. CGH on spotted microarrays accurately identifies S phase replication origins. Our analysis of the replication of a wild type yeast in the S288c background identified 212 replication origins throughout the genome, which is roughly comparable to the numbers obtained by Rhaguraman *et al.* (Raghuraman *et al.*, 2001) (332) and Yabuki *et al.* (Yabuki *et al.*, 2002) (260). Origins on chromosome III (Greenfeder and Newlon, 1992; Poloumienko *et al.*, 2001), VI (Yamashita *et al.*, 1997), V (Tanaka *et al.*, 1996) and X (Wyrick *et al.*, 2001) have been systematically mapped by 2-D gel electrophoresis and and/or ARS plasmid assay, and annotated in the Saccharomyces Genome Database (SGD) (Balakrishnan). For each origin that was identified on chromosome III, V, VI, and X, the distance to the closest annotated origin in SGD was determined and the mean of these distances was calculated (This study, four hybridizations). A similar comparison was performed for the other origins identified by three previously published genome-wide analyses of budding yeast origins (Raghuraman *et al.*, 2001; Yabuki *et al.*, 2002) or potential origins (Wyrick *et al.*, 2001). We note that for screening purposes, our assay can be streamlined even further by using replication profiles from a single microarray (This study, single hybridization.)

	Mean distance
Raghuraman et al. (2001)	6.5 kb
Wyrick et al. (2001)	3.9 kb
Yabuki et al. (2002)	3.5 kb
This study, four hybrizations	3.2 kb
This study, single hybridization	6.1 kb

Figure S1. Example of raw data from a re-replication microarray experiment. For most experiments, two independent sets of genomic DNA were prepared and each set was competitively hybridized in duplicate. The ratio of signal intensity of Cy5 to Cy3 was calculated for each sequence element on the array and normalized such that the average ratio of all elements was set to the median DNA content of the re-replicating cells. Normalized raw ratios of the four hybridizations from the experiment described in Figure 2B are shown for chromosome XIV (top four panels). These normalized ratios were subjected to local averaging and Fourier convolution smoothing to generate a smoothed profile. The four smoothed profiles were then merged (see Supplemental Methods) to generate a composite re-replication profile (bottom panel).

Supplemental Figure 1

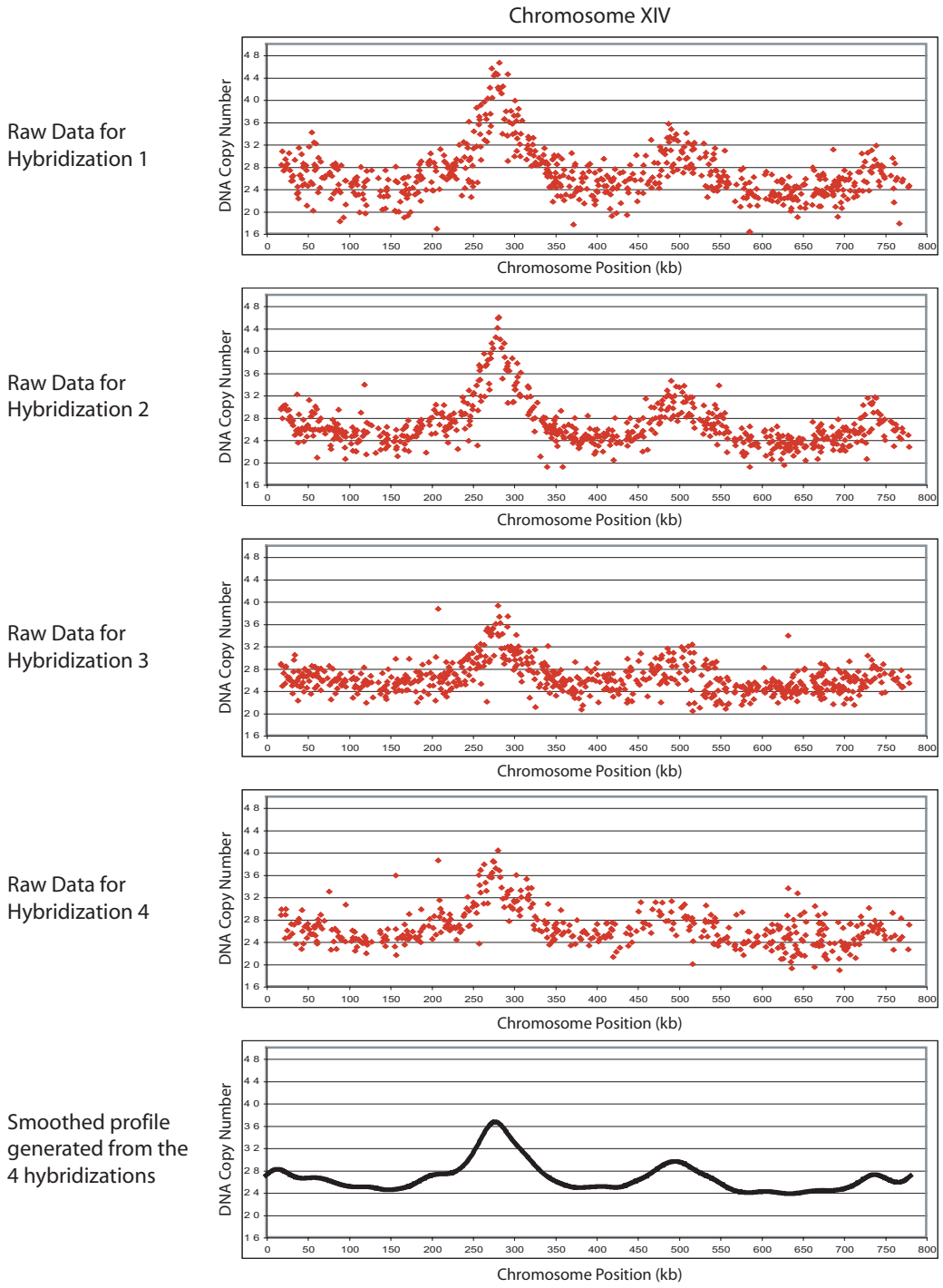

Figure S2. Replication profiles generated by comparative genomic hybridization. CGH replication assay was performed on YJL5038**,** a wild-type yeast strain in the S288c background, in an experiment described in Figure 1B. G1 phase genomic DNA was isolated from cells arrested in alpha factor. S phase genomic DNA was isolated from cells released from an alpha factor arrest in the presence of 100 mM hydroxyurea (HU) for 120 min (DNA content was 1.4 C). The composite replication profiles (blue lines) plus and minus one standard deviation (light gray bands, see Methods) are shown for all sixteen chromosomes. Positions of the 212 origins identified by application of a peak finding algorithm are shown (blue diamonds). Positions of ARSs annotated in the Saccharomyces Genome Database (SGD, (Balakrishnan)) (black open triangles), locations of pro-ARSs mapped by Wyrick *et al.* (Wyrick *et al.*, 2001) (red triangles) and the centromeres (black circles) are marked along the X-axis. Replication profiles derived from Raghuraman *et al.* (Raghuraman *et al.*, 2001) (violet lines) and Yabuki *et al.* (Yabuki *et al.*, 2002) (orange lines) are shown for comparison.

Supplemental Figure 2

S288c S phase Raghuraman *et al.* Yabuki *et al.*

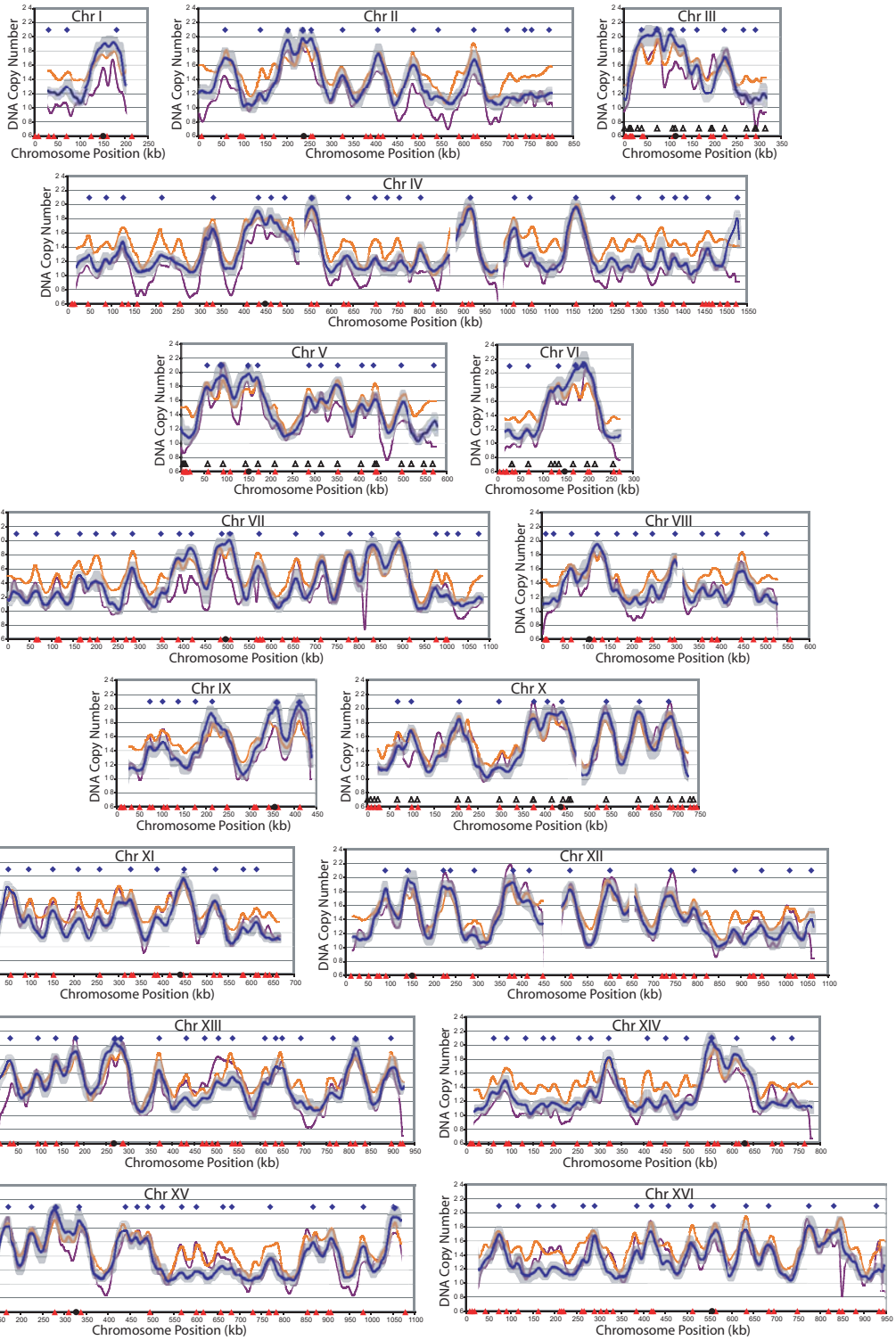

Figure S3. The S phase replication profile of the re-replication competent OMC strain and the congenic wild-type strain are similar. S phase replication profiles were generated for the OMC strain YJL3248 (*MCM7-2NLS orc2-cdk6A orc6-cdk4A pGAL1-Δntcdc6 pMET3-HA3-CDC20*) and YJL5834 (*pGAL1*), a wild-type yeast strain in the A364a background, in an experiment described in Figure 1D. S phase OMC cells were harvested 180 min after alpha factor release into HU (DNA content was 1.4 C). S phase A364a cells were harvested 135 min after alpha factor release into HU (DNA content was 1.35 C). The S phase replication profiles for the OMC strain (green lines), S phase replication profiles for the A364a strain (red lines), the positions of the 193 origins identified in the OMC strain (green diamonds), and the positions of the 231 origins identified in the A364a strain (red diamonds) are shown for all sixteen chromosomes. Positions of origins annotated in SGD, (Balakrishnan) (black open triangles), locations of pro-ARSs mapped by Wyrick *et al.* (Wyrick *et al.*, 2001) (red triangles) and the centromeres (black circles) are marked along the X-axis.

Supplemental Figure 3

A364a S phase OMC S phase

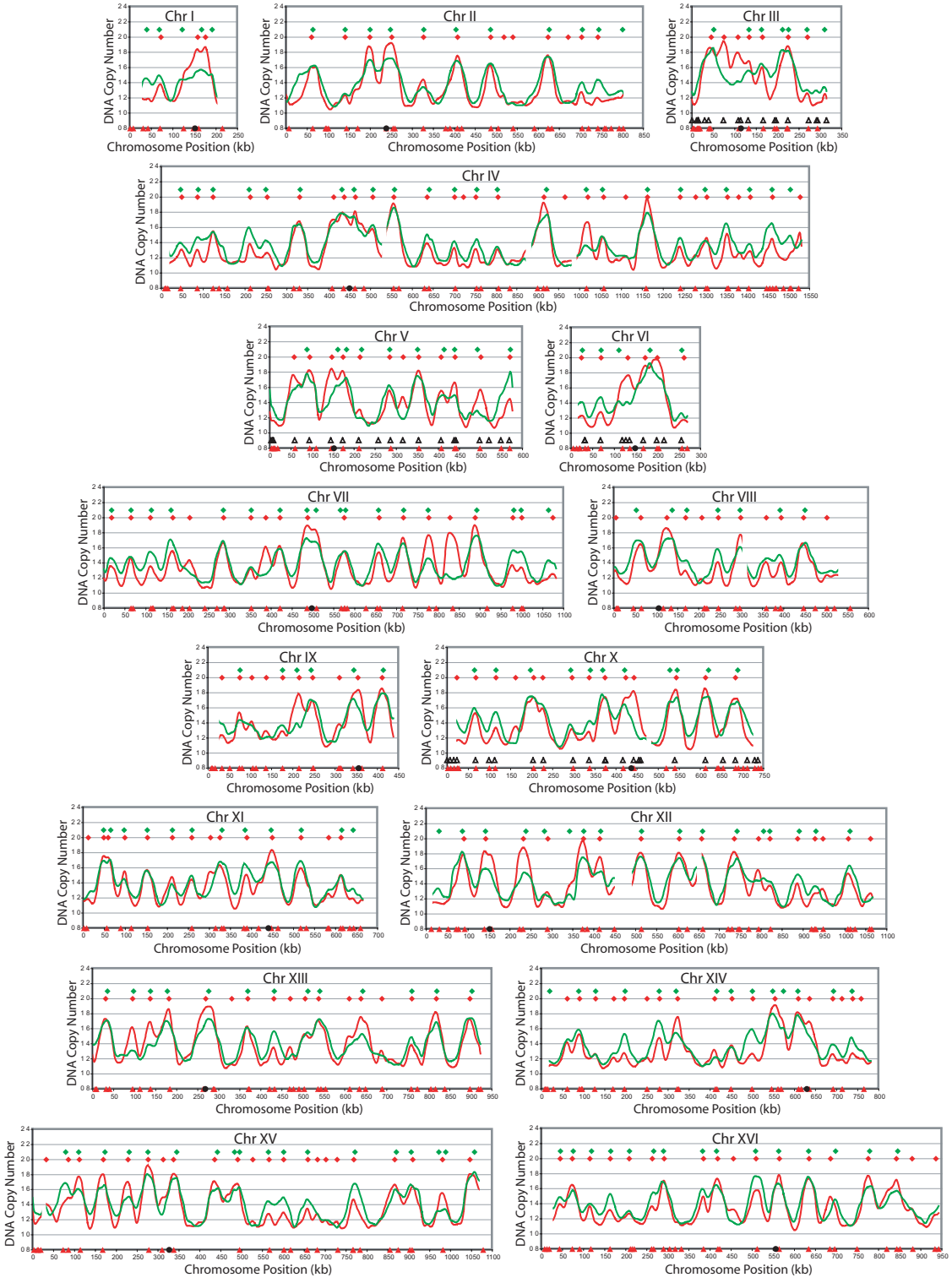

Figure S4. Replication timing in the OMC re-replication competent mutant correlates with replication timing in the A364a background. Application of a peak finding algorithm to the S phase replication profiles in Figure S3 identified 193 origins in the OMC strain YJL3248 (*MCM7-2NLS orc2-cdk6A orc6-cdk4A pGAL1-*Δ*ntcdc6 pMET3-HA3-CDC20*), and 231 origins in the A364a strain YJL5834 (*pGAL1*). 166 (86%) of the origins identified from the OMC strain had a corresponding origin within 10kb in the wild-type A364a strain. For each of the shared origins, the S phase copy number in the A364a replication profile from Figure S3 was plotted against that for the OMC strain in Figure S3. A linear regression line fitted to these points showed a good correlation, with an R^2 value of 0.58.

Supplemental Figure 4

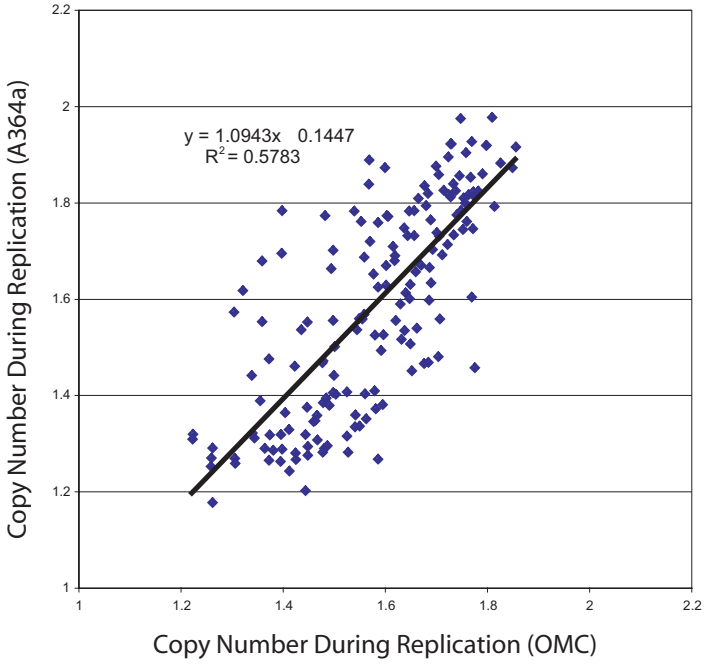

Figure S5. Different strain backgrounds have very similar replication timing profiles. The replication profiles (red lines) and identified origins (red diamonds) from the congenic wild-type A364a strain YJL5834 (*pGAL1*) from Figure S3 are compared to the replication profiles (blue lines) and identified origins (blue diamonds) from the S288c strain in Figure S2. Positions of origins annotated in SGD (Balakrishnan) (black open triangles), locations of pro-ARSs mapped by Wyrick *et al.* (Wyrick *et al.*, 2001) (red triangles) and the centromeres (black circles) are marked along the X-axis.

Supplemental Figure 5

S288c S phase A364a S phase

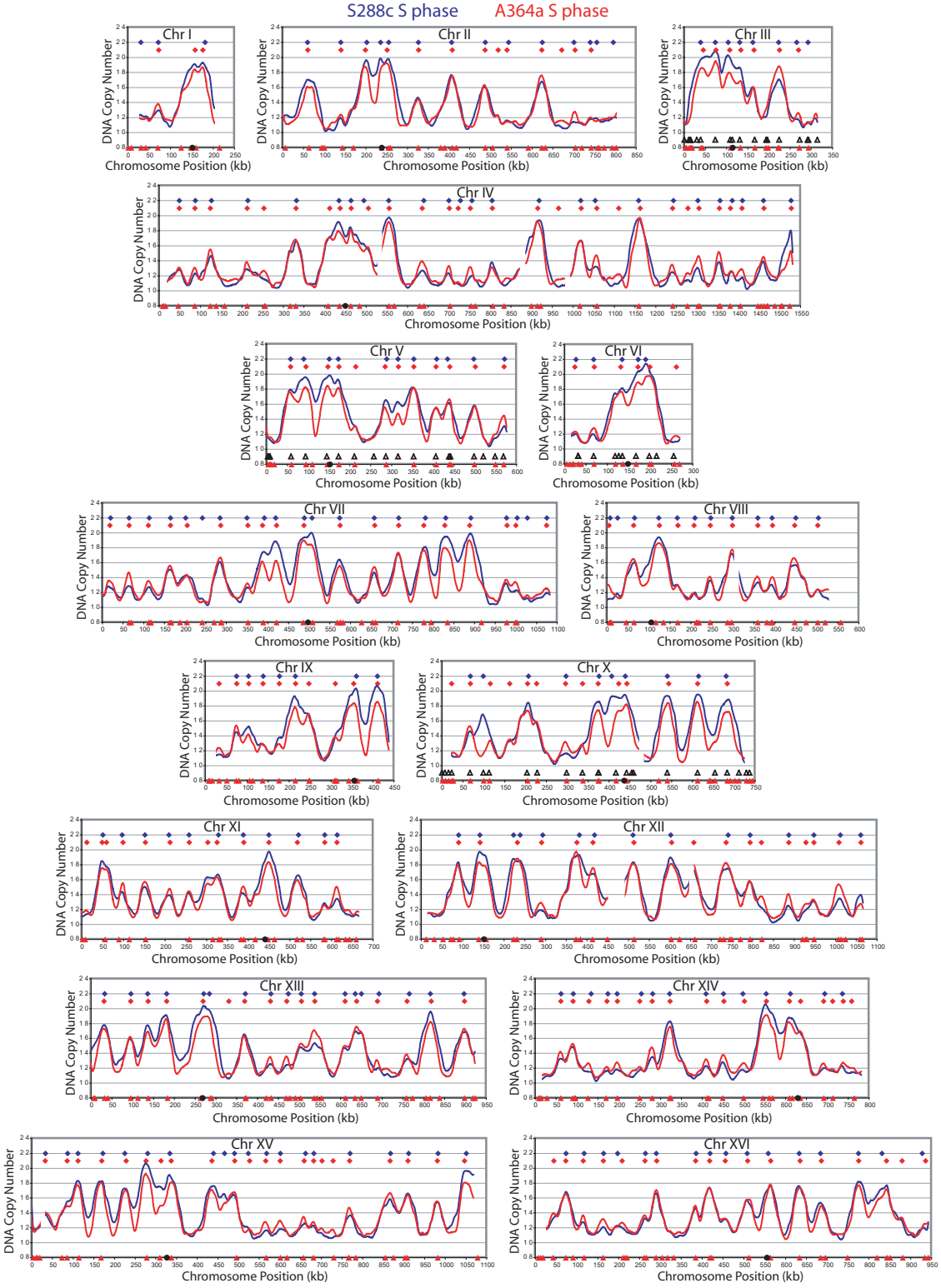

Figure S6. Replication timing in the S288c background strongly correlates with replication timing in the A364a background. Application of a peak finding algorithm to the S phase replication profiles in Figure S5 identified 212 origins in the S288c strain, YJL5038 and 231 origins in the A364a strain YJL5834 (*pGAL1*). Origin usage during S phase was closely matched between the two strain backgrounds; 193 (92%) of origins identified in the S288c background were within 10kb of origins identified in the A364a background. The mean distance between these corresponding origins was 2.1 kb. For each shared origin, the S phase copy number in the A364a background was plotted against that for the S288c background. A linear regression line fitted to these points showed very strong correlation, with an R^2 value of 0.92.

Supplemental Figure 6

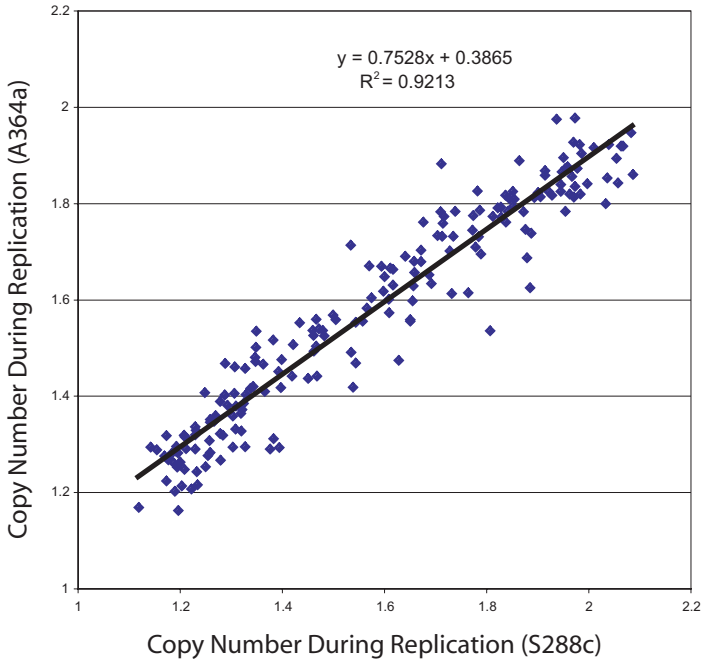

Figure S7. Re-replication induced during G2/M phase when ORC, Mcm2-7 and Cdc6 are deregulated. Genomic DNA was purified from the OMC strain YJL3248 (*orc2-cdk6A orc6-cdk4A MCM7-2NLS pGAL1-*Δ*ntcdc6 pMET3-HA3-CDC20)* and the control OM strain YJL3244 (*orc2-cdk6A orc6-cdk4A MCM7-2NLS pGAL1 pMET3-HA3-CDC20*) after 3 hr of galactose induction from G2/M arrest in an experiment described in Figure 2 (DNA content for the OMC strain was 2.7 C at 3 hr). The OMC G2/M phase re-replication profiles (blue lines, right axis), the positions of the 106 re-replicating peaks identified by application of a peak finding algorithm (blue diamonds), the OMC S phase replication profile (green line, left axis) and identified origins (green diamonds) replotted from Figure S3 are shown for all sixteen chromosomes. The locations of pro-ARSs mapped by Wyrick *et al.* (Wyrick *et al.*, 2001) (red triangles) and the centromeres (black circles) are marked along the X-axis. In the course of these experiments, we observed that the control OM strain YJL3244 (*orc2-cdk6A orc6-cdk4A MCM7-2NLS pGAL1 pMET3-HA3-CDC20*) contained a duplication of a region of chromosome IV (515kb to 645 kb) and that the OMC strain YJL3248 (*orc2-cdk6A orc6-cdk4A MCM7-2NLS pGAL1-*Δ*ntcdc6 pMET3-HA3-CDC20)* had an extra copy of chromosome XI in much of the population. Shown for chromosomes IV and XI are data from a replicate experiment using an isogenic OM strain YJL5493 (*orc2-cdk6A orc6-cdk4A MCM7-2NLS pGAL1 pMET3-HA3-CDC20*) and an isogenic OMC strain YJL3249 (*orc2-cdk6A orc6-cdk4A MCM7-2NLS pGAL1-*Δ*ntcdc6 pMET3-HA3-CDC20*), lacking these genomic alterations (yellow lines).

Supplemental Figure 7

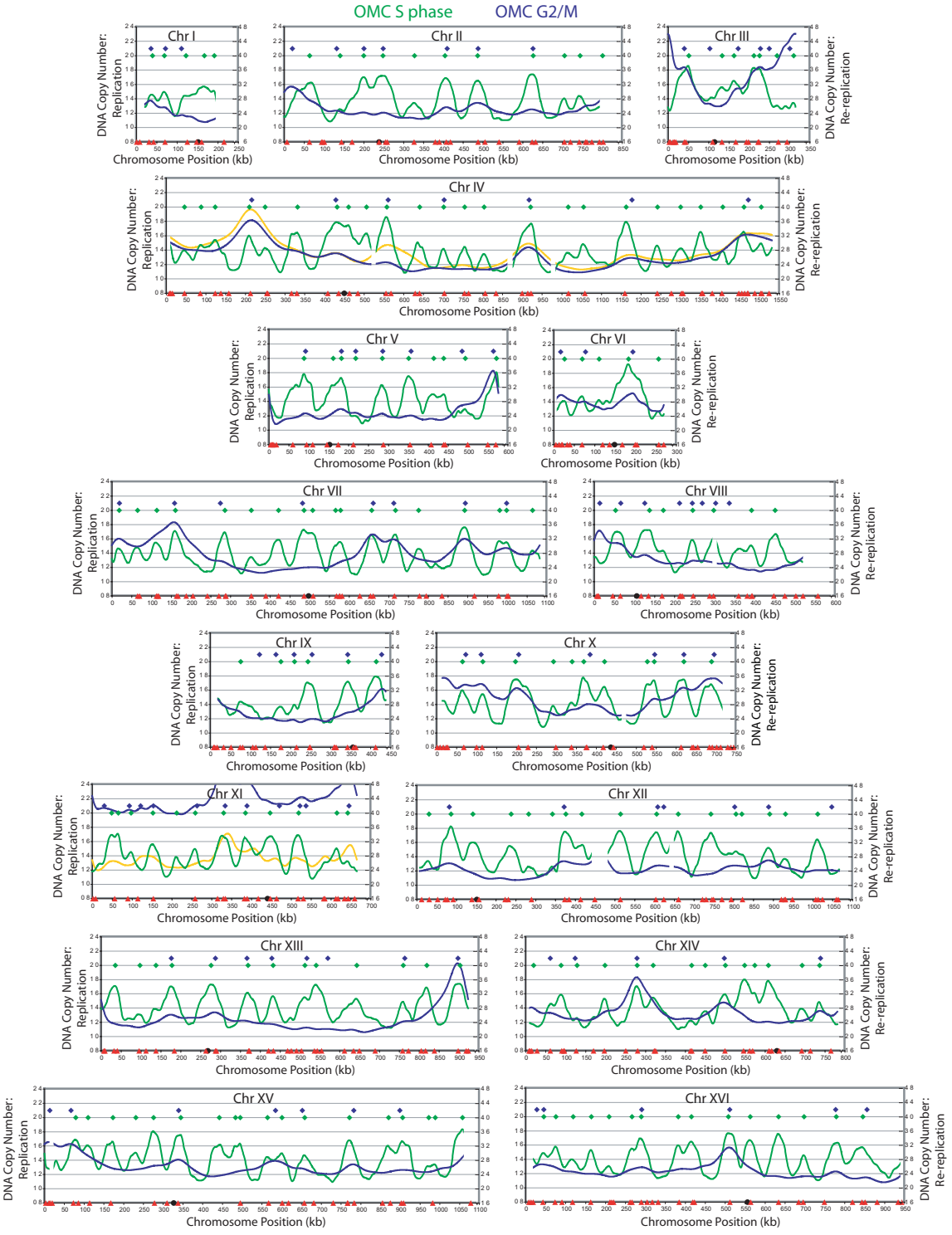

Figure S8. The observed mean distance from re-replication peaks to pro-ARSs is highly significant. When re-replication was induced in G2/M, 106 re-replicating origins were identified (Figure S7). The mean distance from those origins to the closest potential S phase origin defined by Wyrick *et al.* (Wyrick *et al.*, 2001) (pro-ARSs) was 7.0 kb. To determine the significance of this value, 106 random chromosomal loci were selected and the mean distance to the closest pro-ARS was calculated. This was repeated 100,000 times and a histogram was generated showing the percent of the random samples with the indicated mean distances. The actual observed mean, which is greatly below the expected random mean, is indicated with an arrow.

Supplemental Figure 8

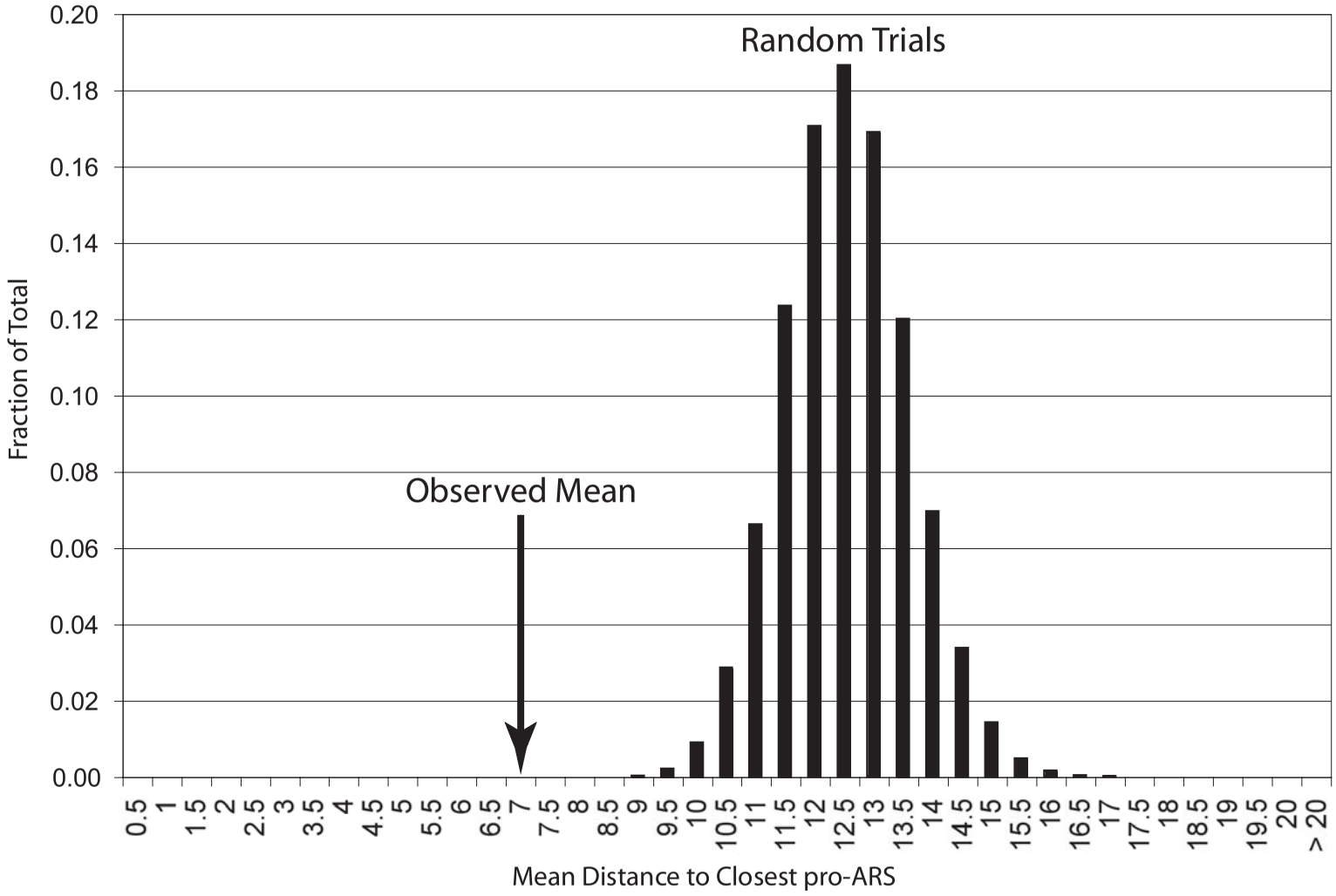

Figure S9. OMC cells can re-initiate and re-replicate within S phase. The OMC strain YJL3249 (*orc2-cdk6A orc6-cdk4A MCM7-2NLS pGAL1-Δntcdc6 pMET3-HA3-CDC20*) was induced to re-replicate while still in S phase in an experiment described in Figure 3. The cells were arrested in G1 phase with alpha factor, induced to express Δntcdc6 by the addition of 2% galactose, then released from the arrest into YEPGal containing 100 mM hydroxyurea (HU) to delay cells from exiting S phase. Genomic DNA from the OMC strain was isolated at the 0 hr (G1 phase) and 4 hr (S phase, DNA content 1.4 C) time points and competitively hybridized against each other. The resulting profiles shown for all sixteen chromosomes reflect copy number increases due to both replication and re-replication. The locations of pro-ARSs mapped by Wyrick *et al.* (Wyrick *et al.*, 2001) (red triangles) and the centromeres (black circles) are plotted along the X-axis.

Supplemental Figure 9

OMC S Re-rep

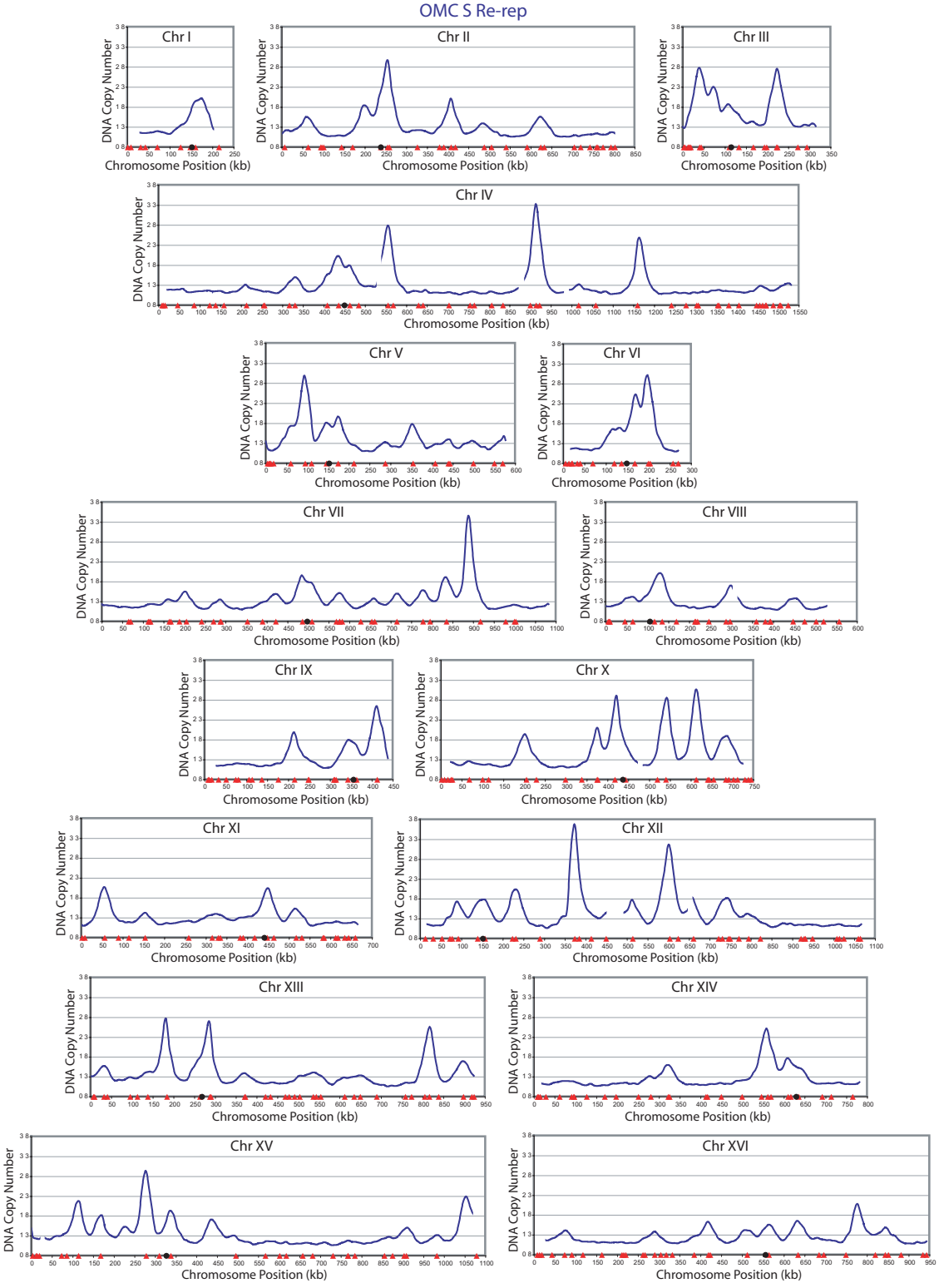

Figure S10. Re-replication induced upon release from a G1 arrest when ORC, Mcm2-7 and Cdc6 are deregulated. The OMC strain YJL3248 (*orc2-cdk6A orc6-cdk4A MCM7-2NLS pGAL1-Δntcdc6 pMET3-HA3-CDC20)* was induced to re-replicate during G1 release in an experiment described in Figure 4. Genomic DNA was purified from the OMC strain and the OM strain YJL3244 (*orc2-cdk6A orc6-cdk4A MCM7-2NLS pGAL1 pMET3-HA3-CDC20*) after 3 hr of galactose induction while cells were released from G1 into G2/M phase (DNA content for the OMC strain was 3.2 C at 3 hr). The two DNA preparations were labeled and competitively hybridized against each other to generate the OMC G1 release re-replication profiles shown for all sixteen chromosomes (blue lines) and to identify 87 re-replicating peaks (blue diamonds). The locations of pro-ARSs mapped by Wyrick *et al.* (Wyrick *et al.*, 2001) (red triangles) and the centromeres (black circles) are plotted along the X-axis. In the course of these experiments, we observed the same genomic alterations of Chromosome IV and XI described in Figure S7. Shown for chromosomes IV and XI are data from a replicate experiment using an isogenic OM strain YJL5493 (*orc2-cdk6A orc6-cdk4A MCM7-2NLS pGAL1 pMET3-HA3-CDC20*) and an isogenic OMC strain YJL3249 (*orc2-cdk6A orc6-cdk4A MCM7-2NLS pGAL1-Δntcdc6 pMET3-HA3-CDC20*), lacking these genomic alterations (yellow lines).

Supplemental Figure 10

OMC G1 to G2/M

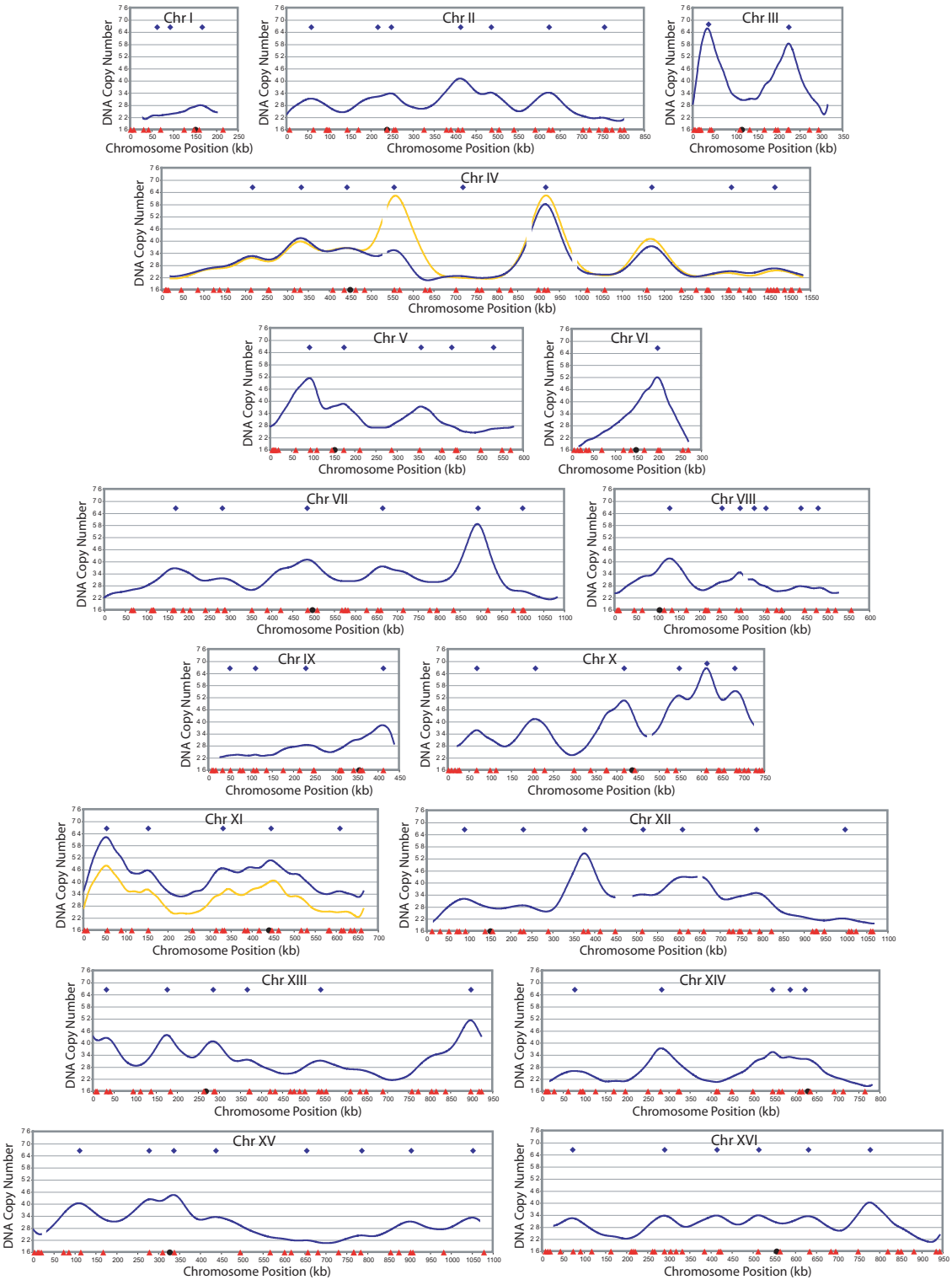

Figure S11. Re-replication can be induced when only ORC and Cdc6p are deregulated. The OC strain YJL3240 (*orc2-cdk6A orc6-cdk4A pGAL1-*Δ*ntcdc6 pMET3-HA3-CDC20)* and the control O strain YJL4832 (*orc2-cdk6A orc6-cdk4A pGAL1 pMET3-HA3-CDC20*) were induced to re-replicate in G2/M phase or during a G1 release in experiments described in Figures 5A and 5B, respectively. The DNA content of the OC strain was 2.0 C for the G2/M induction and 2.6 C for the G1 release. For each induction protocol, OC and O strain genomic DNA were prepared and competitively hybridized against each other as described in Figure1A. Shown for all sixteen chromosomes are OC G2/M phase re-replication profiles (blue lines), OC G1 release re-replication profiles (green lines), locations of pro-ARSs mapped by Wyrick *et al.* (Wyrick *et al.*, 2001) (red triangles), and centromeres (black circles).

Supplemental Figure 11

OC G2/M OC G1 to G2/M

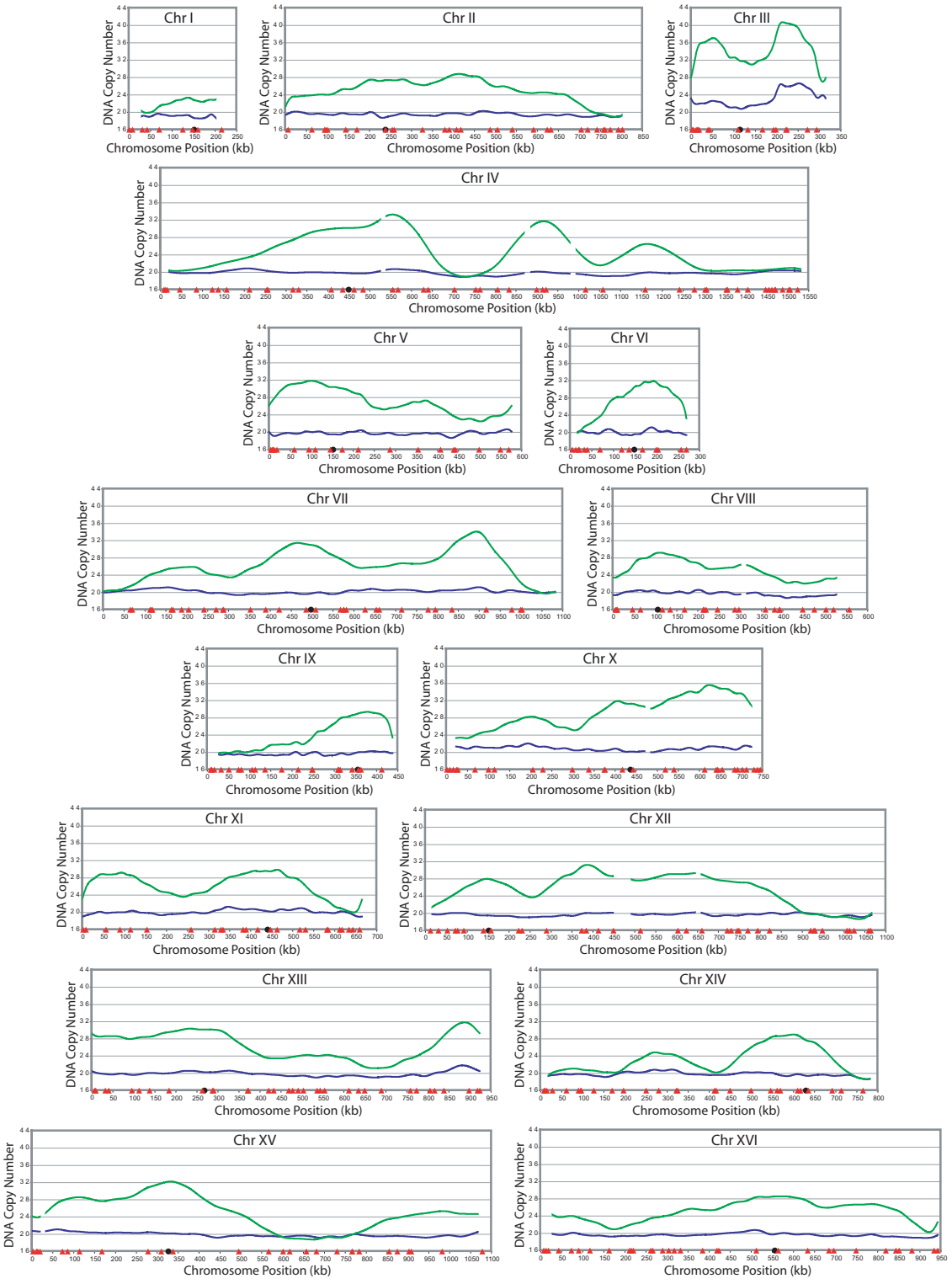

Figure S12. Re-replication occurs primarily on a single chromosome when Mcm2-7 and Cdc6 are deregulated. Re-replication in the MC_{2A} strain occurs primarily on chromosome III. The MC_{2A} strain YJL4489 (*MCM7-NLS pGAL1-Δntcdc6-cdk2A pMET3-HA3-CDC20*) and the control M strain YJL4486 (*MCM7-2NLS pGAL1 pMET3-HA3-CDC20*) were induced to re-replicate in G2/M phase or during a G1 release in experiments described in Figures 6A and 6B, respectively. The DNA content of the MC_{2A} strain was 2.0 C for both the G2/M induction and for the G1 release. For each induction protocol, MC_{2A} and M strain genomic DNA were prepared and competitively hybridized against each other as described in Figure1A. Shown for all sixteen chromosomes are MC_{2A} G2/M phase re-replication profiles (blue lines), MC_{2A} G1 release re-replication profiles (green lines), locations of pro-ARSs mapped by Wyrick *et al.* (Wyrick *et al.*, 2001) (red triangles) and the centromeres (black circles).

Supplemental Figure 12

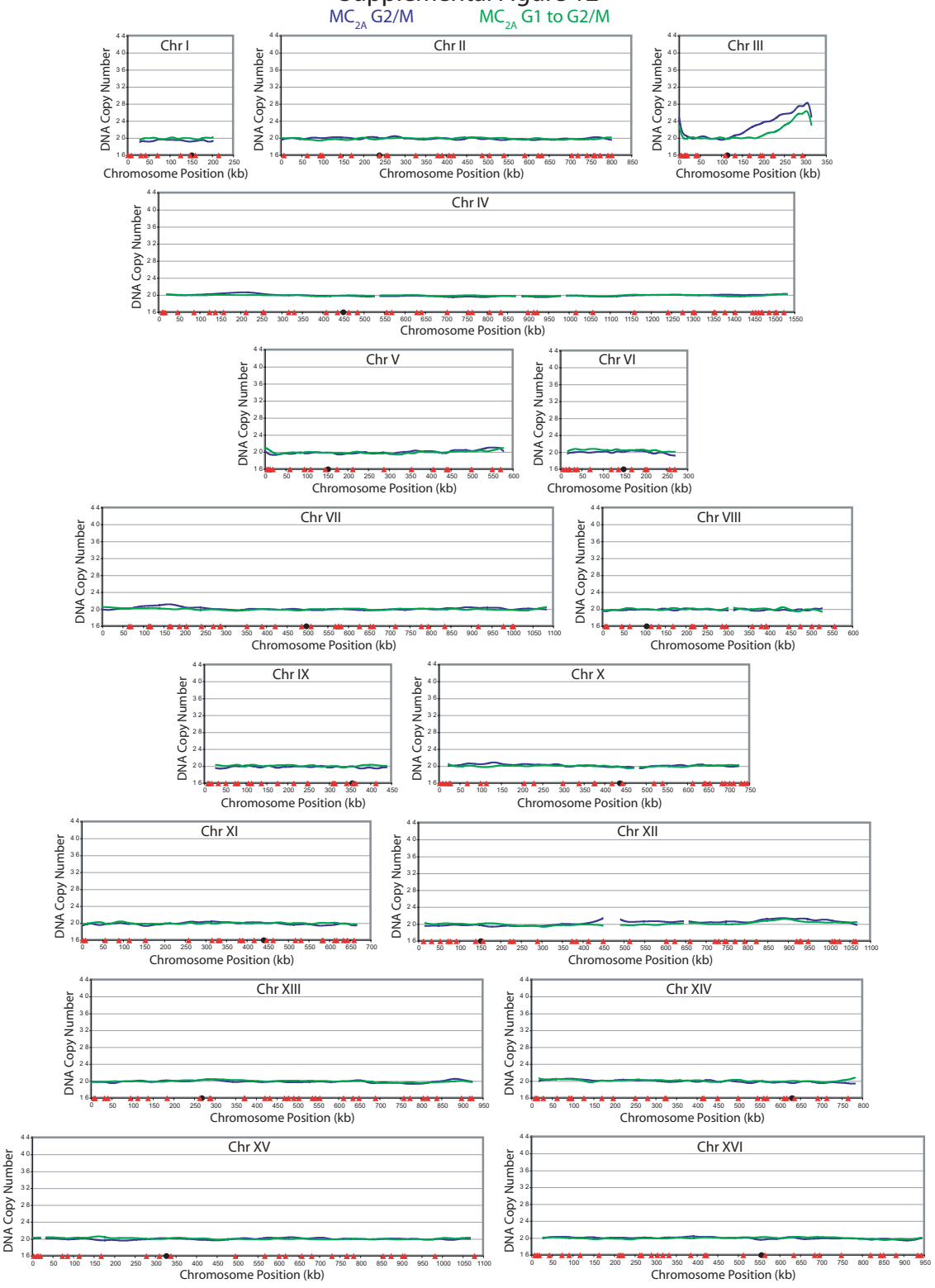

Figure S13. MC_{2A}-*cdc7* strain is competent to re-replicate at the permissive temperature. The MC_{2A} strain YJL4489 (*MCM7-2NLS pGAL1-*Δ*ntcdc6-2A pMET3-HA3-CDC20*), the congenic MC_{2A}-*cdc7* strain YJL5821 (*MCM7-2NLS pGAL1-*Δ*ntcdc6-2A pMET3-HA3-CDC20 cdc7-1*) and their respective controls, the M strain YJL4486 (*MCM7-2NLS pGAL1 pMET3-HA3-CDC20*) and the M-*cdc7* strain YJL5816 (*MCM7-2NLS pGAL1 pMET3-HA3-CDC20 cdc7-1*) were induced with galactose as described in Figure 7C, except that following the initial arrest at 23° C, the arrested cells were maintained at 23° C for 1 hr, before the addition of galactose. Genomic DNA was isolated 4 hr after galactose addition and competitively hybridized (MC_{2A} versus M and MC_{2A}-*cdc7* versus M-*cdc7*) as described in Figure 1A. Re-replication profiles for the MC_{2A} (blue line) and MC_{2A}-*cdc7* (green line) strains are shown for chromosome III. The locations of pro-ARSs mapped by Wyrick *et al.* (Wyrick *et al.*, 2001) (red triangles), and the centromere (black circle) are plotted along the X-axis.

Supplemental Figure 13

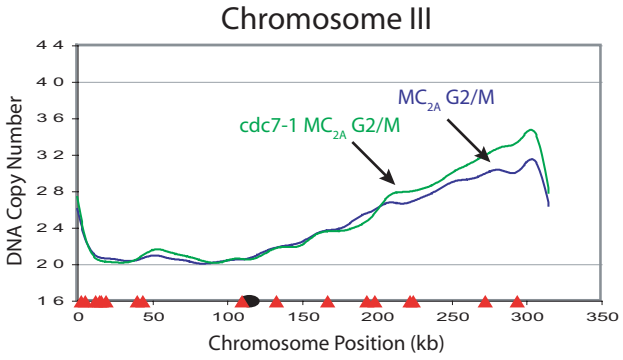

APPENDIX 2

Supplemental data for Chapter 3

SUPPLEMENTAL MATERIALS AND METHODS

Strain construction

All strains (Table 2) were derived from YJL1737 (*MAT*a *orc2-cdk6A orc6-cdk4A leu2 ura3-52 trp1-289 ade2 ade3 bar1*Δ*::LEU2*) (Nguyen *et al.*, 2001). The *orc2-cdk6A* and *orc6-cdk4A* alleles encode mutant proteins in which alanine is substituted for the phosphoacceptor serines or threonines at all full CDK consensus phosphorylation sites (residues 16, 24, 70, 174, 188, and 206 for *orc2-cdk6A*, and residues 106, 116, 123, and 146 *orc6-cdk4A*). Plasmid pR306-ARS-ACS2 (*ars1413-ACS2, URA3/*MluI) was used in a 2-step gene replacement to mutate the ACS of ARS1413 (Friedman *et al.*, 1996). Plasmids pJL806 (*pGAL1, URA3*/StuI) and pJL1489 (*pGAL1-*Δ*ntcdc6, URA3*/StuI) (Nguyen *et al.*, 2001) were inserted at the *URA3* locus by one step integration. The plasmid pJL1489 expresses a truncated Cdc6 with amino acids 2-47 replaced by amino acids S-G-R. YIp22 (*pMET3-HA3-CDC20, TRP1*/MscI) (Uhlmann *et al.*, 2000) and pBO1555 (*pMET3-HA3-CDC20, NatMX4*/MscI) (Green and Li, 2005) were used in one-step gene replacements at the CDC20 locus.

ARS1411 and *ARS1412* were deleted using PCR fragments containing NatMX4 or loxp-KanMX4-loxp that were amplified, respectively, from pAG25 (Goldstein and McCusker, 1999) or pUG6 (Guldener *et al.*, 1996) using oligonucleotide primers shown in Table 3. The *ars1411*Δ removes a XXX kb sequence containing *ARS1411* and replaces it with a NatMX4 cassette. The *ars1412*Δ removes a XXX kb sequence containing ARS1412 replaces it with a loxp-KanMX4-loxp cassette. Genomic DNA

from the Saccharomyces Genome Deletion Project (Winzeler *et al.*, 1999) was used as a template to generate a wtm1Δ::KanMX PCR fragment using OJL1912 and OJL1915.

Array Design and Fabrication

PCR products representing every ORF and intergenic region were designed and amplified as previously described (DeRisi *et al.*, 1997; Iyer *et al.*, 2001). Intergenic regions larger than 1.5 kb were amplified in segments of at most 1.5 kb. Each of the PCR products was resuspended in 3X SSC and robotically arrayed with Silicon Microcontact Spotting Pins (Parallel Synthesis Technologies, San Francisco, CA) onto poly-L-lysine coated glass slides (VWR 48382-232, West Chester, PA) as previously described (DeRisi *et al.*, 1997). The remaining poly-L-lysine was then blocked as previously described (DeRisi *et al.*, 1997) with the following modifications. The hydration step was omitted and instead slides were incubated in 3X SSC 0.2% SDS at 65˚C for 5 min. Slides were washed successively with H_2O and 95% ethanol, and then dried by centrifugation for 2 min at 500 rpm in a SX4750 rotor using a GS-6 centrifuge (Beckman) and processed as described previously.

Genomic DNA preparation for CGH

450 ml of culture was mixed with 2.25 ml of 20% sodium azide and added to 50 ml of frozen, –80 ˚C, 0.2 M EDTA, 0.1% sodium azide. Cells were pelleted, washed with 50 ml 4 ˚C TE (10 mM TrisCl 1 mM EDTA pH 7.5) and stored frozen at –80˚C. Pellets were resuspended in 4 ml Lysis buffer (2% Triton X-100, 1% SDS, 100 mM NaCl, 10 mM Tris-Cl, 1 mM EDTA pH8.0) and mixed with 4 ml of

phenol:$CHCl_3$:isoamyl alcohol (25:25:1) and 8 ml 0.5 mm glass beads (BioSpec Products, Inc., Bartlesville, OK). The suspension was vortexed seven times for 2 min separated by 2 min intervals at room temperature until greater than 95% of the cells lysed. The lysate was diluted with 8 ml phenol:$CHCl_3$:isoamyl alcohol and 8 ml TE, and then centrifuged at 18,500 x g for 15 min at RT. After collecting the aqueous phase, the interphase was re-extracted with 8 ml TE, and the second aqueous phase from this re-extraction pooled with the first. The combined aqueous phases were extracted with an equal volume of $CHCl_3$. The bulk of the RNA in the extract was selectively precipitated by addition of 0.01 volume 5 M NaCl to 50 mM and 0.4 volumes isopropanol and centrifugation at 12,000 x g for 15 min at RT. The RNA pellet was discarded and an additional 0.4 volumes of isopropanol was added to the supernatant. The sample was pelleted, washed with 70% ethanol, dried, and resuspended with 5.3 ml 10 mM Tris-Cl, (pH 8) 1 mM EDTA. RNase A (Qiagen, Valencia, CA) was added to 225 µg/ml followed by incubation at 37ºC for 30 min. Proteinase K was then added to 350 µg/ml followed by incubation at 55 ˚C for 30 min. NaCl was added to a final concentration of 1M. Finally, 0.6 ml of 10% (w/v) Cetyltrimethylammonium Bromide (CTAB) in 1 M NaCl (prewarmed to 65 °C) was added and the sample was incubated for 20 min at 65 ˚C before being extracted with 8 ml $CHCl_3$ and centrifuged at 6000 x g for 15 min at RT. The DNA in the aqueous phase was precipitated with 0.8 volumes isopropanol at RT, washed with 70% ethanol, dried, and resuspended in 10 ml Qiagen buffer QBT. DNA was loaded and purified on a Qiagen Genomic-tip 100/G column as per the manufacturer's instructions (Qiagen, Valencia, CA). The eluted DNA was precipitated with 0.8 volumes isopropanol at 4 ˚C, washed with 70% ethanol, dried, and resuspended

in 250 µl 2 mM Tris pH 7.5. This highly purified genomic DNA (OD 260/280 1.82-1.86) was sheared by sonication with a Branson Sonifier 450 to an average fragment size of 500 bp. Isolating DNA of this purity is important for generating reproducible replication profiles.

Labeling and Hybridization

2.5 µg of sheared genomic DNA was randomly primed with 10 µg of N_9 nonomer by boiling for 5 min, then cooling on ice for 5 min. 5-(3-Aminoallyl)-2'-deoxyuridine 5'-triphosphate (Sigma A0410, St. Louis, MO) was incorporated into the primed genomic DNA in a 50 µl reaction containing 10 mM TrisHCl pH 7.5, 5 mM MgCl2, 7.5 mM dithiothreitol, 120 µM dATP, 120 µM dCTP, 120 µM dGTP, 20 µM dTTP, 100 µM 5-(3-Aminoallyl)-2'-deoxyuridine 5'-triphosphate, and 5 U Klenow fragment. The reaction was incubated at 37˚C for 4 hr, and the DNA was purified using the DNA Clean and Concentrator kit (Zymo Research, Orange, California). 15-40 nmol of Cy3 and Cy5 (Amersham, Piscataway, NJ) were then separately coupled to the appropriate DNA with 0.1 M $NAHCO_3$, pH 9.0 for 1 hr (Bozdech *et al.*, 2003), and the fluorescently labeled DNA purified using the DNA Clean and Concentrator kit (Zymo Research, Orange, California). For most hybridizations, the replicating or re-replicating DNA was labeled with Cy5 and the non-replicating competitor DNA was labeled with Cy3.

Cy3 and Cy5 labeled DNA were pooled in a 40 µl mixture containing 3X SSC, 25 mM HEPES pH 7.0, and 0.25% SDS. Samples denatured for 2 min at 100˚C and hybridized under a glass mSeries Lifterslip (Erie Scientific 25x40I-M-5227, Portsmouth, NH) to a microarray for 18-24 hours at 63˚C. Microarrays were washed successively in

0.85X SSC, 0.02%SDS and 0.035X SSC immediately before scanning. The microarrays were spun dry and scanned with a GenePix 4000B scanner (Axon Instruments Union City, California) in an enclosed chamber where atmospheric ozone was maintained below 10 ppb using two OI-45 Ozone Interceptors (Ozone solutions, Sioux Center, Iowa).

Data analysis

Genepix Pro 4.0 software (Axon Instruments, Union City, CA) was used for micorarray image analysis and quantification. Data were filtered to remove features that had (1) obvious defects, (2) saturated pixels, (3) regression R^2 values less than 0.5, or (4) fewer than 55% of their pixels with fluorescence intensity greater than 2 standard deviations above background. Data was also filtered to remove 1572 features that contain repetitive sequences from the analysis. The median of the ratios for each element was used for the raw Cy5/Cy3 value.

The raw ratios were normalized by multiplying each value by a scalar normalization factor chosen so that the average of the normalized values was equal to the DNA content of the cells. DNA content was calculated from the median of the flow cytometry profile after correcting for signal increase due to mitochondrial replication (detailed information on the calculation of DNA content is provided below). The raw data were then binned and smoothed essentially as described (Raghuraman *et al.*, 2001). In short, a moving median was calculated over a 10 kb window for every 0.5 kb location along the genome. If a given 10 kb window did not contain any raw data points after filtering it was defined as a no data zone and the binned value from the previous window was used for smoothing purposes. The binned data were then smoothed using Fourier

Convolution Smoothing essentially as described (Raghuraman *et al.*, 2001). However, the equation for k(S) was incorrectly provided in part II.3 of the supplemental information of that paper. The correct equation is as follows (personal communication, Collingwood D.):

$$k(S) = \{\exp(-2^{-S} n^2) : \text{n is an integer satisfying } -\left[\frac{T}{2}\right] \le n \le T - 1 - \left[\frac{T}{2}\right]\}$$

In Raghuraman *et al.* (Raghuraman *et al.*, 2001) the optimal value for S was computationally determined for each chromosome for each experiment. While this was effective for replication profiles, we found that predetermined values for S resulted in better re-replication profiles. Thus, for all G2/M re-replication profiles, the following values for S were used for each chromosome: I: 7.5, II: 9.5, III: 8, IV: 10.25, V: 9, VI: 7.75, VII: 9.75, VIII: 9, IX: 8.5, X: 9.25, XI: 9, XII: 9.75, XIII: 9.75, XIV: 9.25, XV: 9.75, XVI: 9.5.

Two hybridizations were performed from each of two independent genomic DNA preparations. For presentation purposes, the resulting four replication profiles were averaged into one composite profile. Table S1 contains the value at each chromosomal locus for each of the composite profiles in this manuscript. In the final replication profiles, no data regions as described above are presented as gaps in the profiles.

Fork Progression Measurements:

The rate of elongation was measured by calculating what we call the "Peak spread". This is simply a measure of how far a given peak in replication profile was able to spread in a certain amount of time. For a given peak spread there are three parameters: the origin from which the fork originated (the x coordinate), the profile containing the

initial peak height (the y coordinate), and the time interval over which the measurement is being made. The horizontal distance from the apex of a peak to where it reaches the subsequent curve is measured. This distance represents how far forks starting at the origin were able to travel in the given time period.

Two independent trials were performed for each experiment in which Peak Spread was calculated. For each interval of interest the peak spread was calculated for the two independent experiments. These values were then averaged for that origin and peak spread interval. For ARS1414 the standard error was calculated using the two independent trials. For a given origin and peak spread interval the value was calculated by averaging the two measurements form the two independent experiments. This value was obtained for each origin in the 'other origins' group. This set of values was then used to obtain an average and standard error for the 'other origins' at that interval.

REFERENCES

Bozdech, Z., Zhu, J., Joachimiak, M.P., Cohen, F.E., Pulliam, B., and DeRisi, J.L. (2003). Expression profiling of the schizont and trophozoite stages of Plasmodium falciparum with a long-oligonucleotide microarray. Genome Biol *4*, R9.

DeRisi, J.L., Iyer, V.R., and Brown, P.O. (1997). Exploring the metabolic and genetic control of gene expression on a genomic scale. Science *278*, 680-686.

Friedman, K.L., Diller, J.D., Ferguson, B.M., Nyland, S.V., Brewer, B.J., and Fangman, W.L. (1996). Multiple determinants controlling activation of yeast replication origins late in S phase. Genes Dev *10*, 1595-1607.

Goldstein, A.L., and McCusker, J.H. (1999). Three new dominant drug resistance cassettes for gene disruption in Saccharomyces cerevisiae. Yeast *15*, 1541-1553.

Green, B.M., and Li, J.J. (2005). Loss of rereplication control in Saccharomyces cerevisiae results in extensive DNA damage. Mol Biol Cell *16*, 421-432.

Guldener, U., Heck, S., Fielder, T., Beinhauer, J., and Hegemann, J.H. (1996). A new efficient gene disruption cassette for repeated use in budding yeast. Nucleic Acids Res *24*, 2519-2524.

Iyer, V.R., Horak, C.E., Scafe, C.S., Botstein, D., Snyder, M., and Brown, P.O. (2001). Genomic binding sites of the yeast cell-cycle transcription factors SBF and MBF. Nature *409*, 533-538.

Nguyen, V.Q., Co, C., and Li, J.J. (2001). Cyclin-dependent kinases prevent DNA re-replication through multiple mechanisms. Nature *411*, 1068-1073.

Raghuraman, M.K., Winzeler, E.A., Collingwood, D., Hunt, S., Wodicka, L., Conway, A., Lockhart, D.J., Davis, R.W., Brewer, B.J., and Fangman, W.L. (2001). Replication dynamics of the yeast genome. Science *294*, 115-121.

Uhlmann, F., Wernic, D., Poupart, M.A., Koonin, E.V., and Nasmyth, K. (2000). Cleavage of cohesin by the CD clan protease separin triggers anaphase in yeast. Cell *103*, 375-386.

Winzeler, E.A., Shoemaker, D.D., Astromoff, A., Liang, H., Anderson, K., Andre, B., Bangham, R., Benito, R., Boeke, J.D., Bussey, H., Chu, A.M., Connelly, C.,

Davis, K., Dietrich, F., Dow, S.W., El Bakkoury, M., Foury, F., Friend, S.H., Gentalen, E., Giaever, G., Hegemann, J.H., Jones, T., Laub, M., Liao, H., Liebundguth, N., Lockhart, D.J., Lucau-Danila, A., Lussier, M., M'Rabet, N., Menard, P., Mittmann, M., Pai, C., Rebischung, C., Revuelta, J.L., Riles, L., Roberts, C.J., Ross-MacDonald, P., Scherens, B., Snyder, M., Sookhai-Mahadeo, S., Storms, R.K., Veronneau, S., Voet, M., Volckaert, G., Ward, T.R., Wysocki, R., Yen, G.S., Yu, K., Zimmermann, K., Philippsen, P., Johnston, M., and Davis, R.W. (1999). Functional characterization of the S. cerevisiae genome by gene deletion and parallel analysis. Science *285*, 901-906.

Xu, W., Aparicio, J.G., Aparicio, O.M., and Tavare, S. (2006). Genome-wide mapping of ORC and Mcm2p binding sites on tiling arrays and identification of essential ARS consensus sequences in S. cerevisiae. BMC Genomics *7*, 276.

SUPPLEMENTAL FIGURE LEGENDS

Figure S1. Replication fork progression in S phase

The S phase replication profile of the re-replication competent *OMC ChrXIV-3ars*Δ strain after release from hydroxyurea (HU). Microarray CGH was performed on *OMC ChrXIV-3ars*Δ cells in the experiment described in Figure 1. S phase replication profiles 180 min after cells were released from G1 phase into media containing hydroxyurea (HU) and 20 min and 40 min following release from HU are shown for all sixteen chromosomes. Positions of nim-ARSs mapped by Xu *et al.* (Xu *et al.*, 2006) (gray triangles) and the centromeres (black circles) are plotted along the X-axis.

Supplementary Figure 1

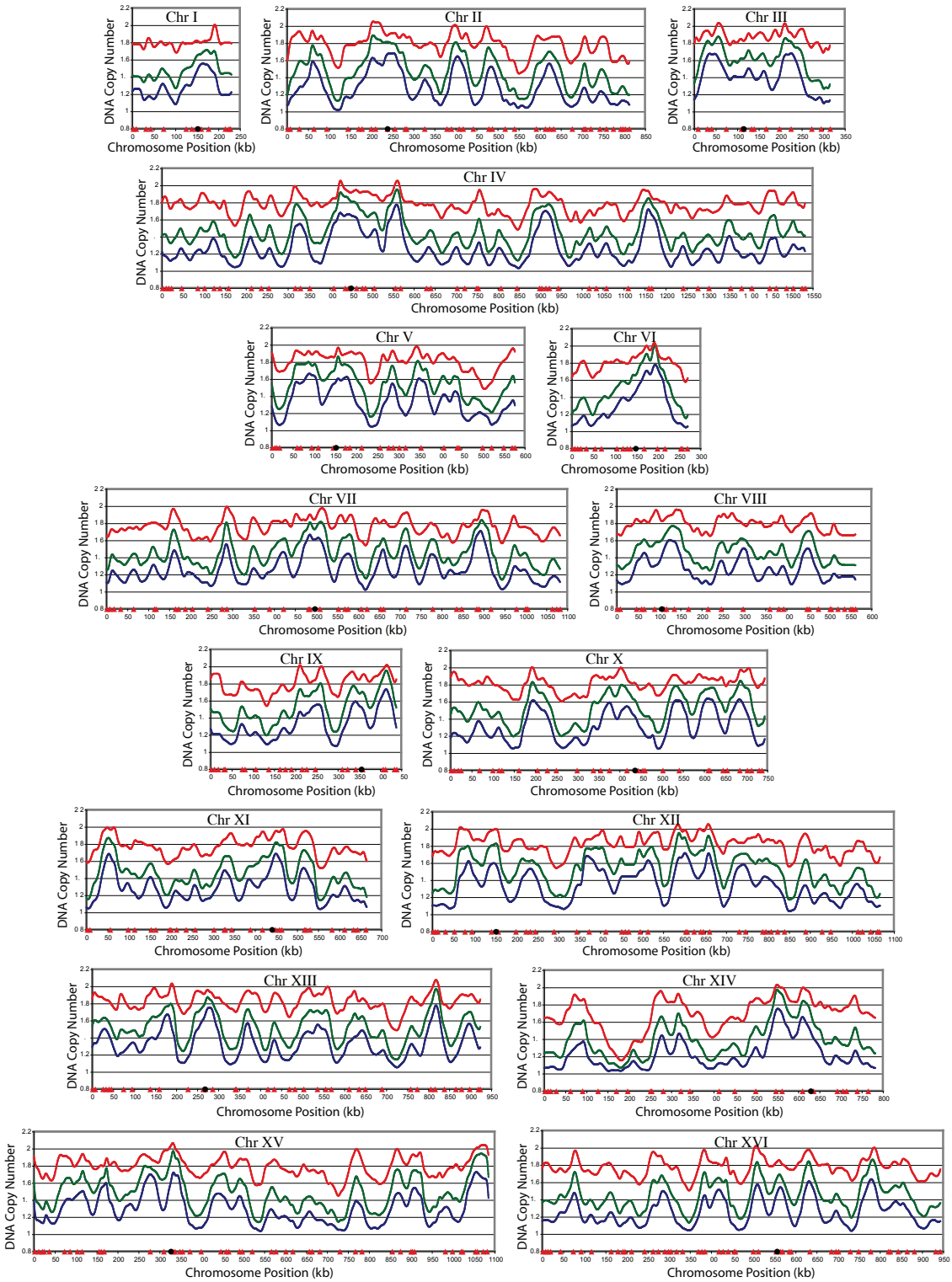

Figure S2. Impaired fork progression across the entire genome during re-replication in G2/M phase. The *OMC ChrXIV-3ars*Δ strain was induced to re-replicate in G2/M phase in the experiment described in Figure 2. The re-replication profiles 180 min, 240 min, and 300 min during continuous galactose induction are shown for all sixteen chromosomes. Positions of nim-ARSs mapped by Xu *et al.* (Xu *et al.*, 2006) (gray triangles) and the centromeres (black circles) are plotted along the X-axis.

Supplementary Figure 2

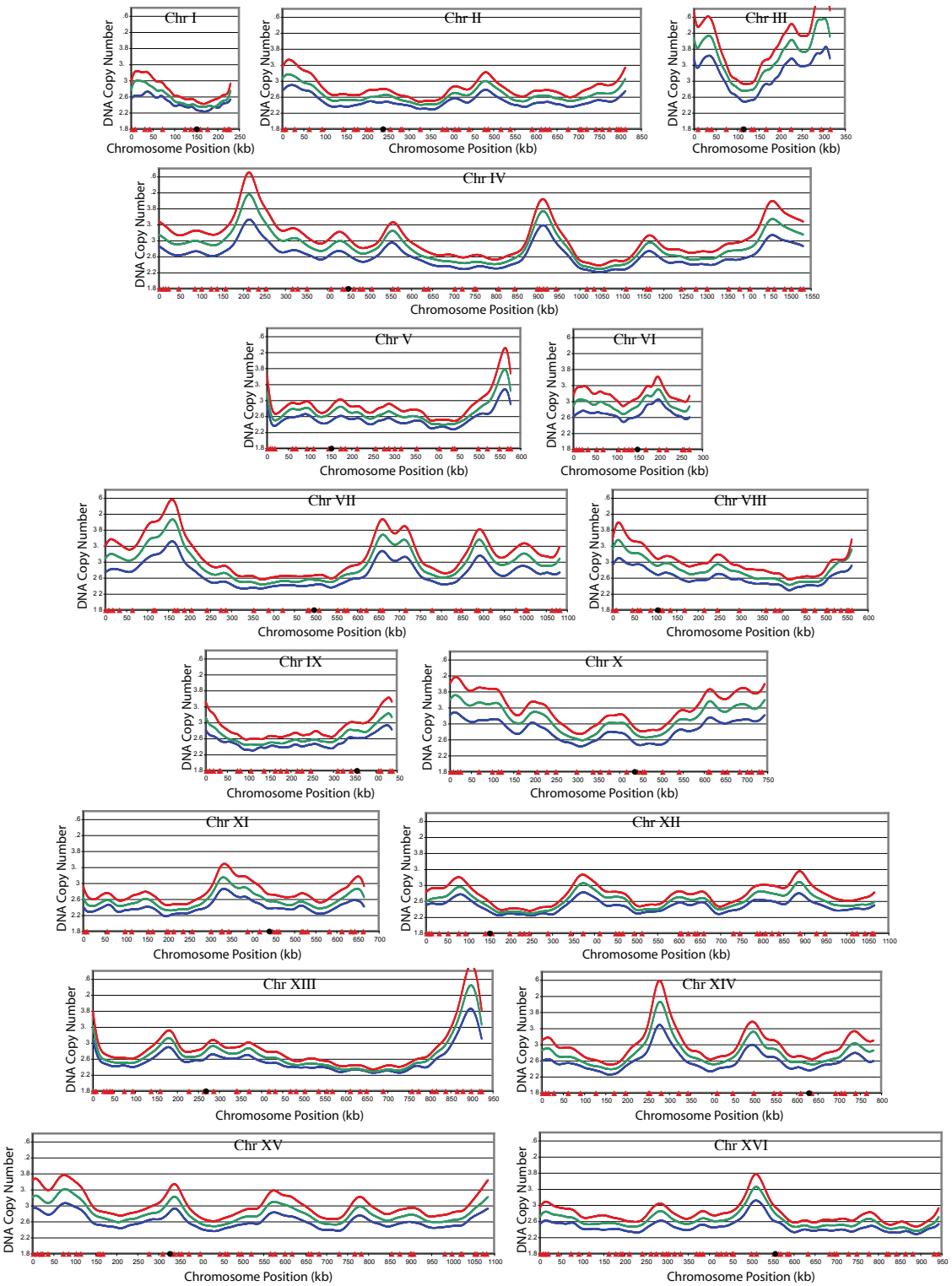

Figure S3. Impaired fork progression across the entire genome following a pulse of re-replication in G2/M phase. The *OMC ChrXIV-3ars*Δ strain was induced to re-replicate for 90 min in G2/M phase in the experiment described in Figure 3. After 90 min dextrose was added to repress re-replication induction. The re-replication profiles 180 min, 240 min, and 300 min after the initial addition of galactose are shown for all sixteen chromosomes. Positions of nim-ARSs mapped by Xu *et al.* (Xu *et al.*, 2006) (gray triangles) and the centromeres (black circles) are plotted along the X-axis.

Supplementary Figure 3

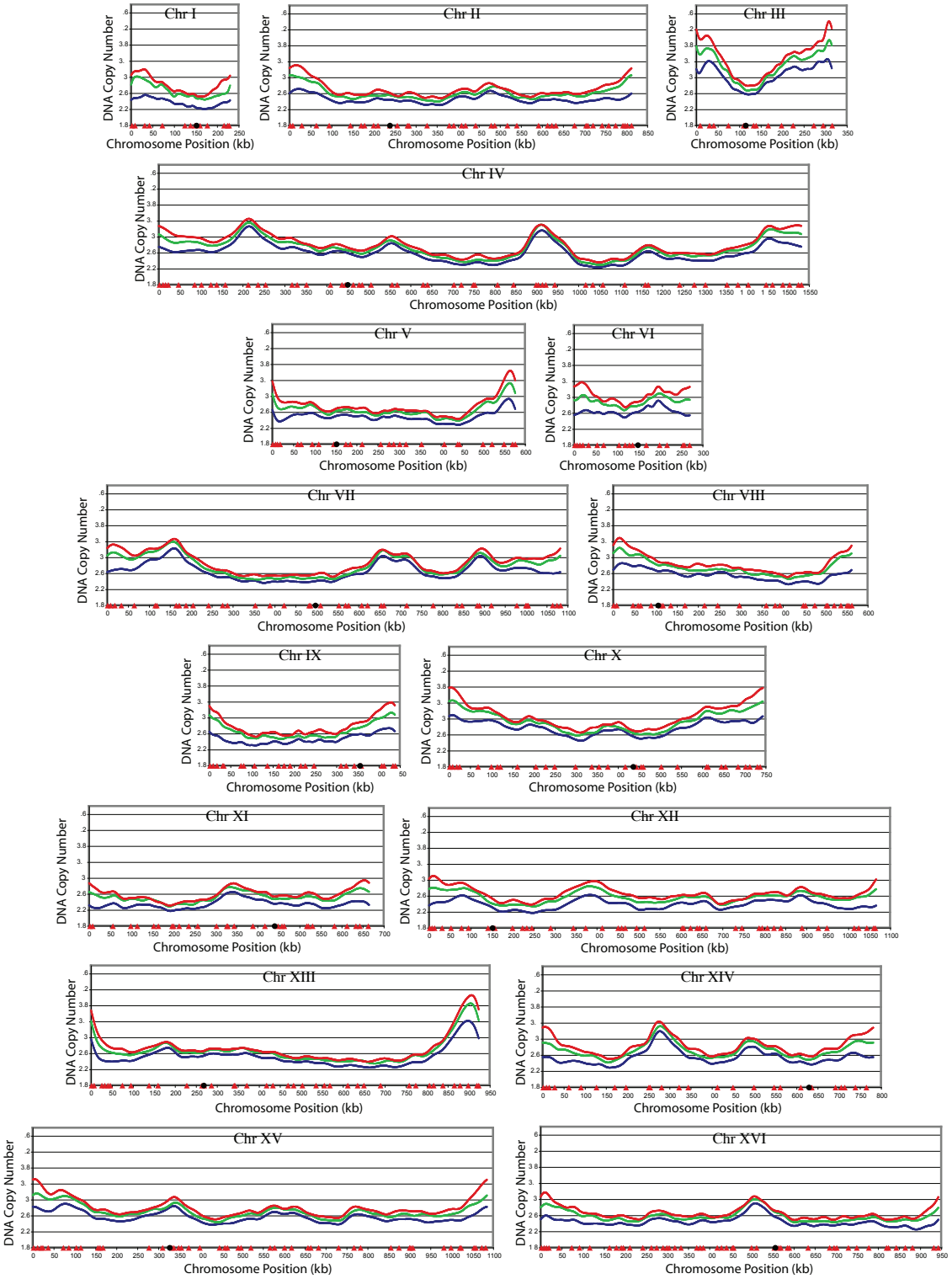

Figure S4. Dextrose repression of pGAL1-Δntdcdc6 transcription is effective at inhibiting new re-initiation events

Re-replication profiles from Figures 2 and 3 are arranged by time point to better visualize effect of dextrose addition on curbing re-replication initiation. On each graph the re-replication in continuous galactose (gray) and when dextrose in added (black) are shown. Positions of nim-ARSs mapped by Xu *et al.* (Xu *et al.*, 2006) (gray triangles) and the centromeres (black circles) are plotted along the X-axis.

Supplementary Figure 4

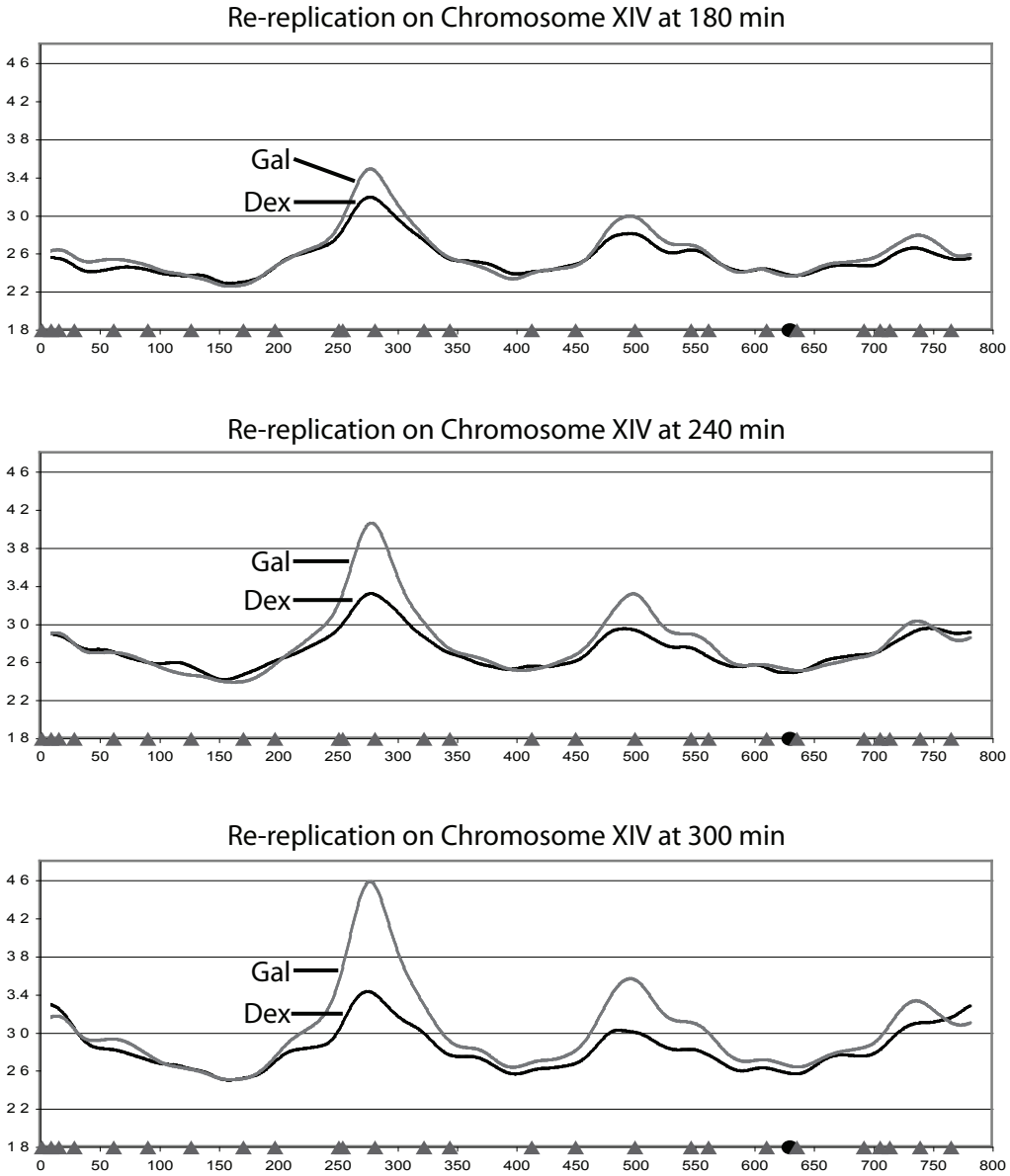

Publishing Agreement

It is the policy of the University to encourage the distribution of all theses and dissertations. Copies of all UCSF theses and dissertations will be routed to the library via the Graduate Division. The library will make all theses and dissertations accessible to the public and will preserve these to the best of their abilities, in perpetuity.

I hereby grant permission to the Graduate Division of the University of California, San Francisco to release copies of my thesis or dissertation to the Campus Library to provide access and preservation, in whole or in part, in perpetuity.

Richard J Mommaerts
Author Signature

7/15/2007
Date